CENTRO DE INVESTIGACIÓN EN TECNOLOGÍAS DE AUDIO
PONTIFICIA UNIVERSIDAD CATÓLICA DE CHILE

AUDICIÓN ESPACIAL

Rodrigo F. Cádiz
Octubre 2011

Audición espacial
(Spatial hearing o Audio 3D)

Localización de sonidos

Azimuth, Elevación, Distancia

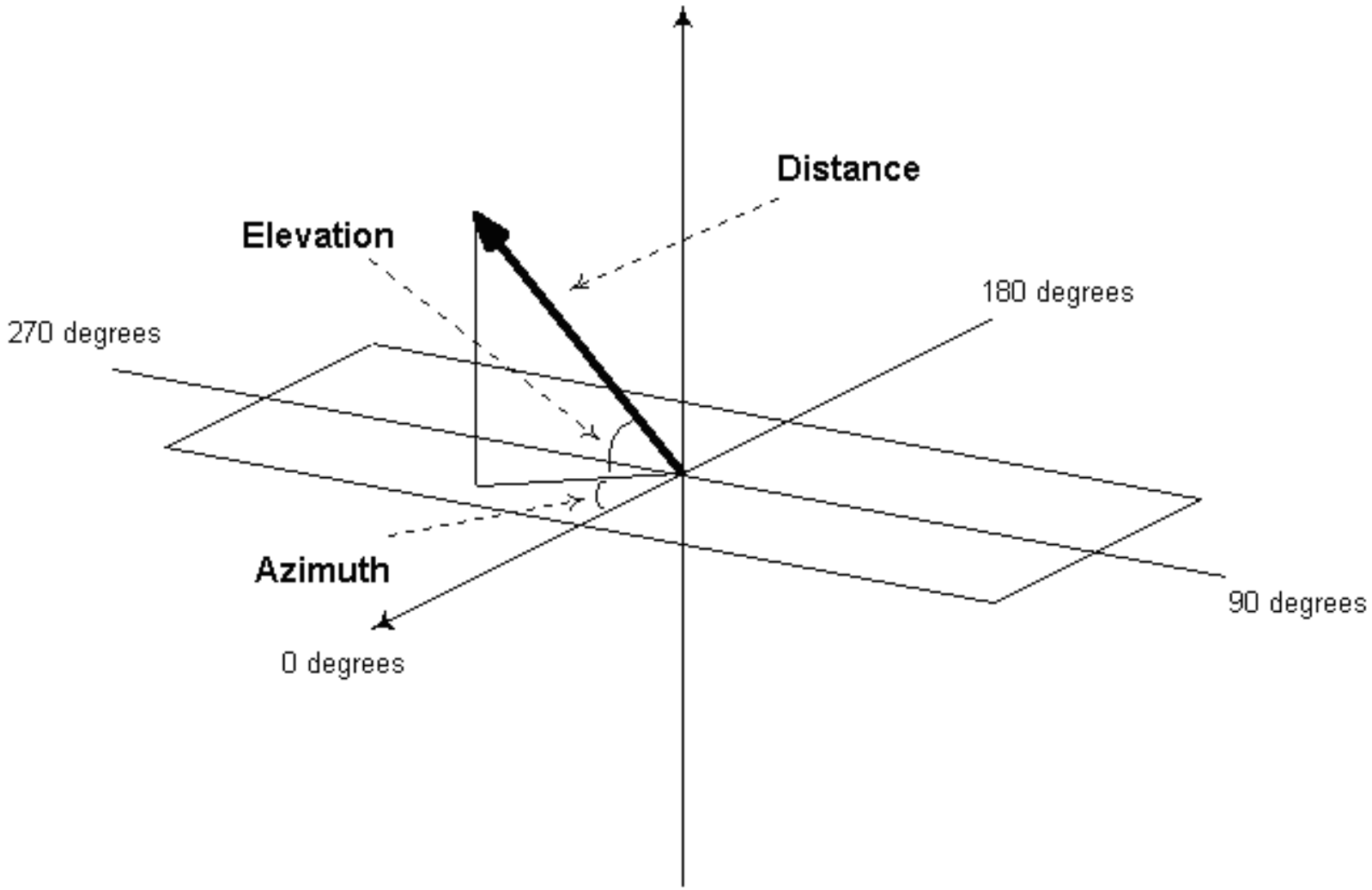

Planos horizontal, medial y frontal

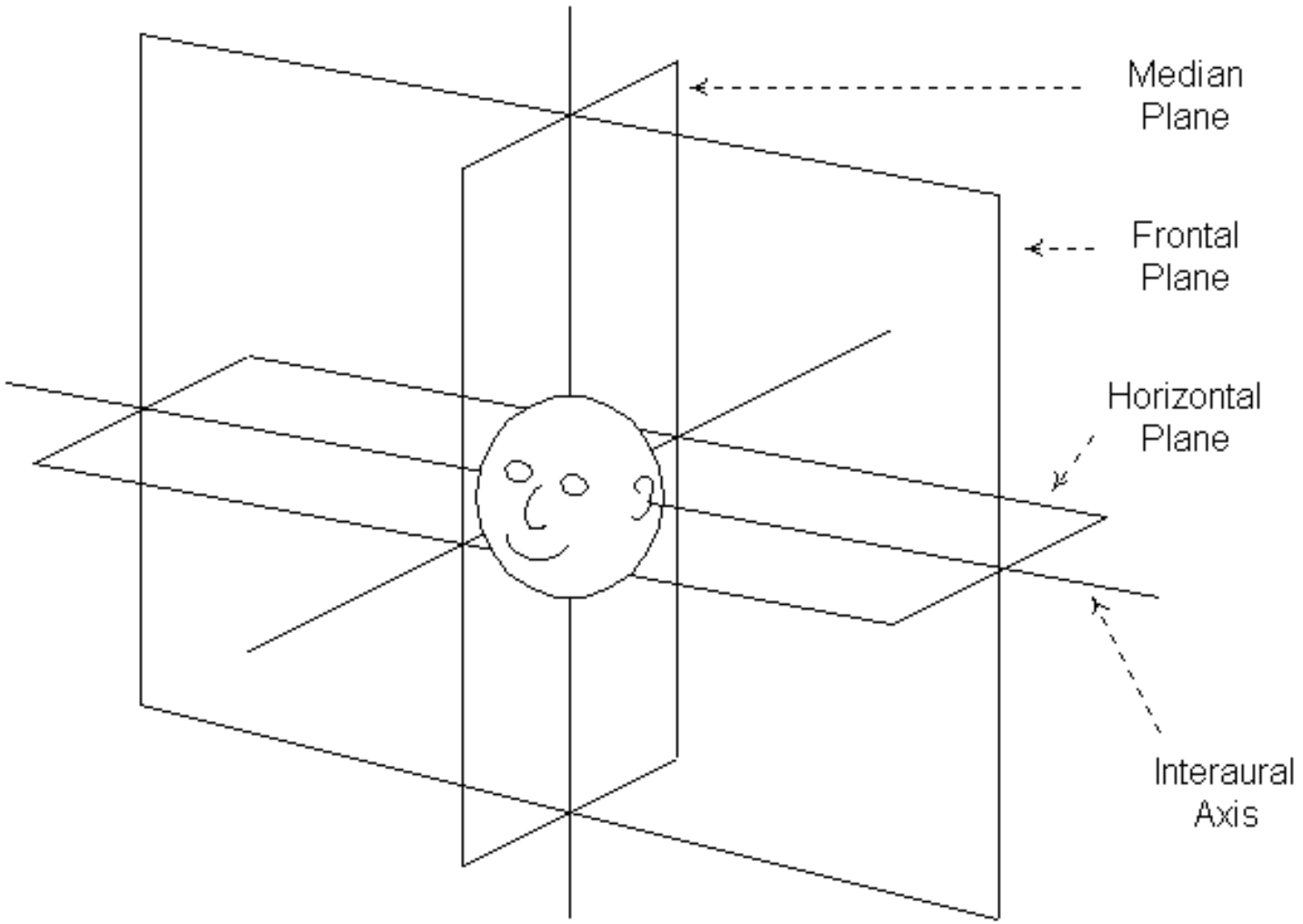

Localización de sonidos

FIG. 1. THE EXPERIMENTAL SET-UP
Note the absence of vertical reflecting surfaces at the level of the observer.

Stevens and Newman (1936)

Localización de sonidos

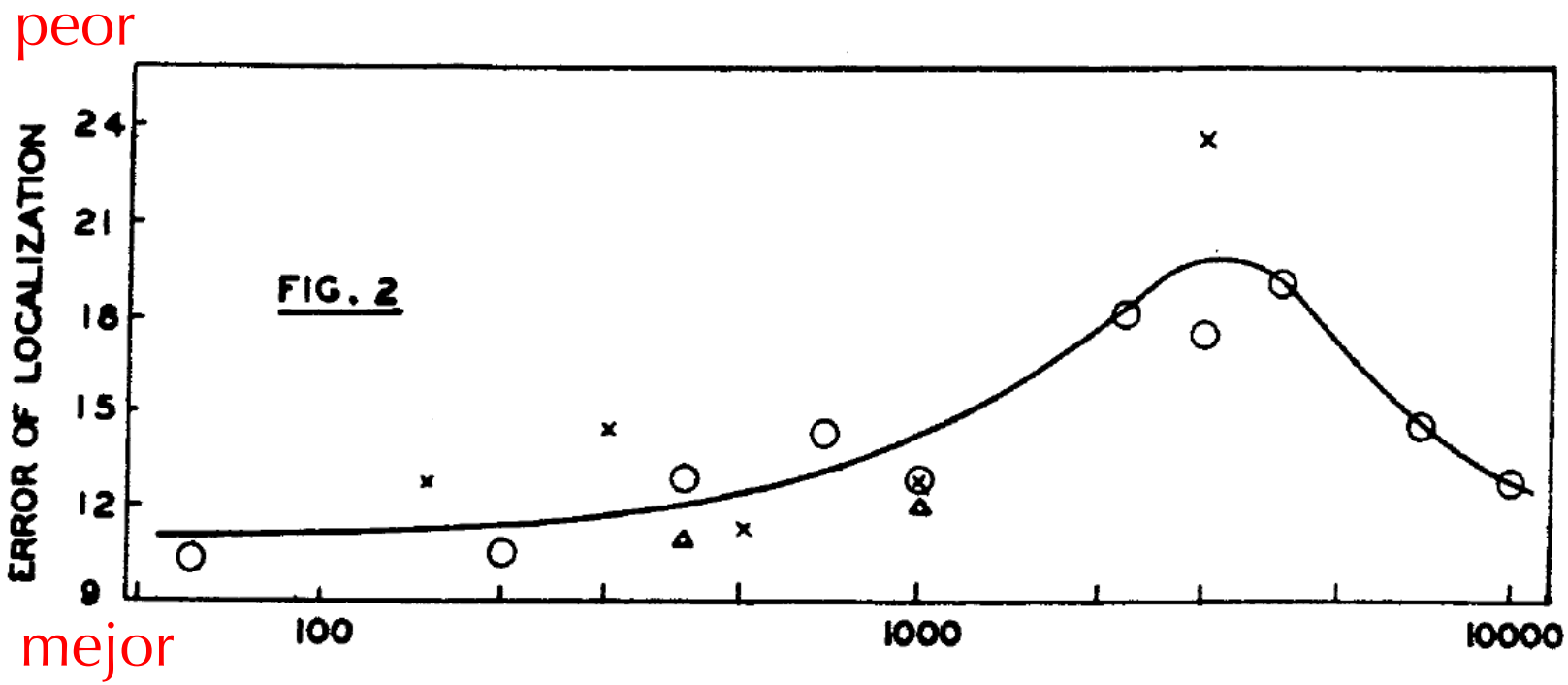

FIG. 2. DEPENDENCE OF LOCALIZATION ON FREQUENCY
The ordinate represents the average of the errors in degrees made by both *Os*. The crosses are for the shorter series of judgments made in 1933. The circles represent the results obtained in 1934. The triangles represent the results obtained with unfiltered tones. Note the critical region at about 3000 cycles.

Stevens and Newman (1936)

Mínimo ángulo audible

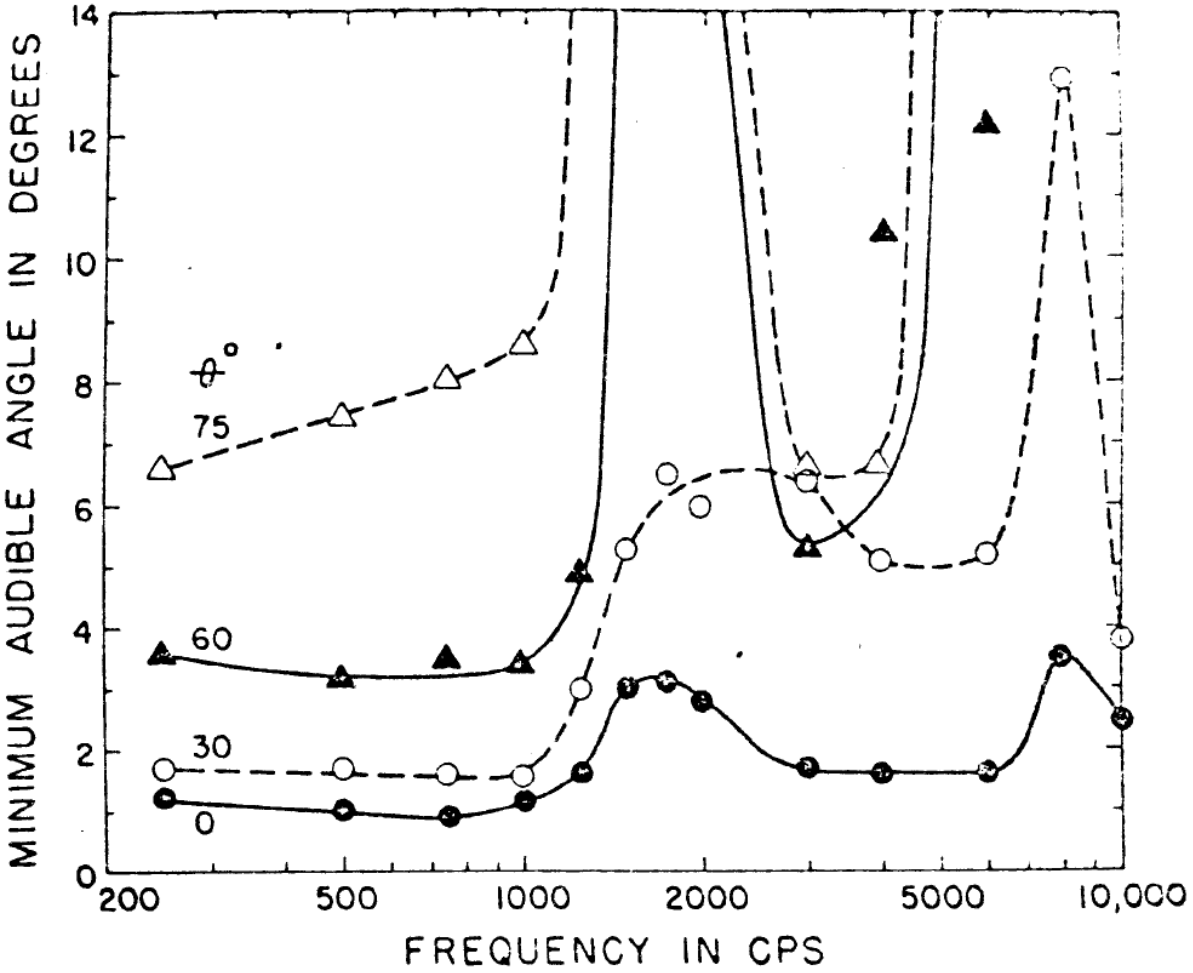

FIGURE 6 Minimum Audible Angle Between Successive Pulses of Tone as a Function of the Frequency of the Tone and the Direction of the Source (17)

Mills (1958)

Teoría dual de la localización de sonidos

Teoría dual de la localización

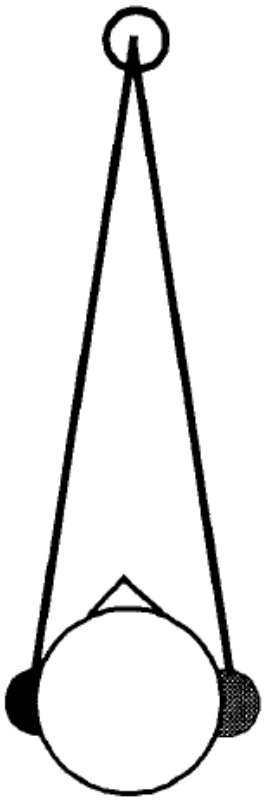

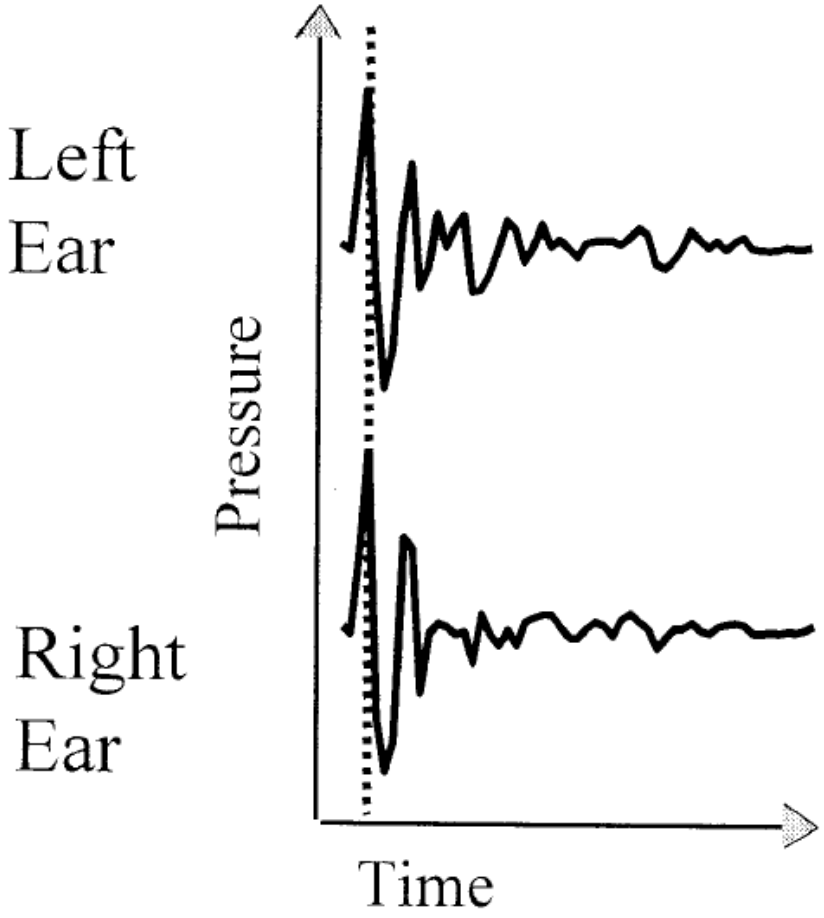

Courtesy of Shinn-Cunningham

Teoría dual de la localización

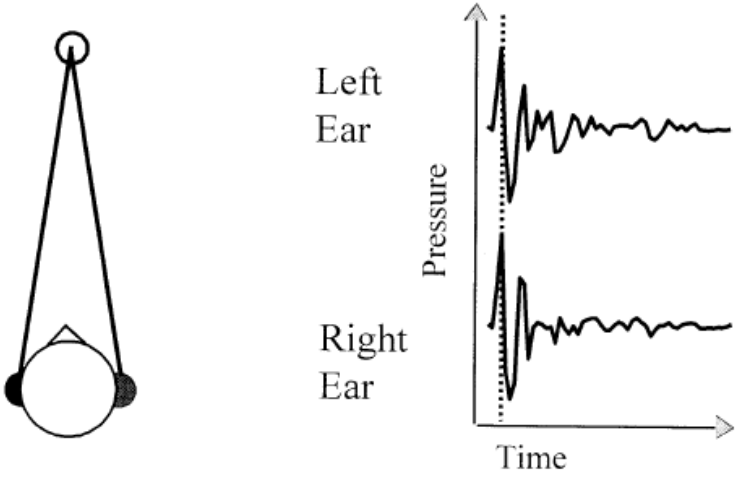

Interaural
Time Difference
(ITD)

Interaural
Level Difference
(ILD)

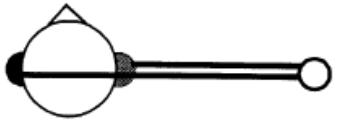

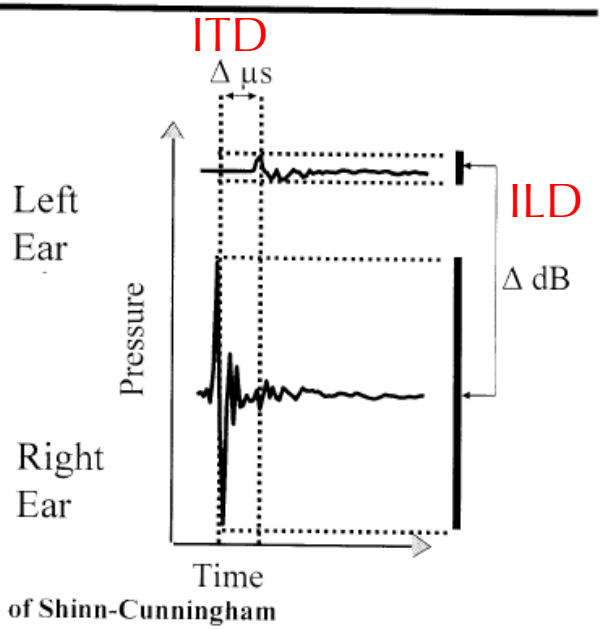

courtesy of Shinn-Cunningham

Teoría dual de la localización

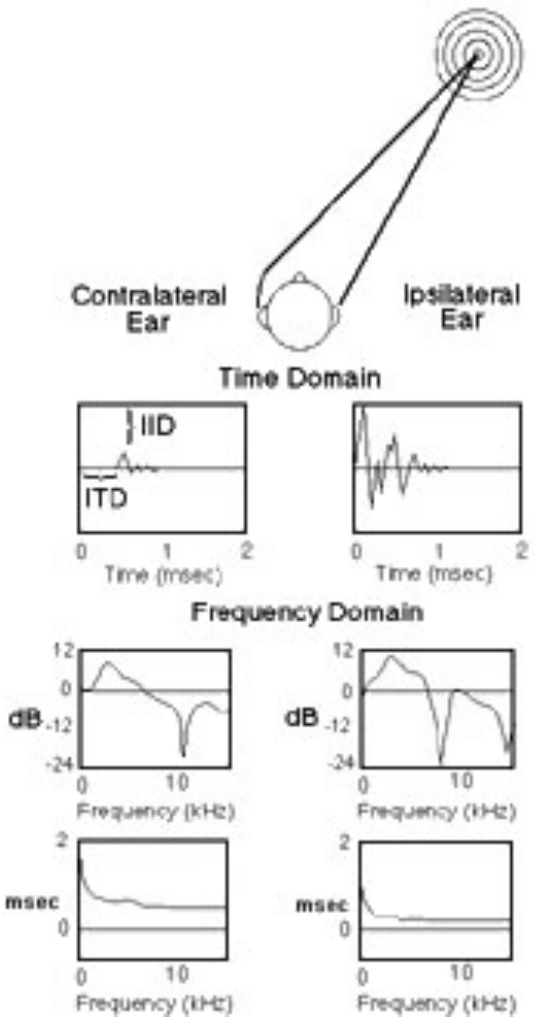

Interaural time difference (ITD)

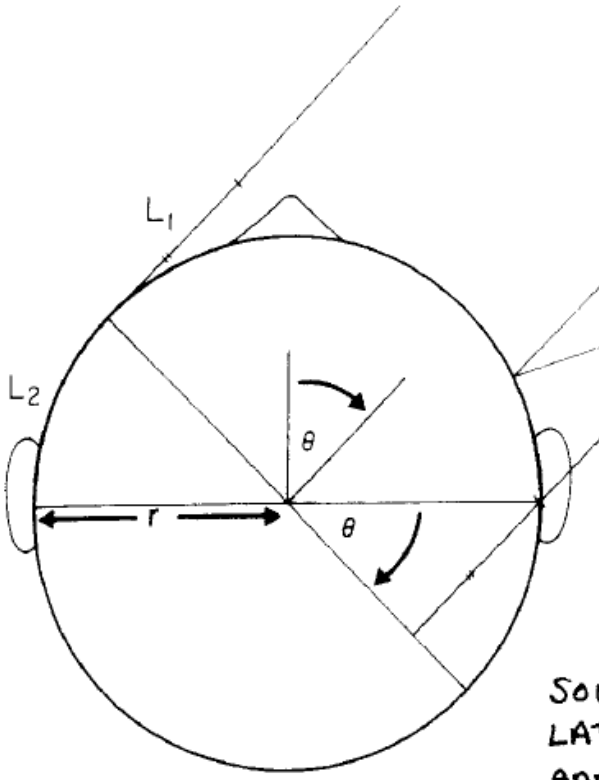

$L_1 = r \sin\theta$

$L_2 = r\theta$

$L_1 + L_2 = r(\theta + \sin\theta)$

$\Delta t = 257(\theta + \sin\theta)$

SOUND REACHES THE FARTHER EAR LATER BY ~29 μsec FOR EACH ADDITIONAL CENTIMETER TRAVELLED.

MICROSECOND (μS)

$1\,\mu S = \frac{1}{1{,}000{,}000}$ SECOND

Woodworth (1938)

Interaural time difference (ITD)

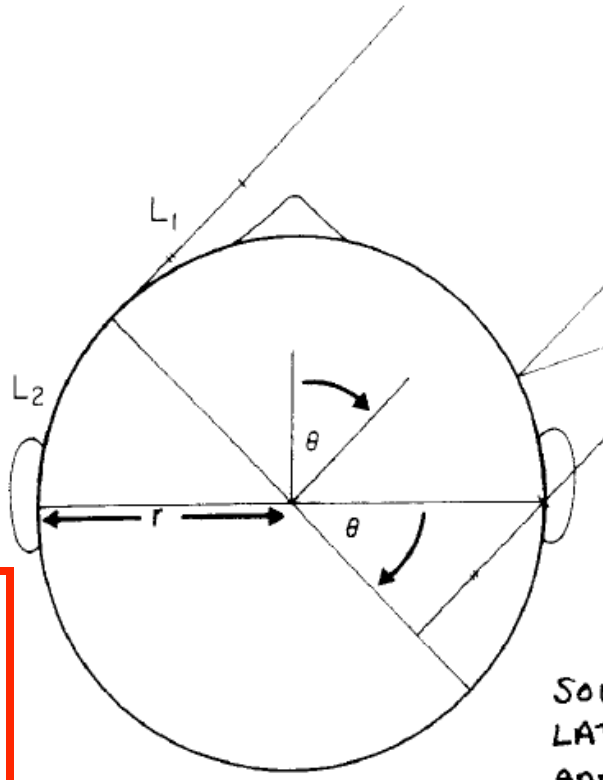

$L_1 = r \sin\theta$

$L_2 = r\theta$

$L_1 + L_2 = r(\theta + \sin\theta)$

$\Delta t = 257(\theta + \sin\theta)$

SOUND REACHES THE FARTHER EAR LATER BY ~29 μsec FOR EACH ADDITIONAL CENTIMETER TRAVELLED.

MICROSECOND (μS)

$1\,\mu S = \frac{1}{1{,}000{,}000}$ SECOND

Woodworth (1938)

Interaural time difference (ITD)

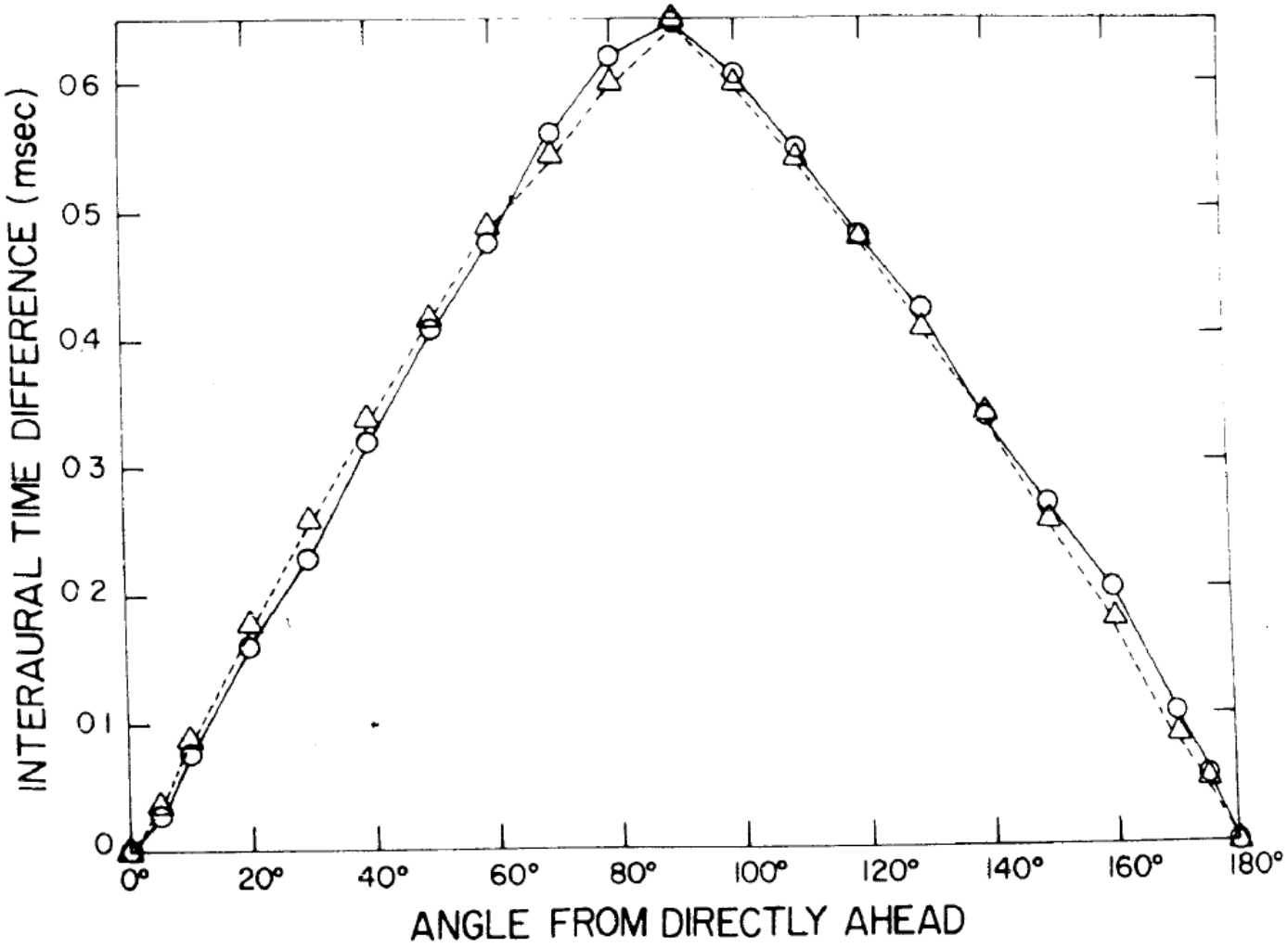

FIG. 8.2 Interaural time differences as measured on a human head (○) compared with Woodworth's formula (△), see Eq. (8.2). (From Feddersen *et al.*, 1957, p. 989.)

Woodworth (1938)

Interaural time difference (ITD)

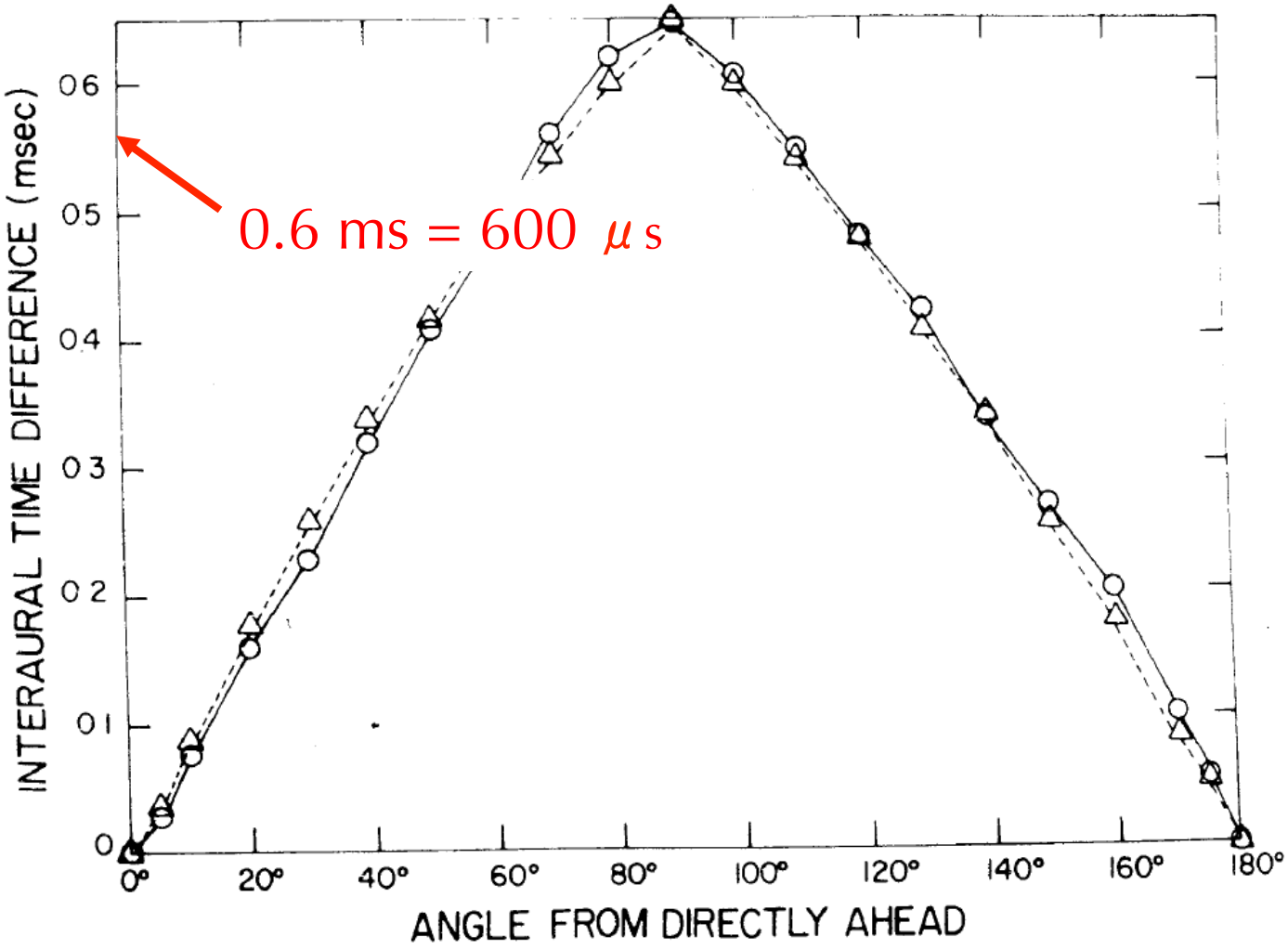

FIG. 8.2 Interaural time differences as measured on a human head (○) compared with Woodworth's formula (△), see Eq. (8.2). (From Feddersen *et al.*, 1957, p. 989.)

Woodworth (1938)

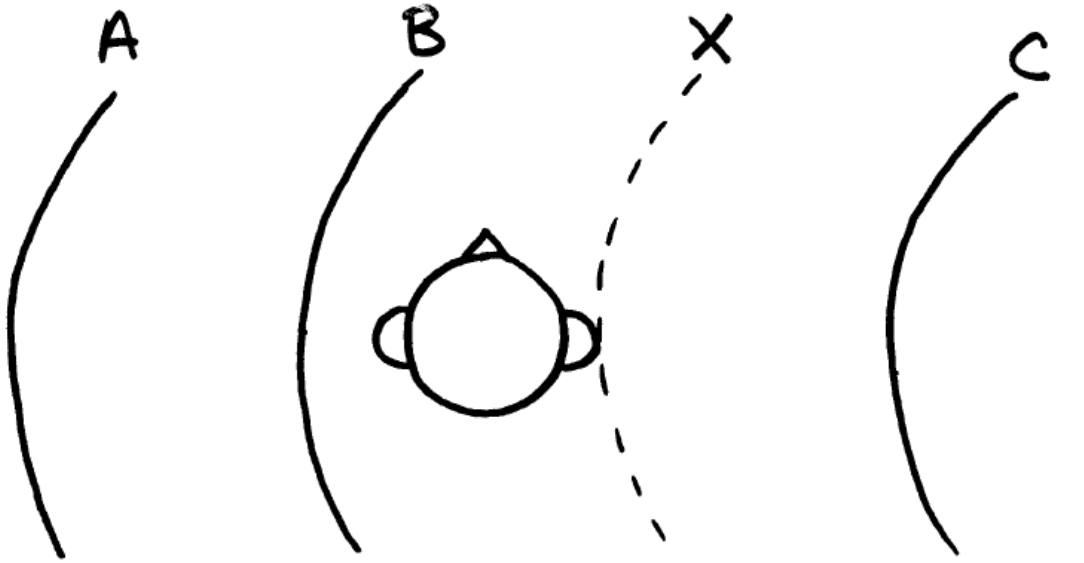

Interaural time difference (ITD)

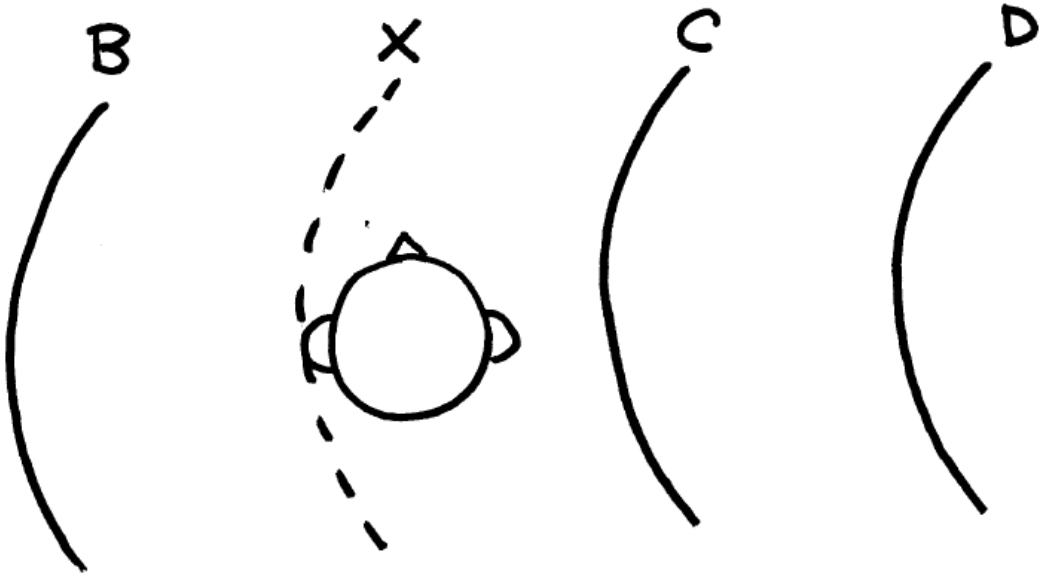

Bajas frecuencias

La onda X llega al oído izquierdo antes que cualquier otra onda — se puede calcular la ITD.

Interaural time difference (ITD)

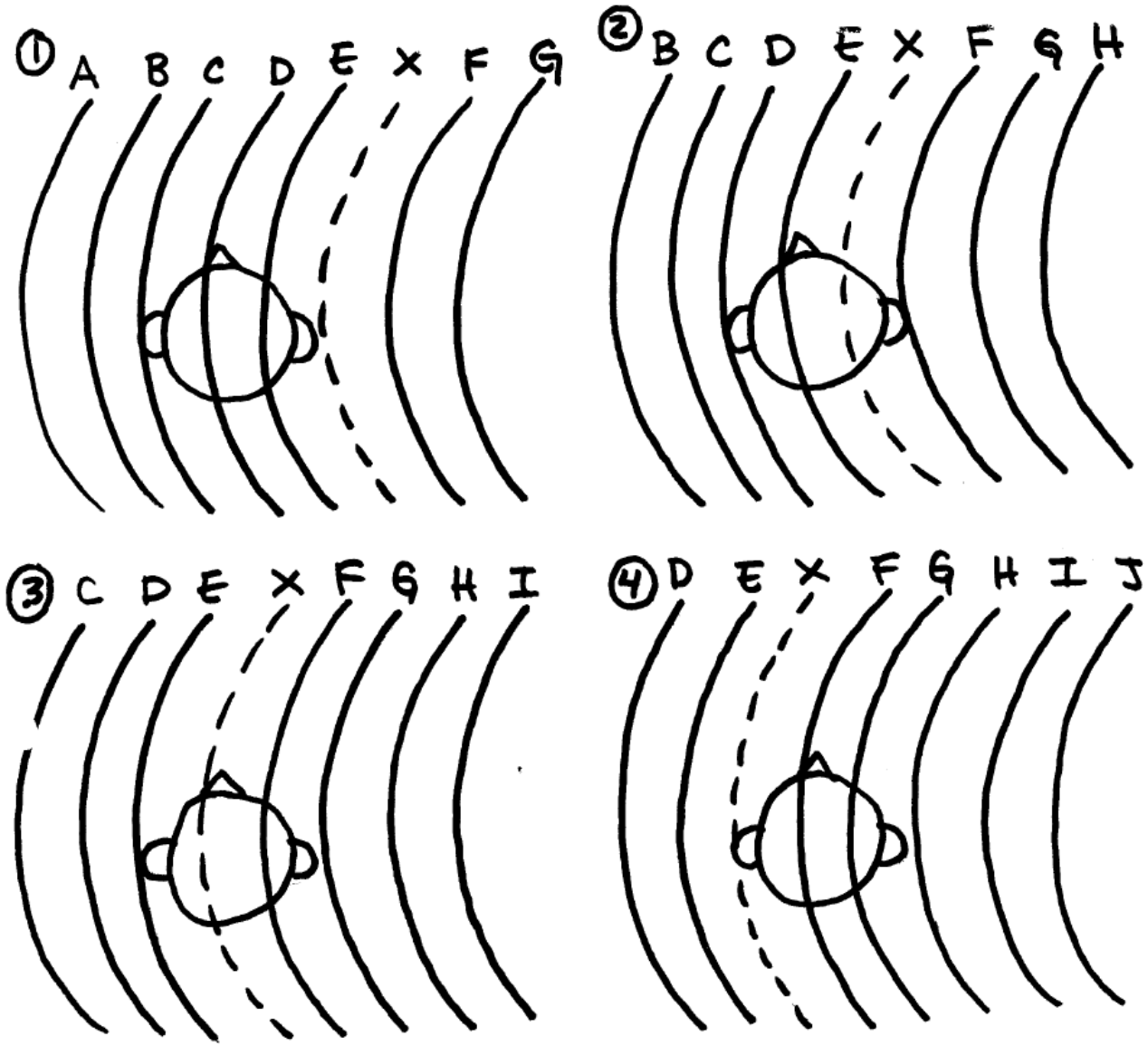

Altas frecuencias

Las ondas C,D, y E llegan al oído antes que X—la ITD es ambigua.

Interaural level difference (ILD)

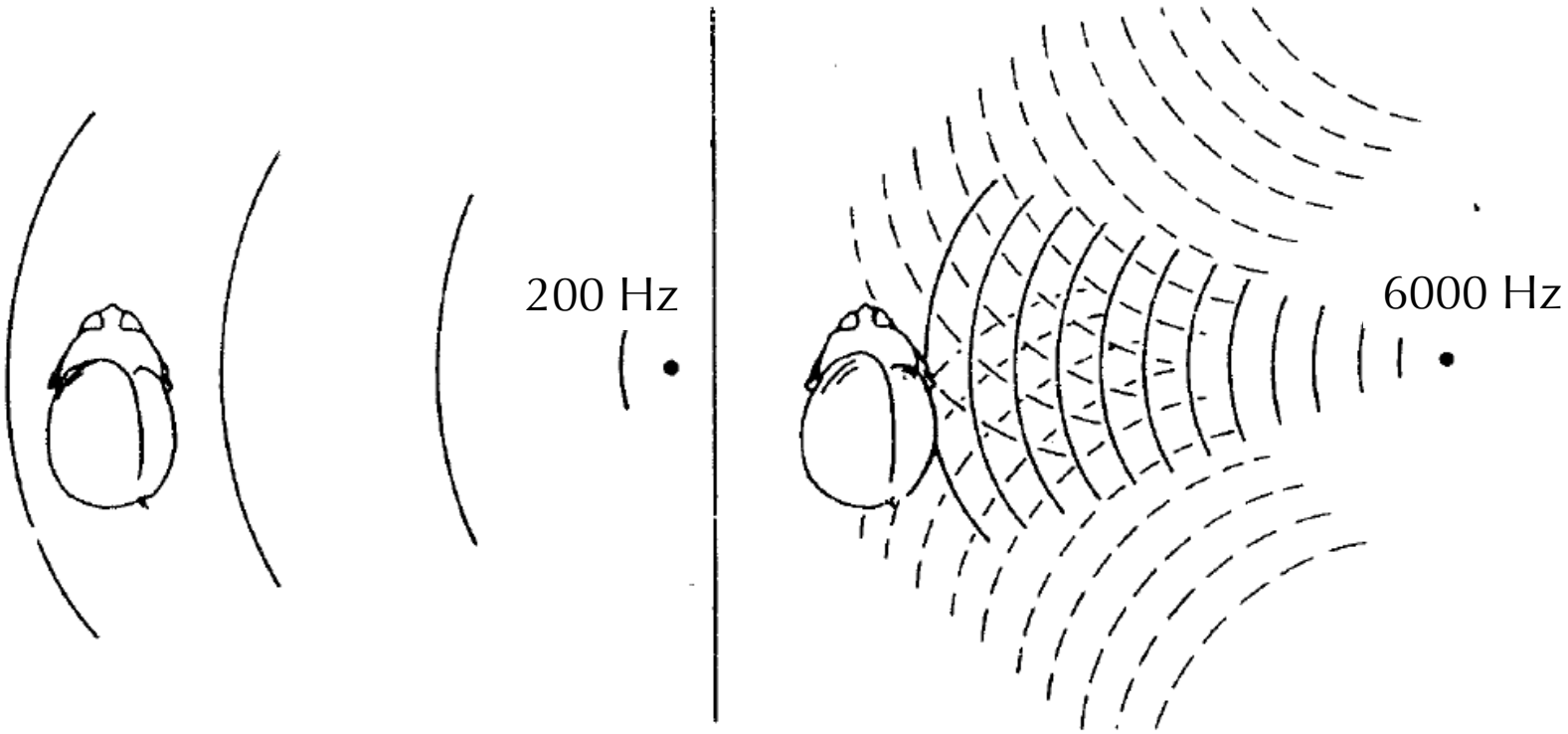

A frecuencias bajas, las ILDs son muy pequeñas porque sonidos de baja frecuencia tienen una longitud de onda mucho mayor en comparación con el ancho de la cabeza y consecuentemente hay sólo pequeñas pérdidas de energía debido a la obstrucción o sombra de la cabeza (head shadow).

Interaural level difference (ILD)

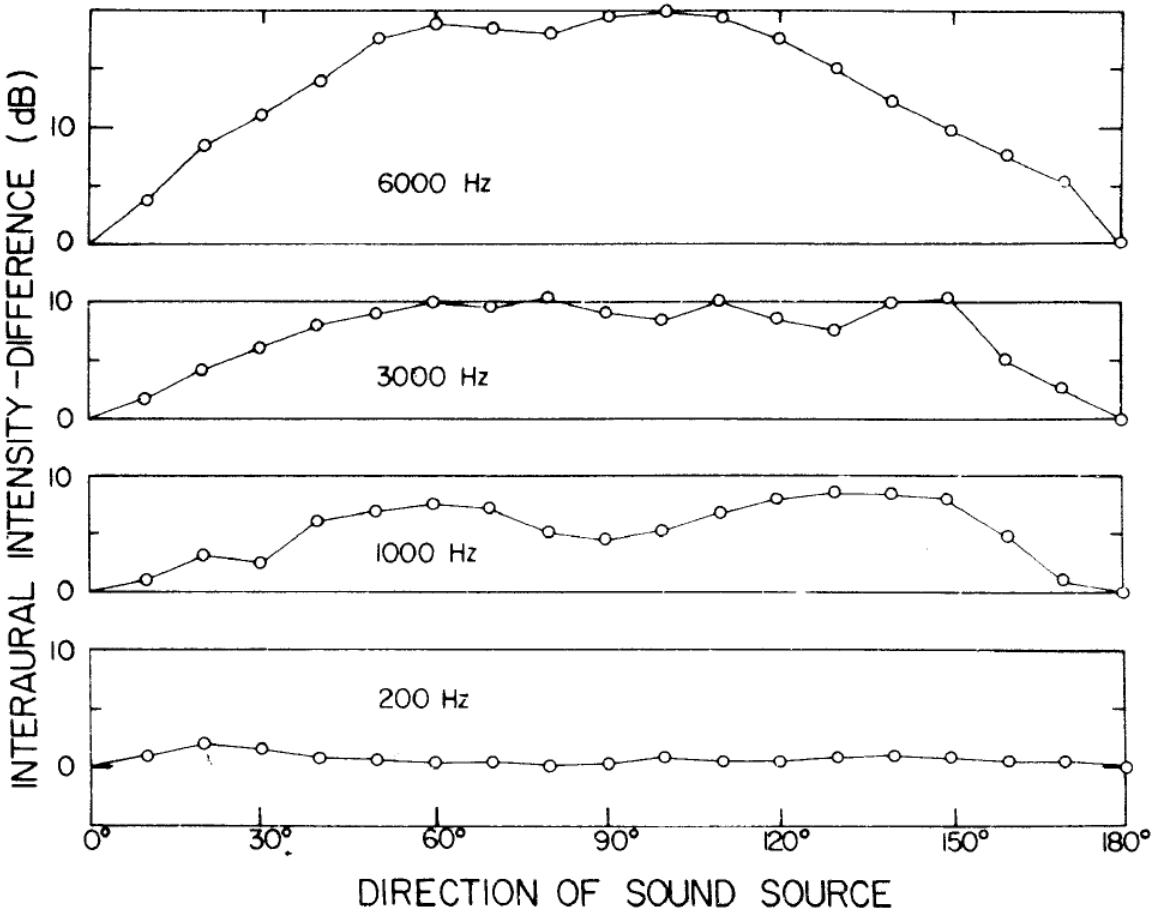

FIG. 8.3 Interaural intensity difference measured at the two ears as a function of the position of the sound source. At 200 Hz there is essentially no sound shadow, whereas at 6000 Hz it is nearly 20 dB when the source is located directly to the side. The lack of symmetry about 90° is caused by the pinna. (From Fedderson *et al.*, 1957, p. 989.)

ITD
Líneas de retraso de Jeffress

ITD: Líneas de retraso de Jeffress

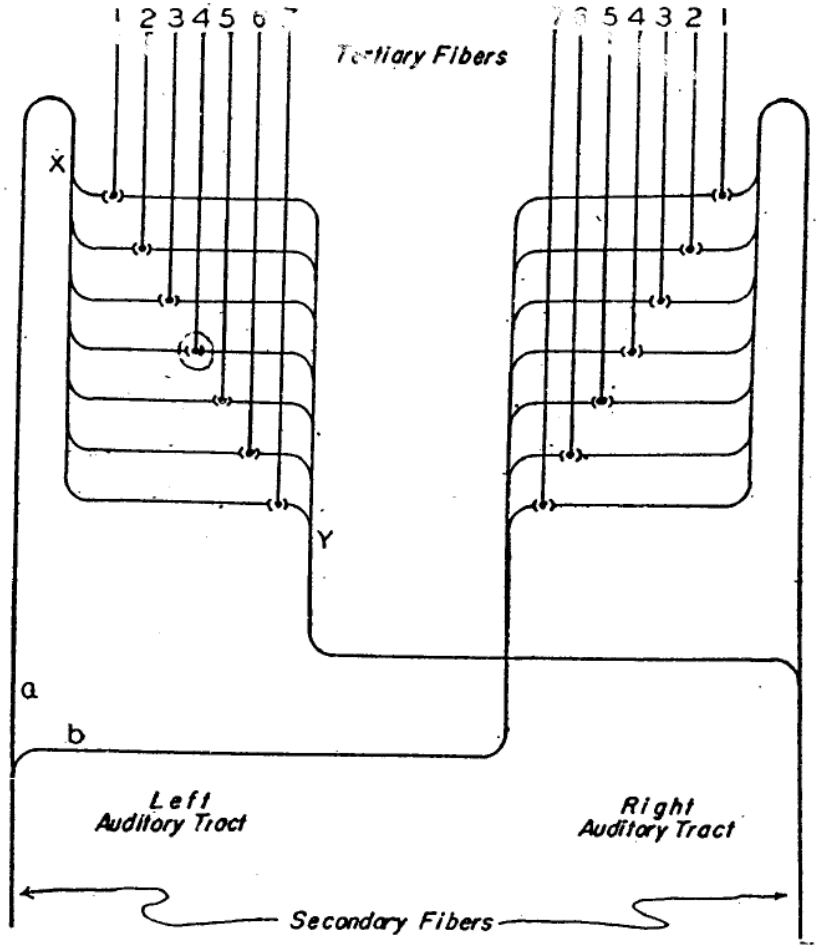

FIGURE 1. HYPOTHETICAL MID-BRAIN MECHANISM FOR THE LOCALIZATION OF LOW FREQUENCY TONES

Jeffress, L.A. (1948). "A place theory of auditory localization," J. Comp. Physiol. Psychol., 41, 35-39.

ITD: Jeffress delay line

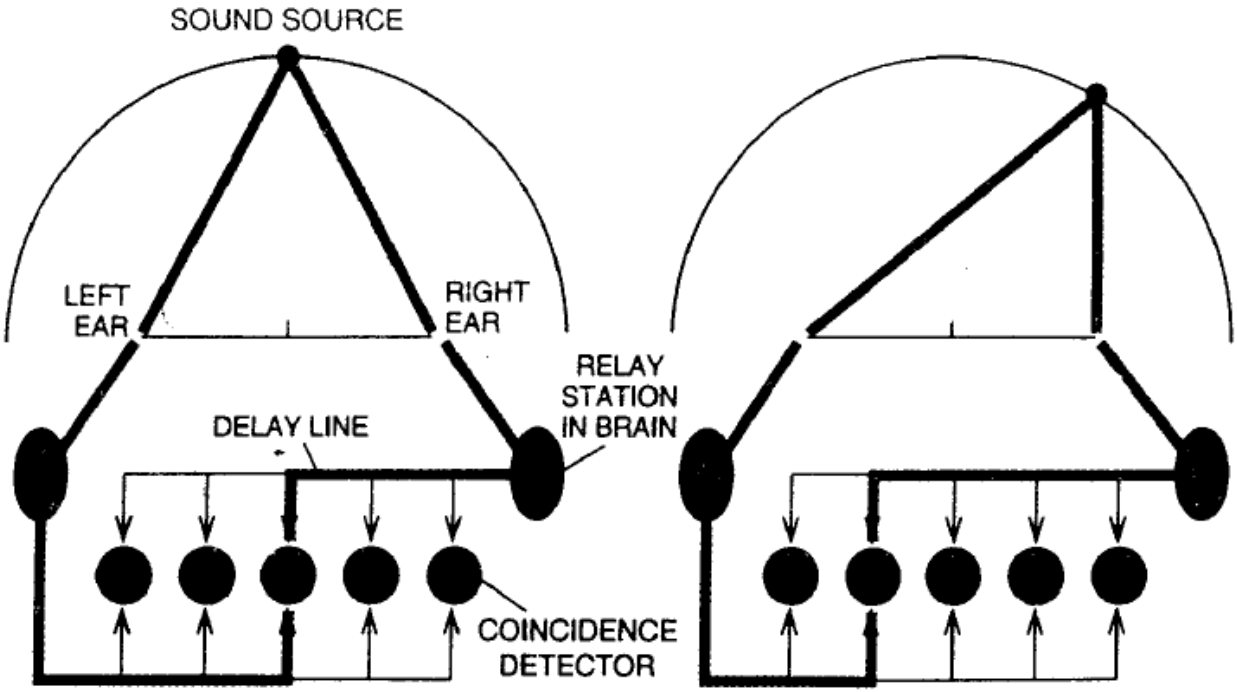

MODEL CIRCUIT for detection of interaural time differences was suggested in 1948. The coincidence detectors receive inputs from both ears. They fire only when impulses from the two sides arrive simultaneously through fibers that serve as delay lines. The detector that responds (*darkly colored circle*) changes as a sound source moves from directly in front of an individual (*left*) to the side (*right*). The owl brain operates in much the way the model proposed.

Konishi, M. (1993). "Listening with two ears," Scientific American, April, 66-73.

Animación de las líneas de retraso de Jeffress

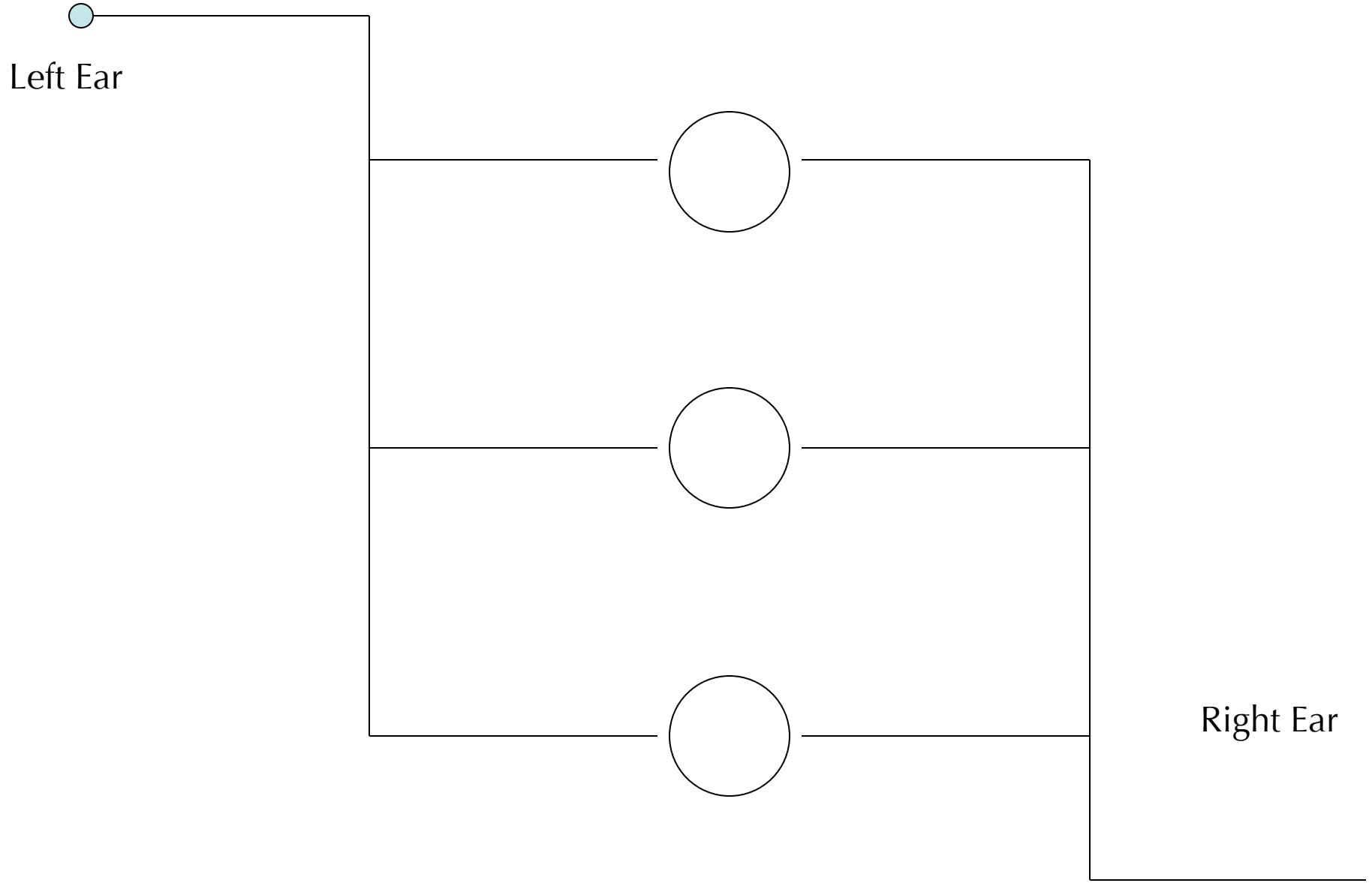
Left Ear
Right Ear

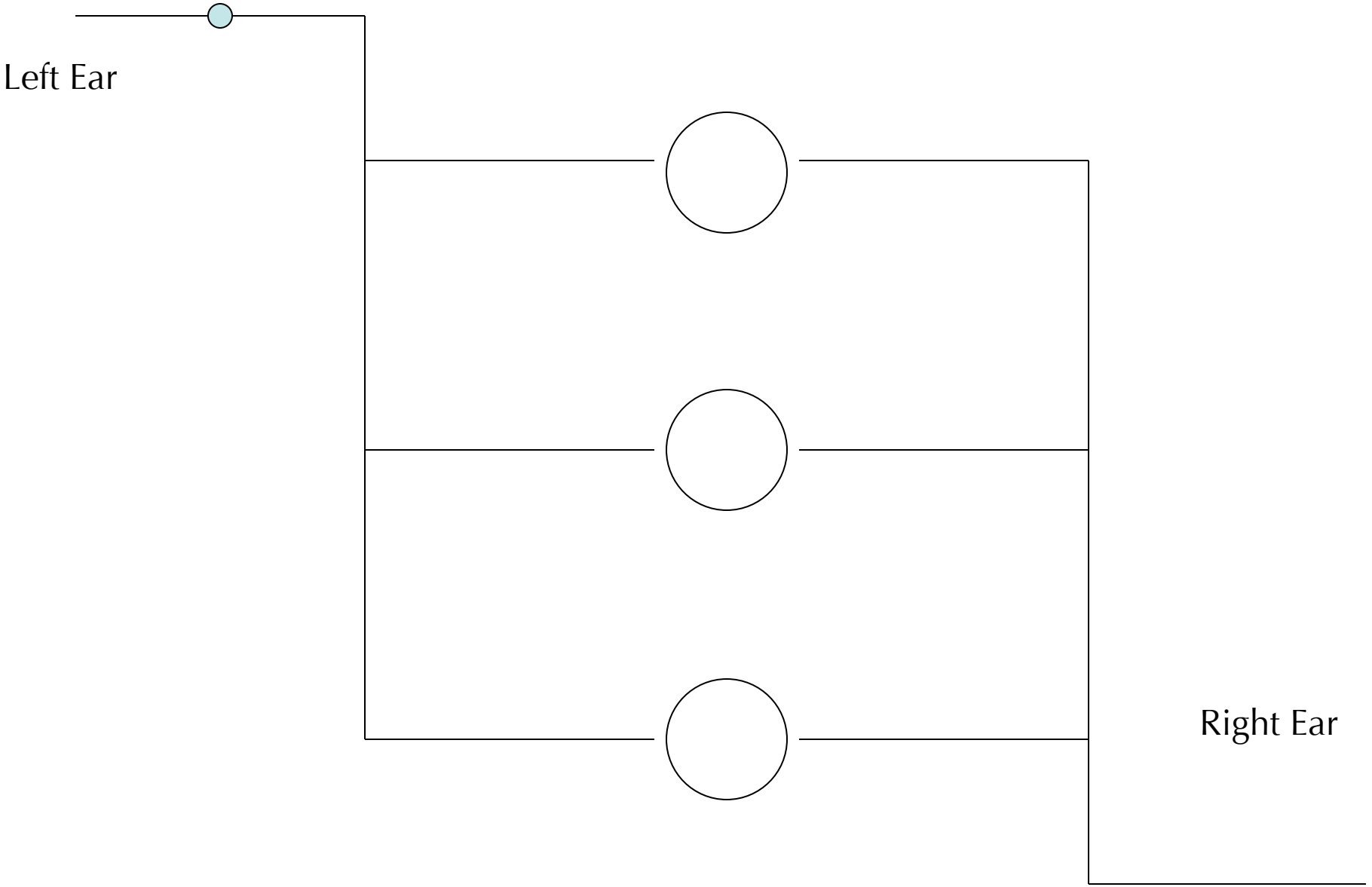
Left Ear
Right Ear

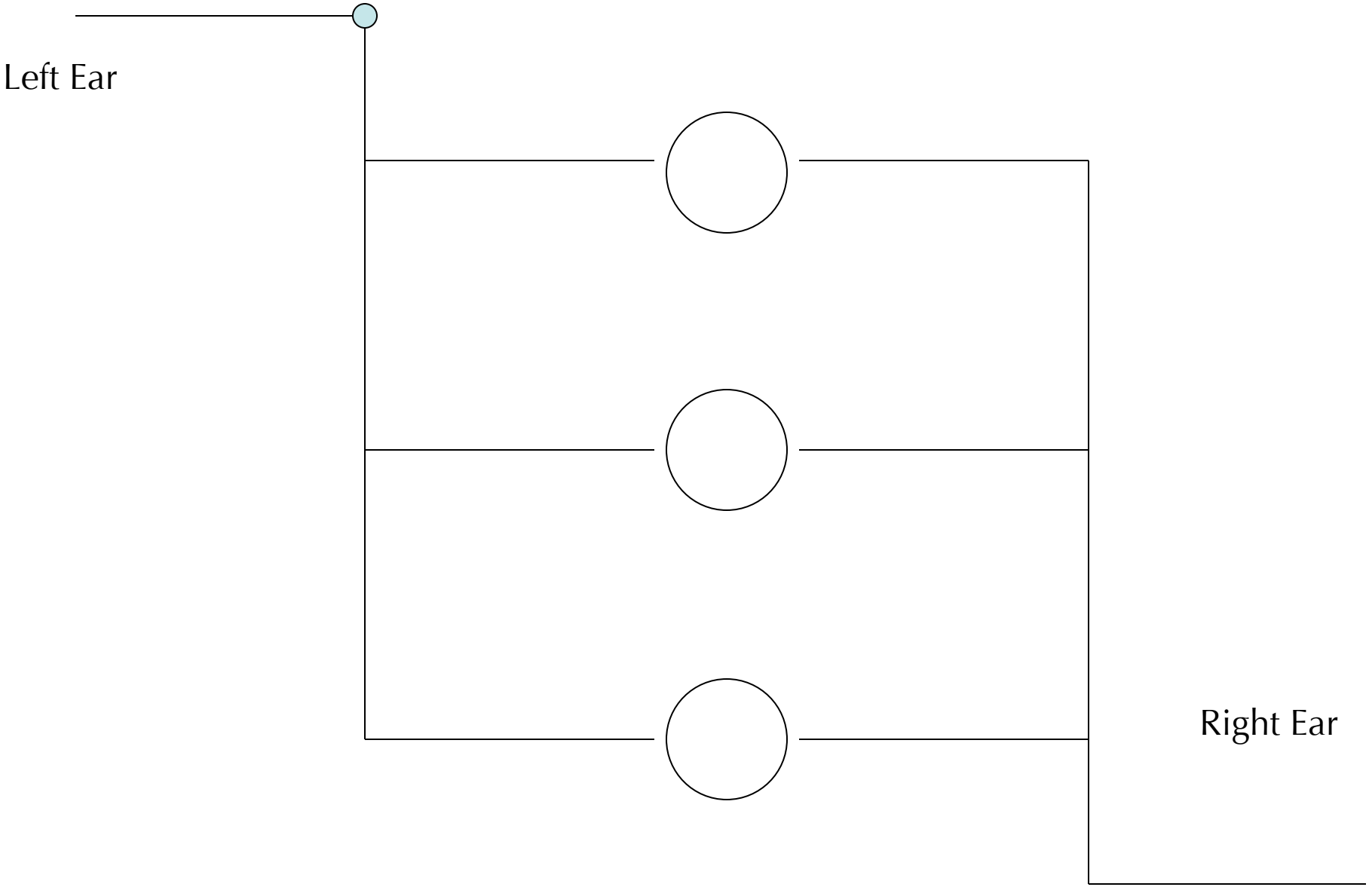
Left Ear
Right Ear

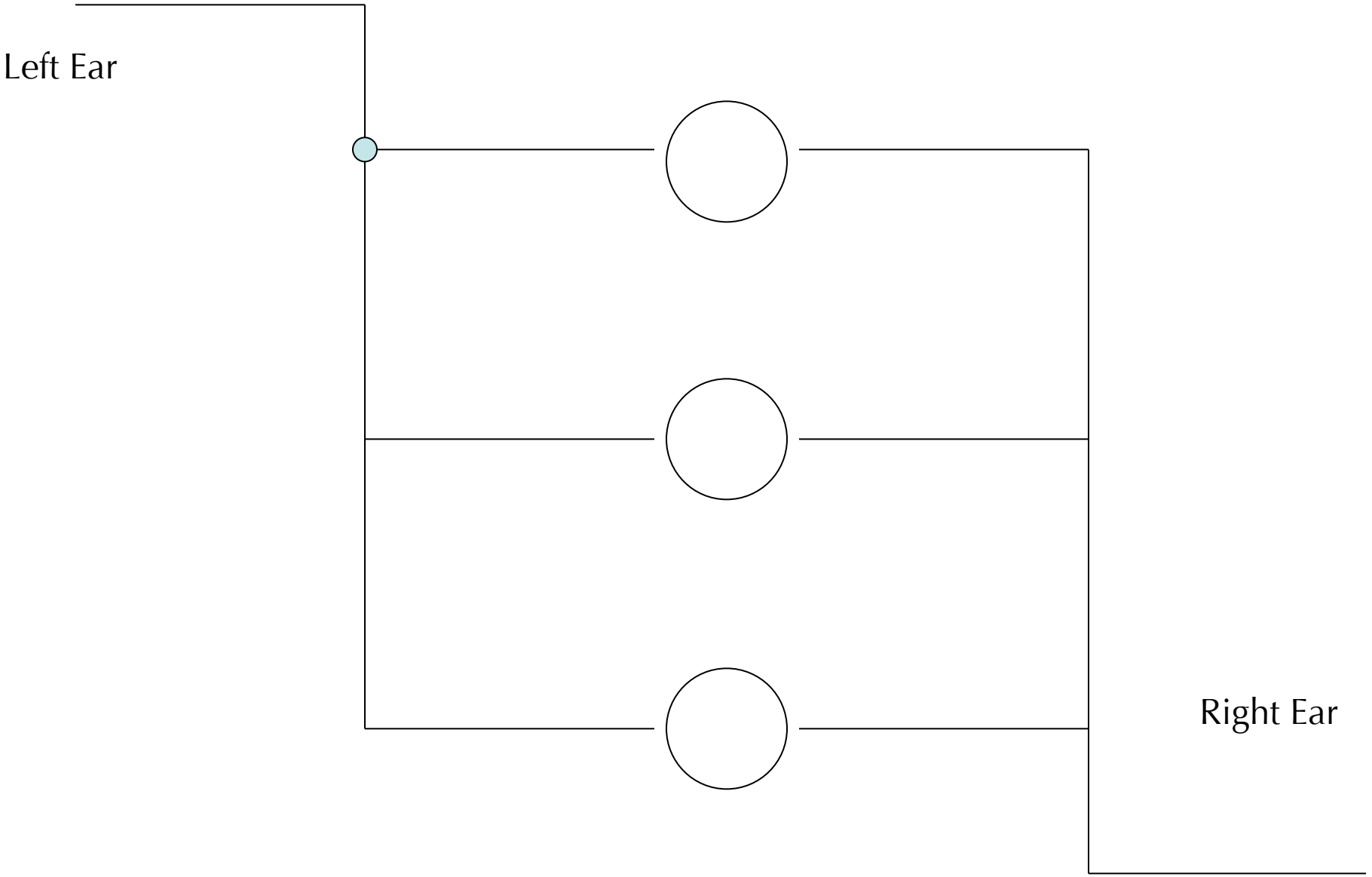
Left Ear
Right Ear

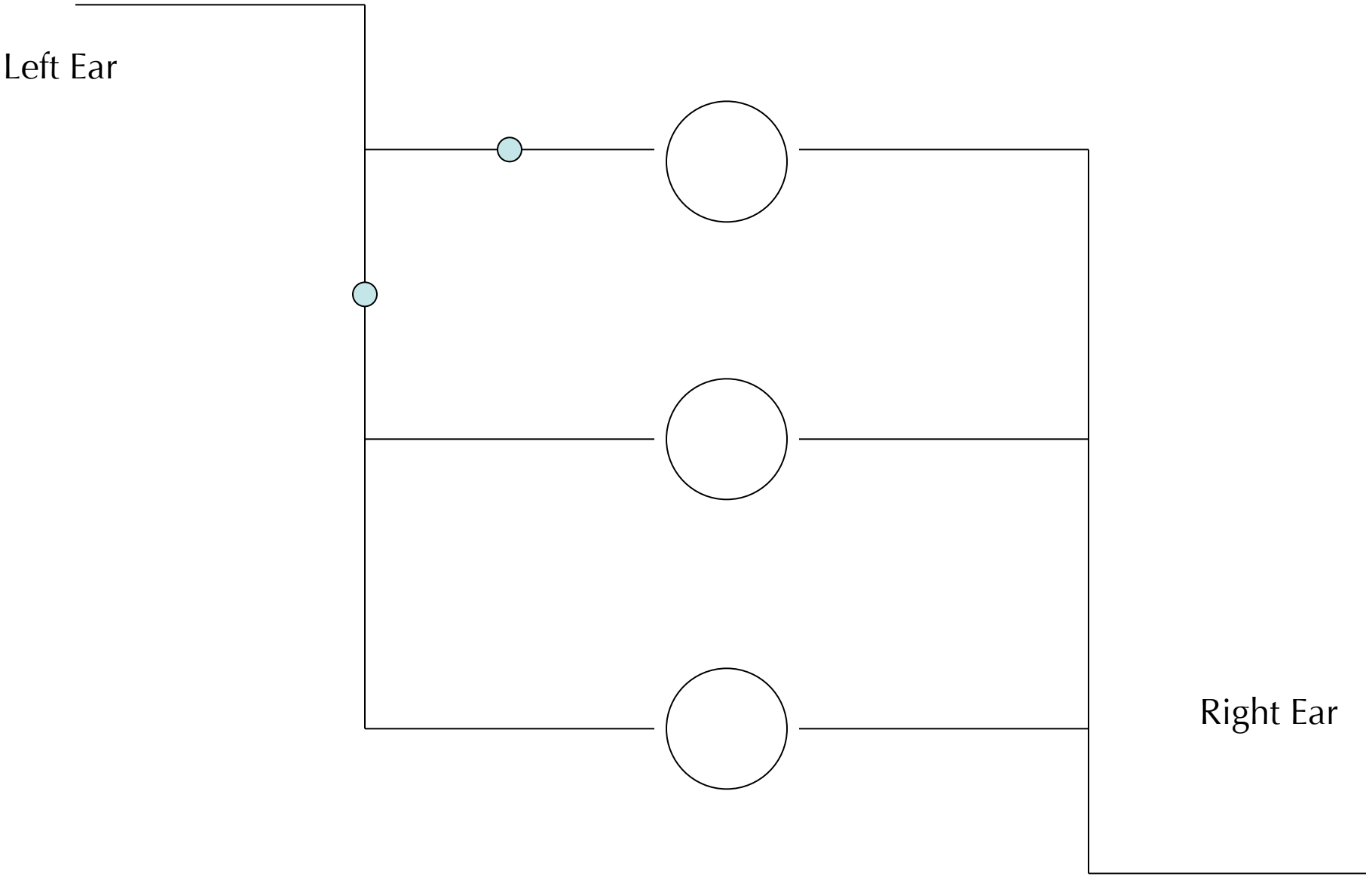
Left Ear
Right Ear

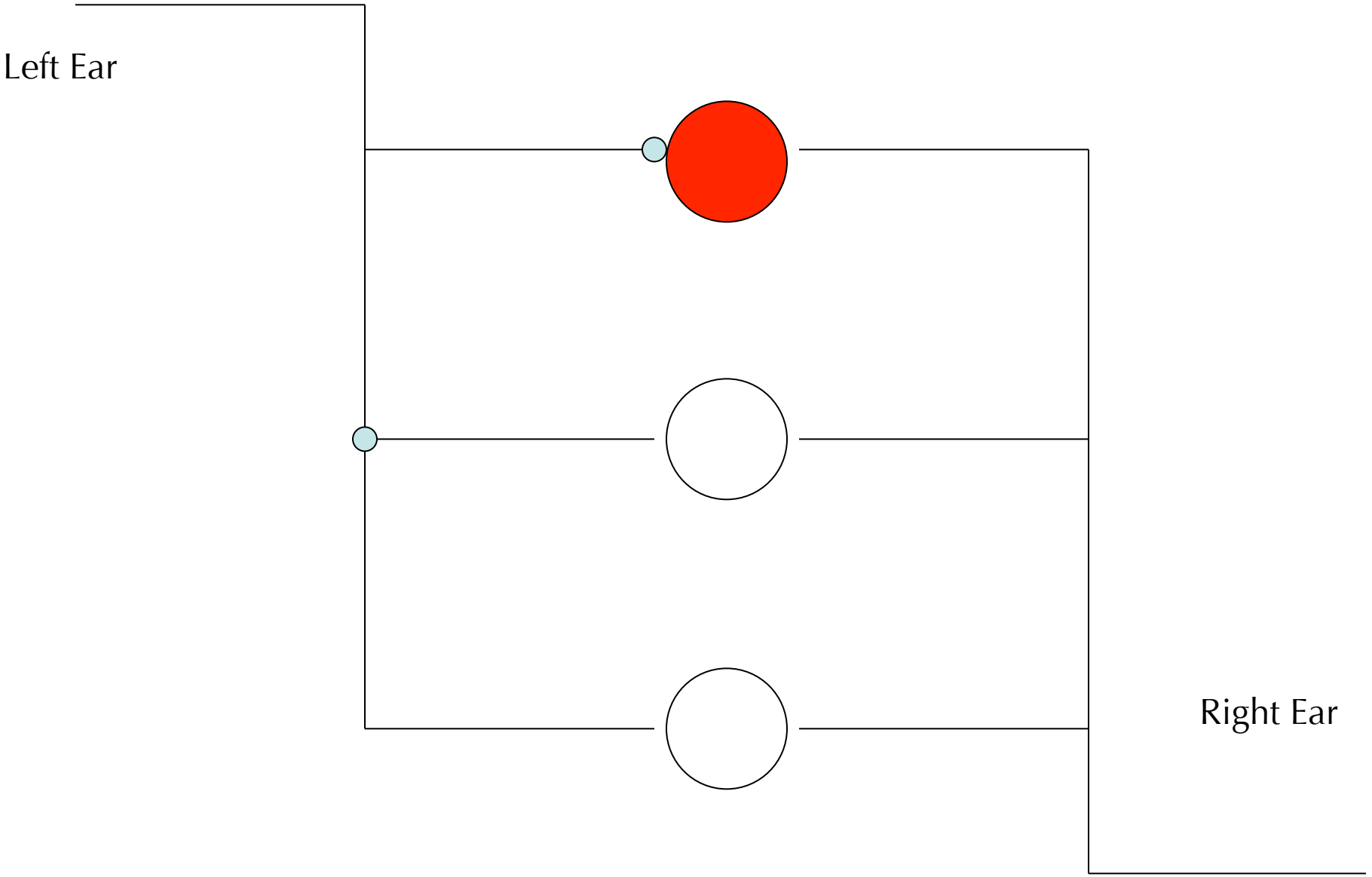
Left Ear
Right Ear

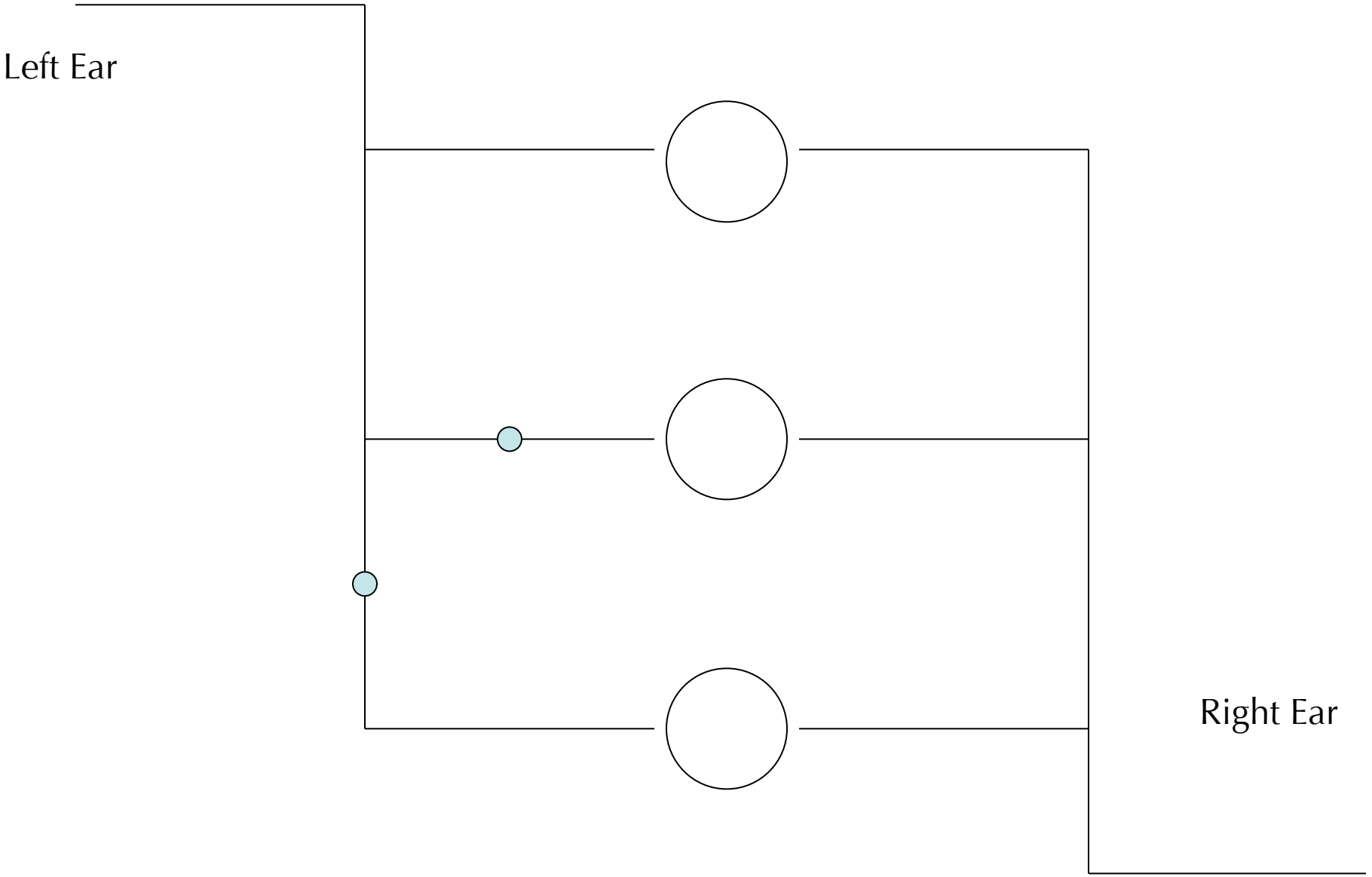
Left Ear
Right Ear

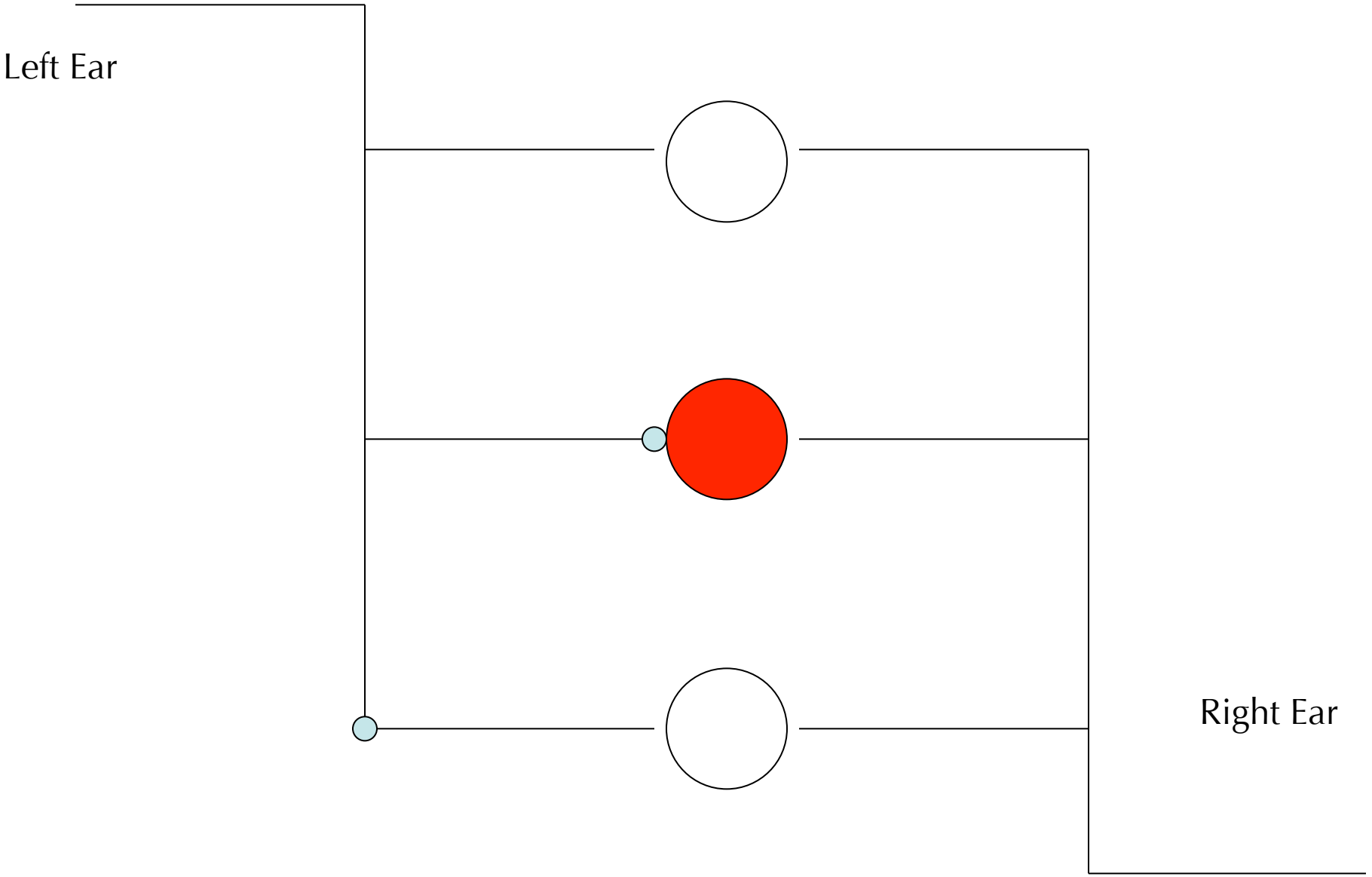
Left Ear
Right Ear

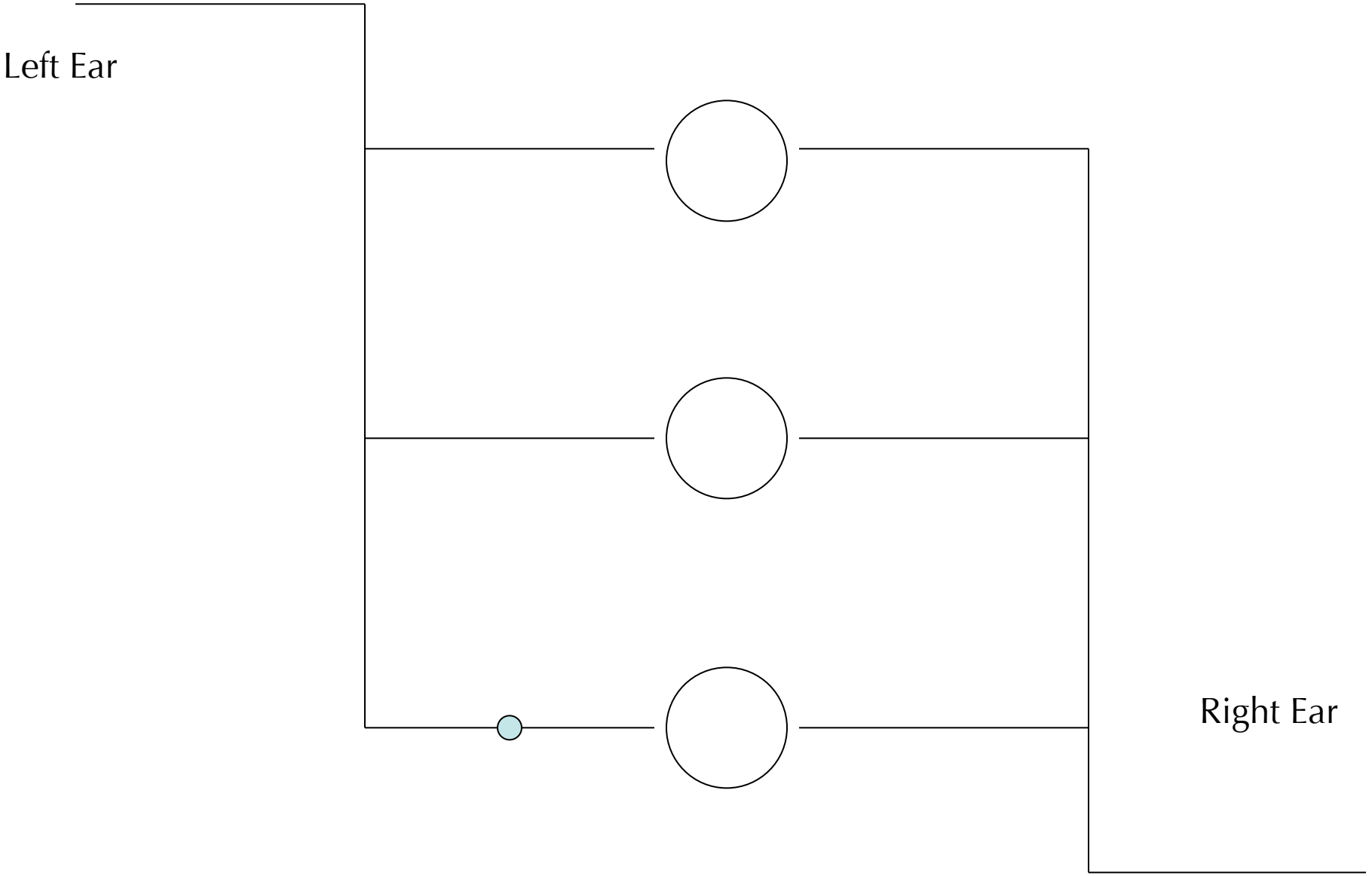
Left Ear
Right Ear

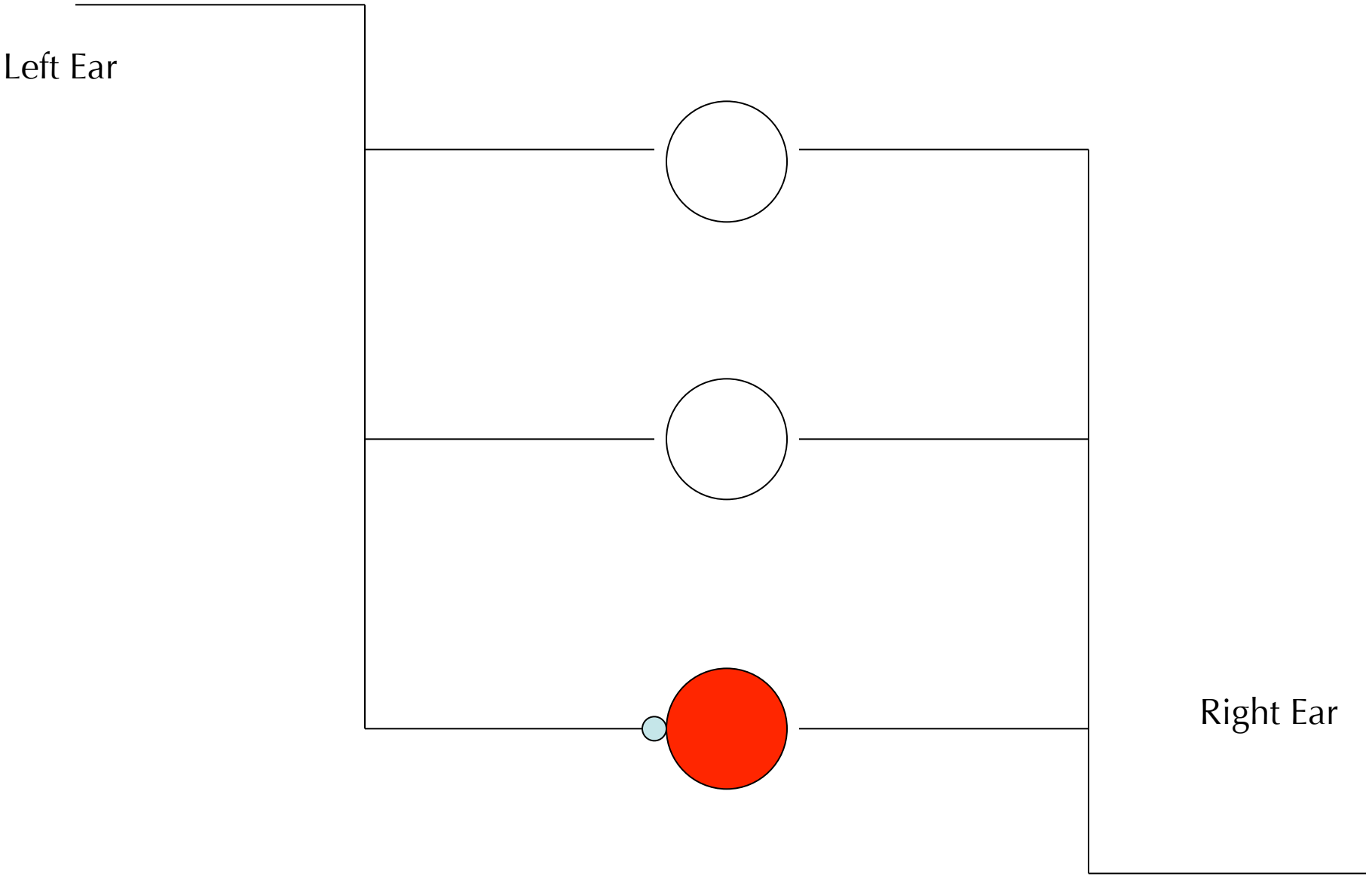
Left Ear
Right Ear

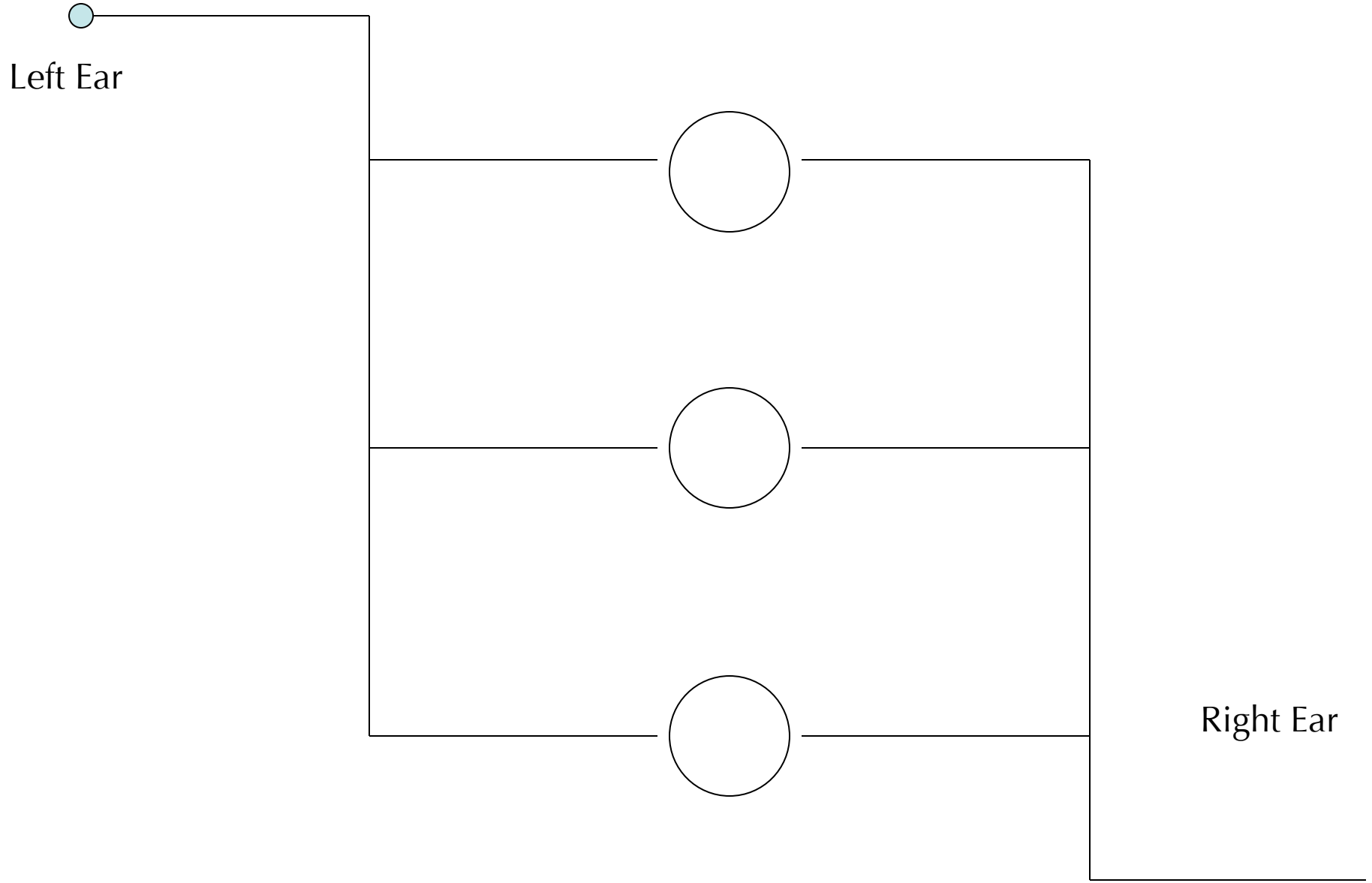
Left Ear
Right Ear

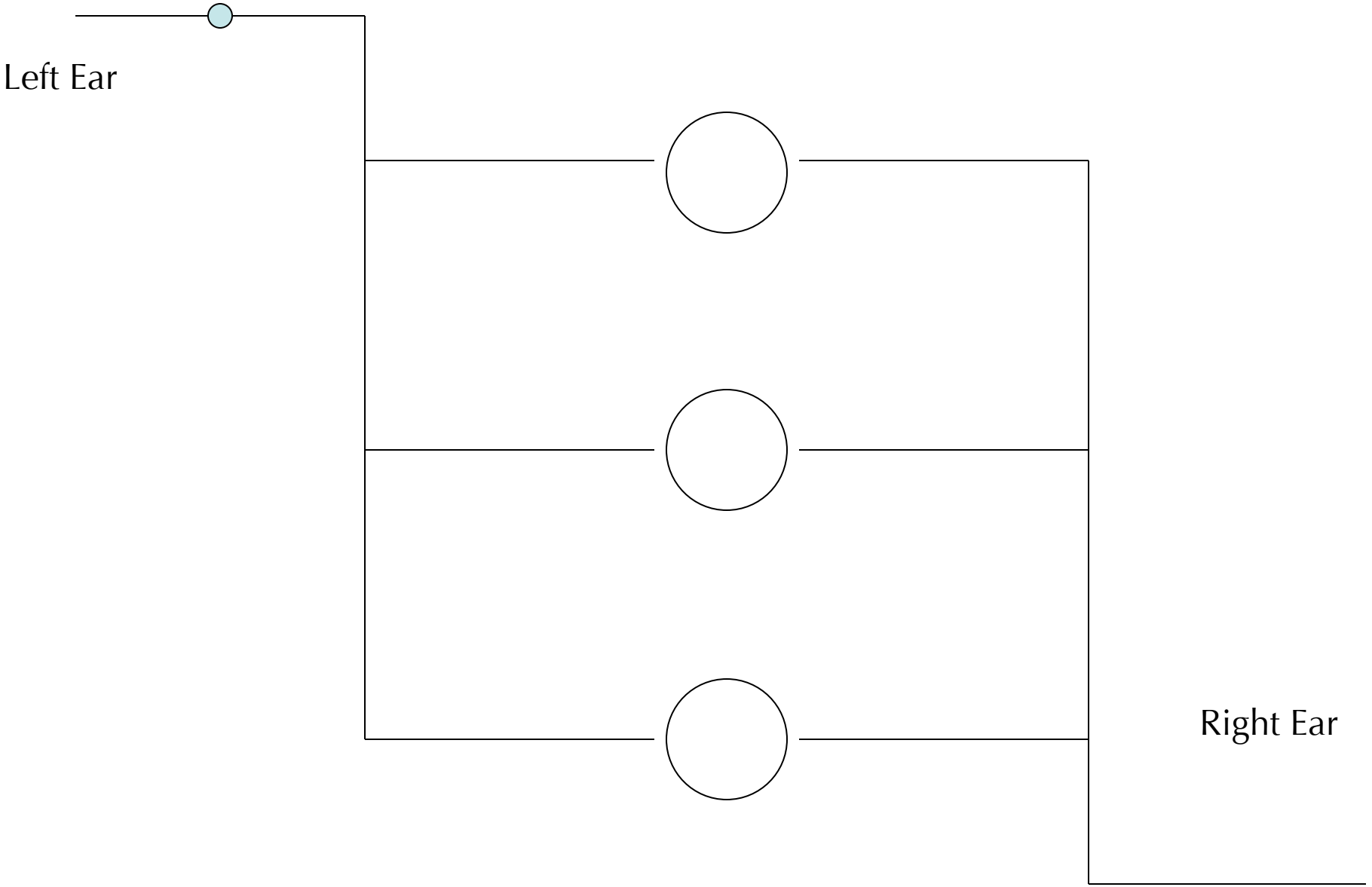
Left Ear
Right Ear

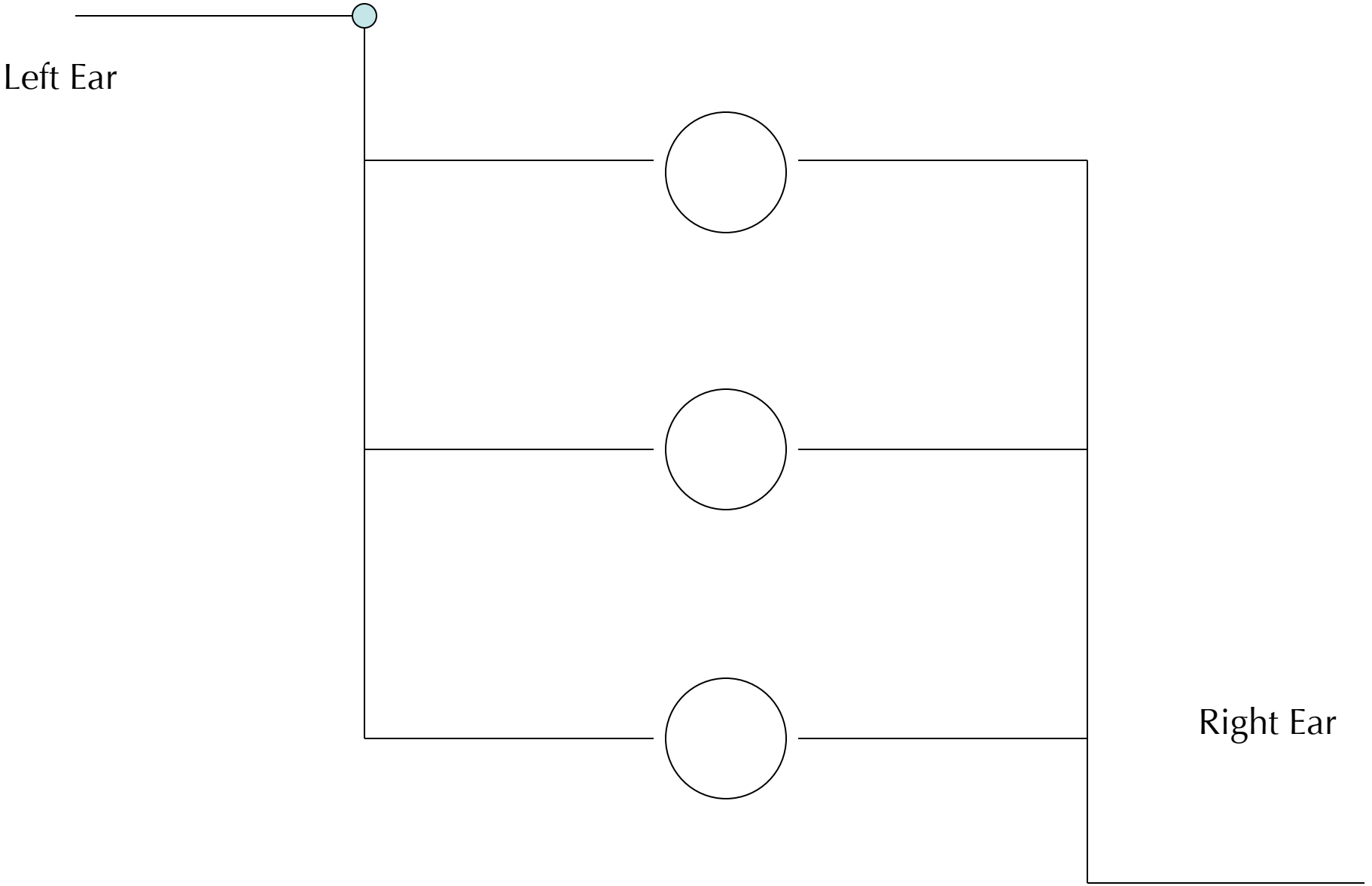
Left Ear
Right Ear

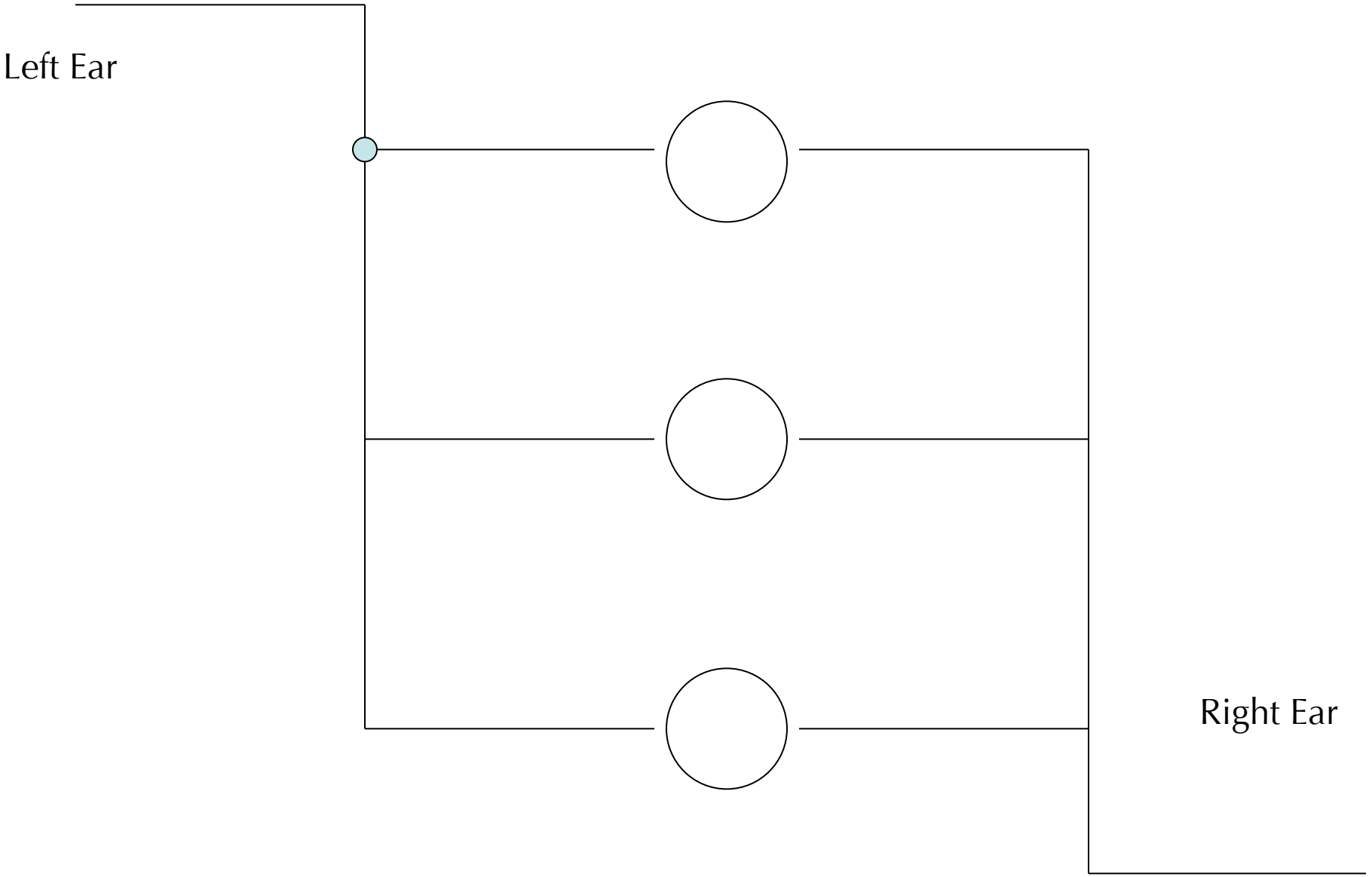
Left Ear
Right Ear

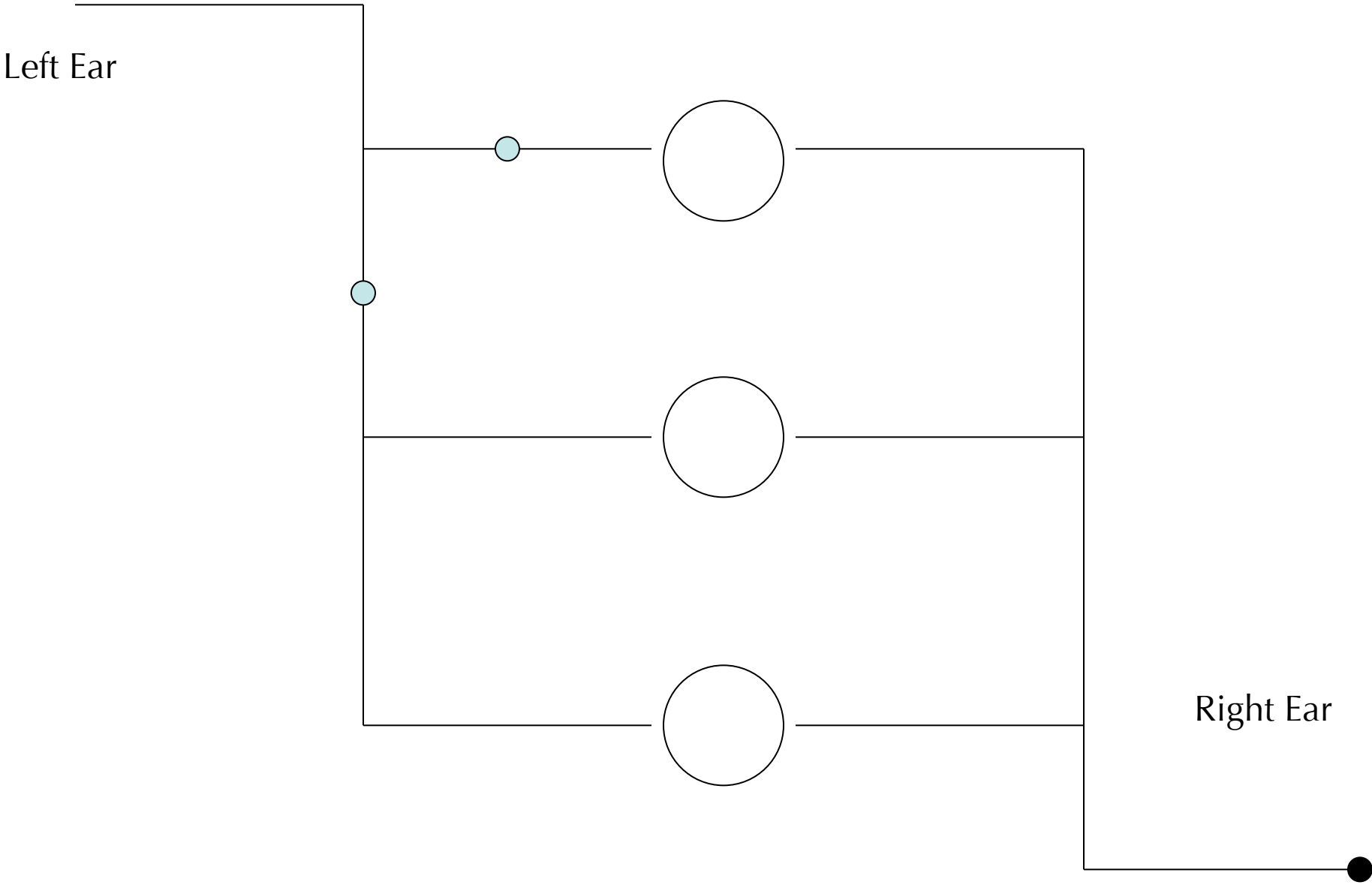
Left Ear
Right Ear

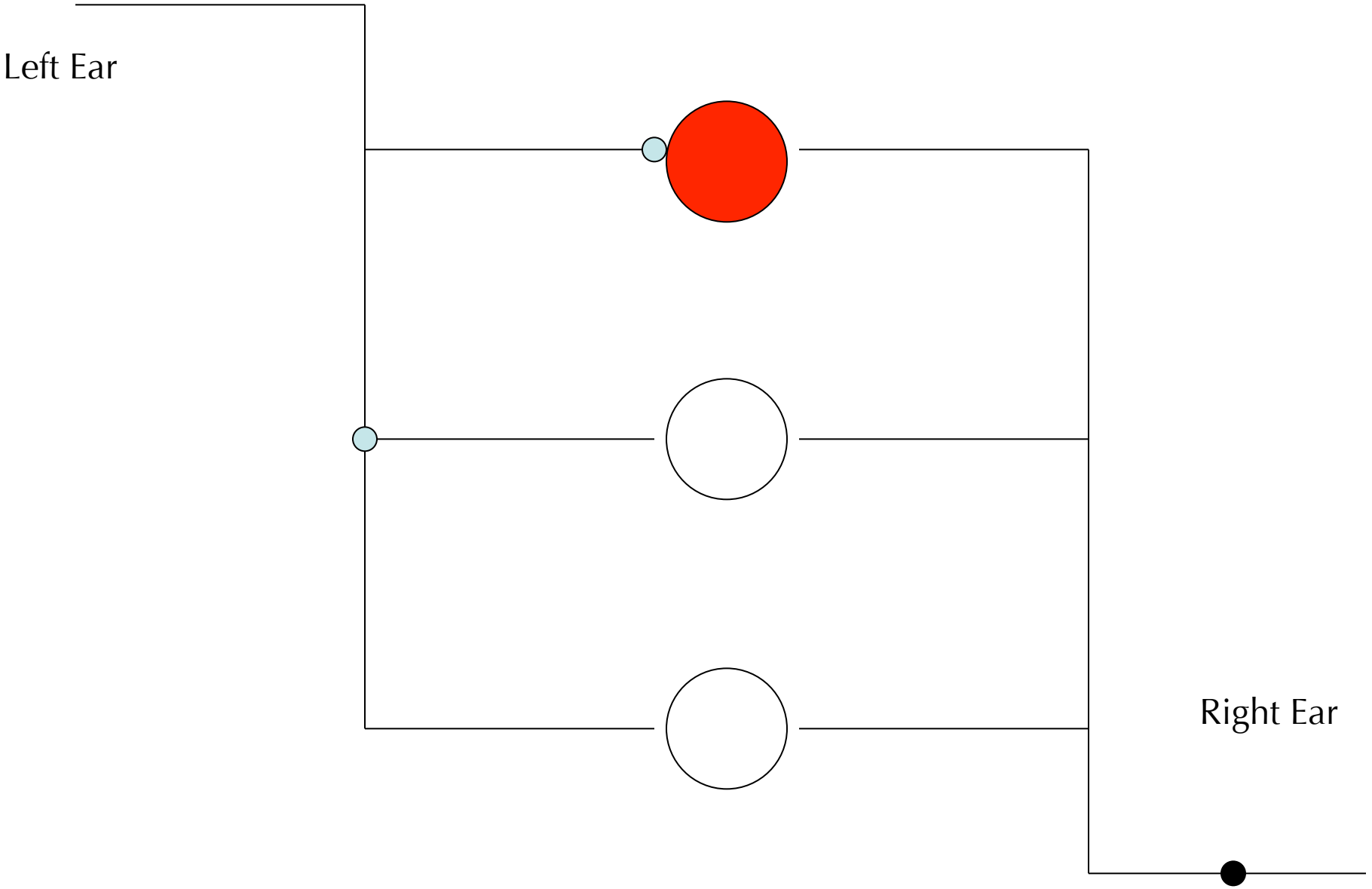
Left Ear
Right Ear

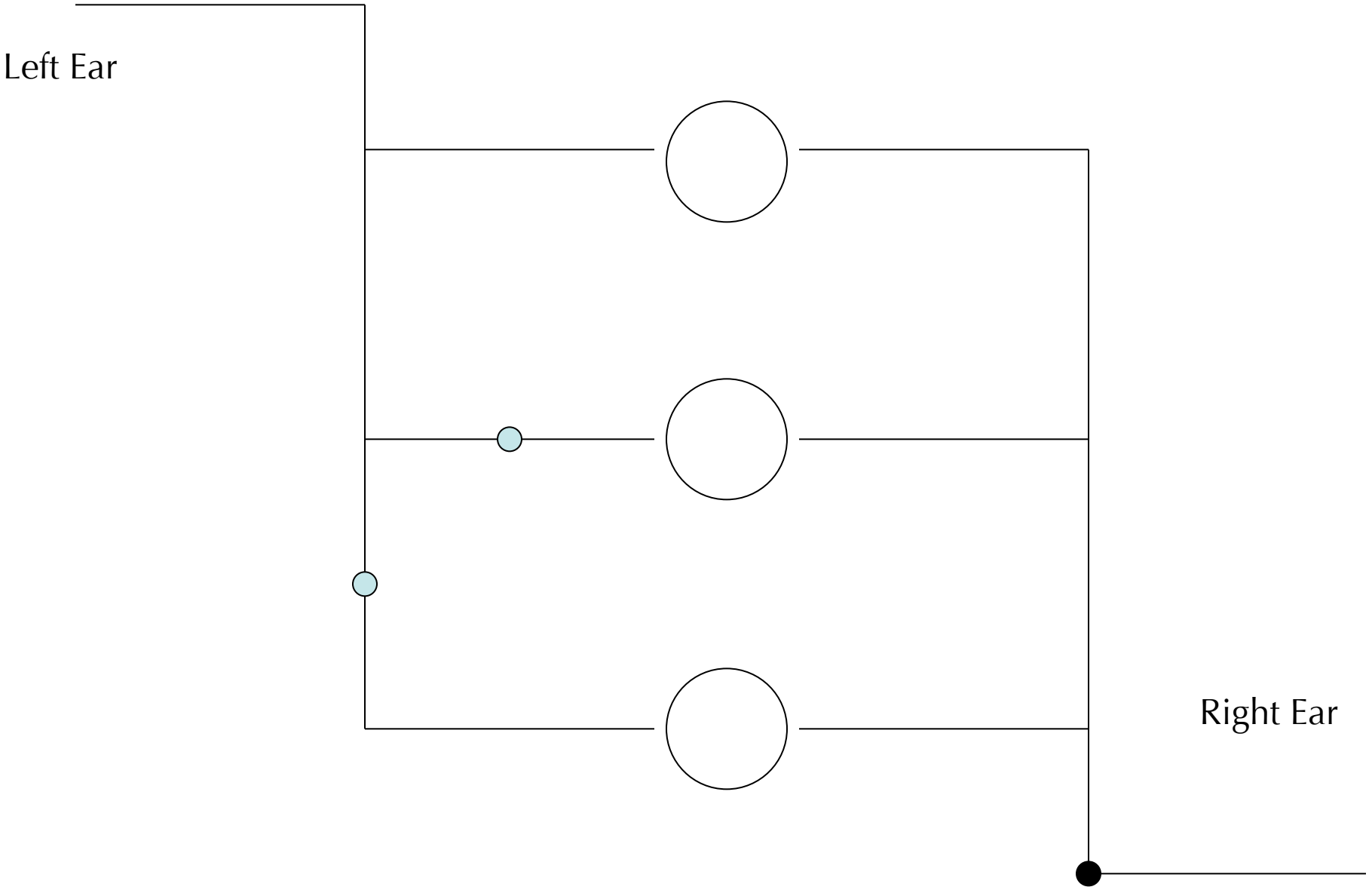
Left Ear
Right Ear

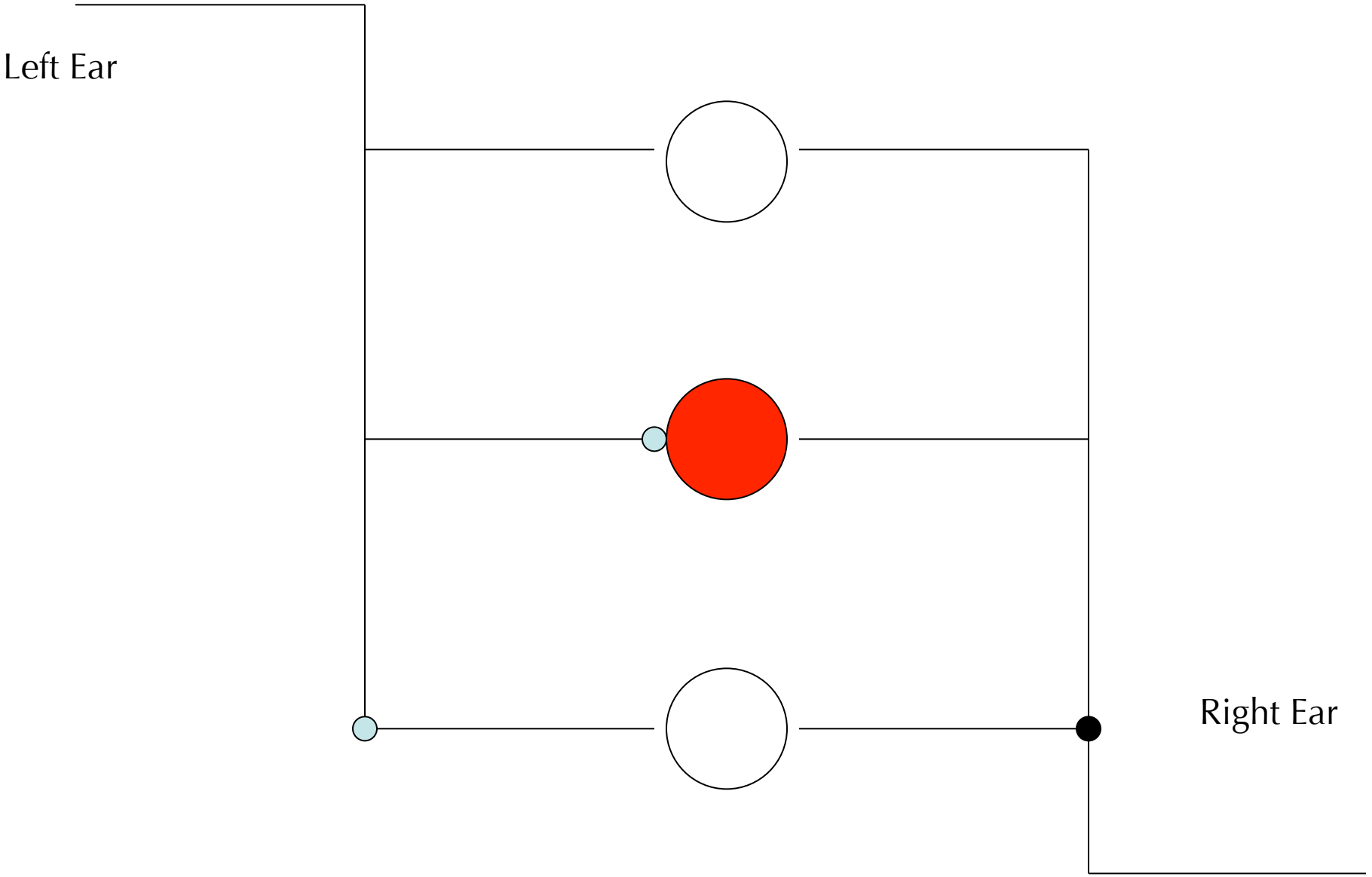
Left Ear
Right Ear

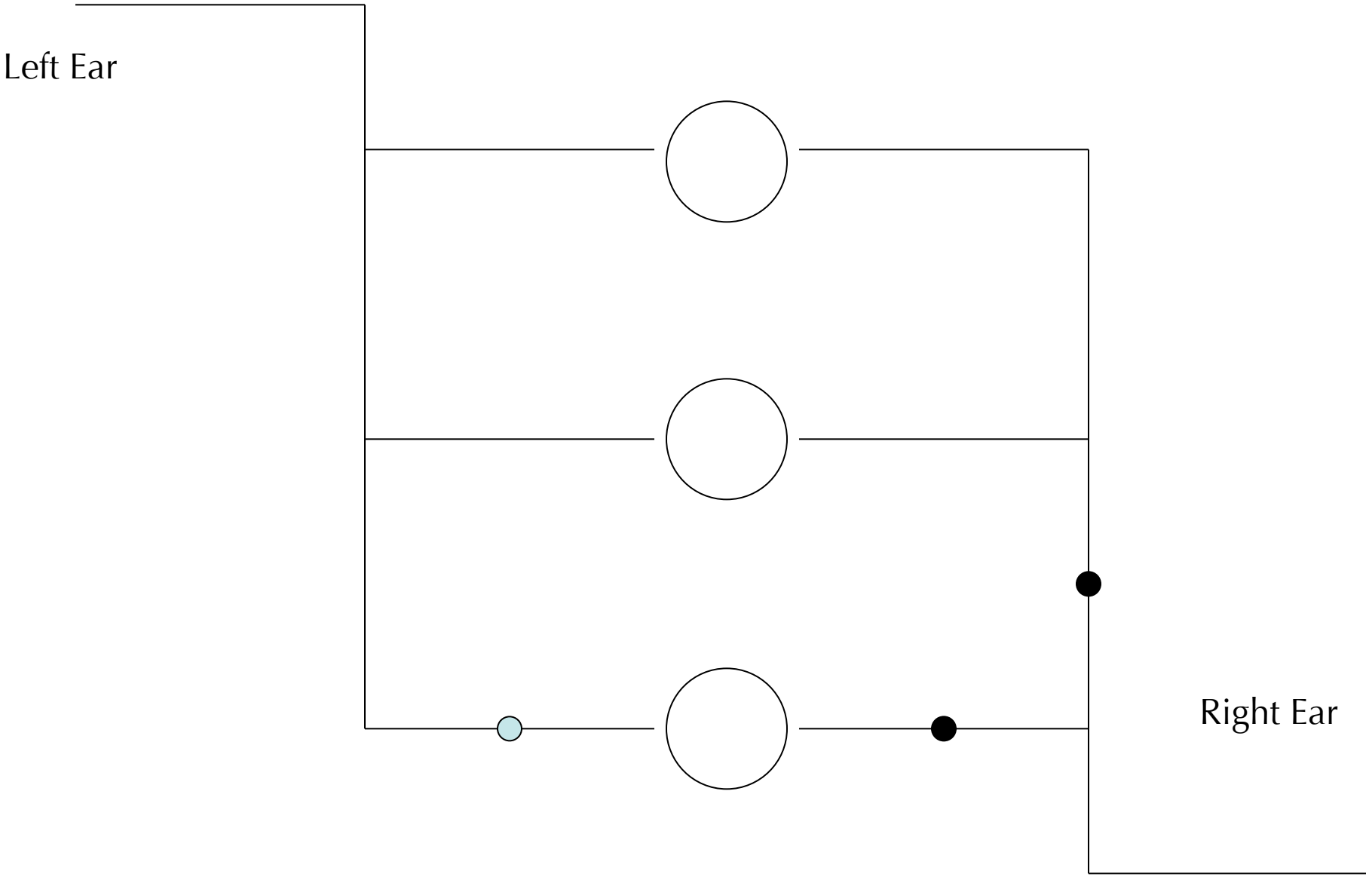
Left Ear
Right Ear

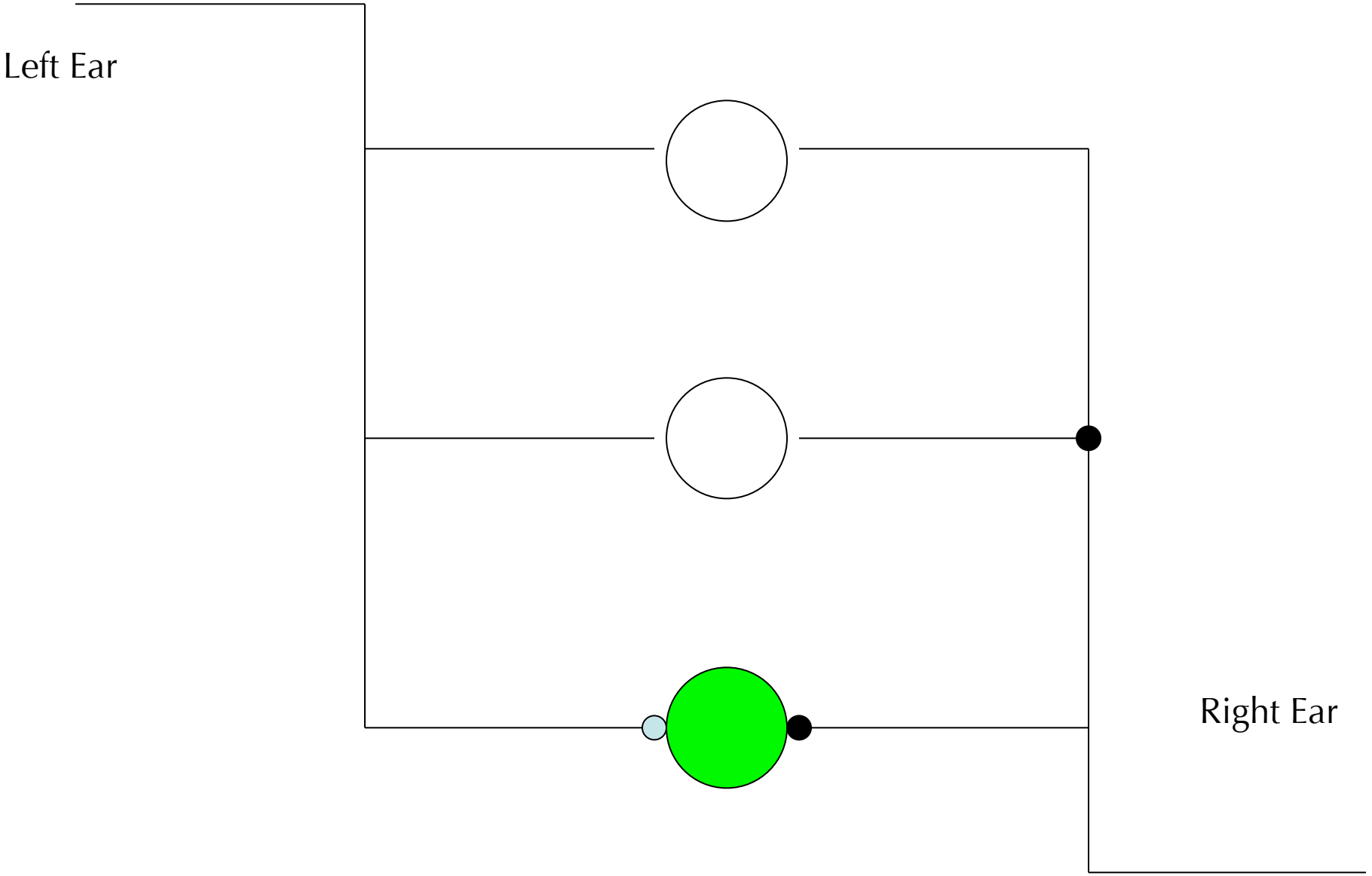
Left Ear
Right Ear

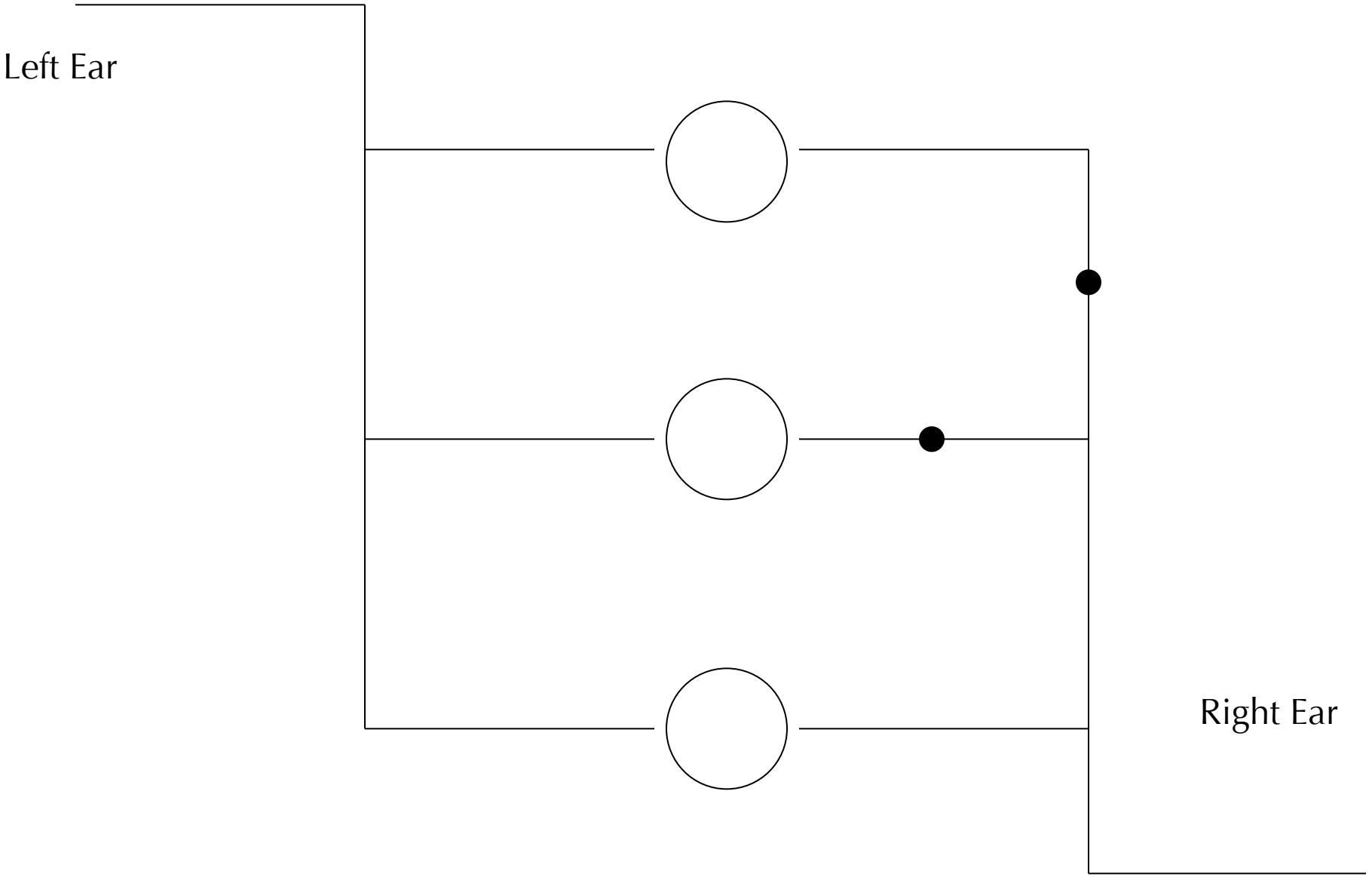
Left Ear
Right Ear

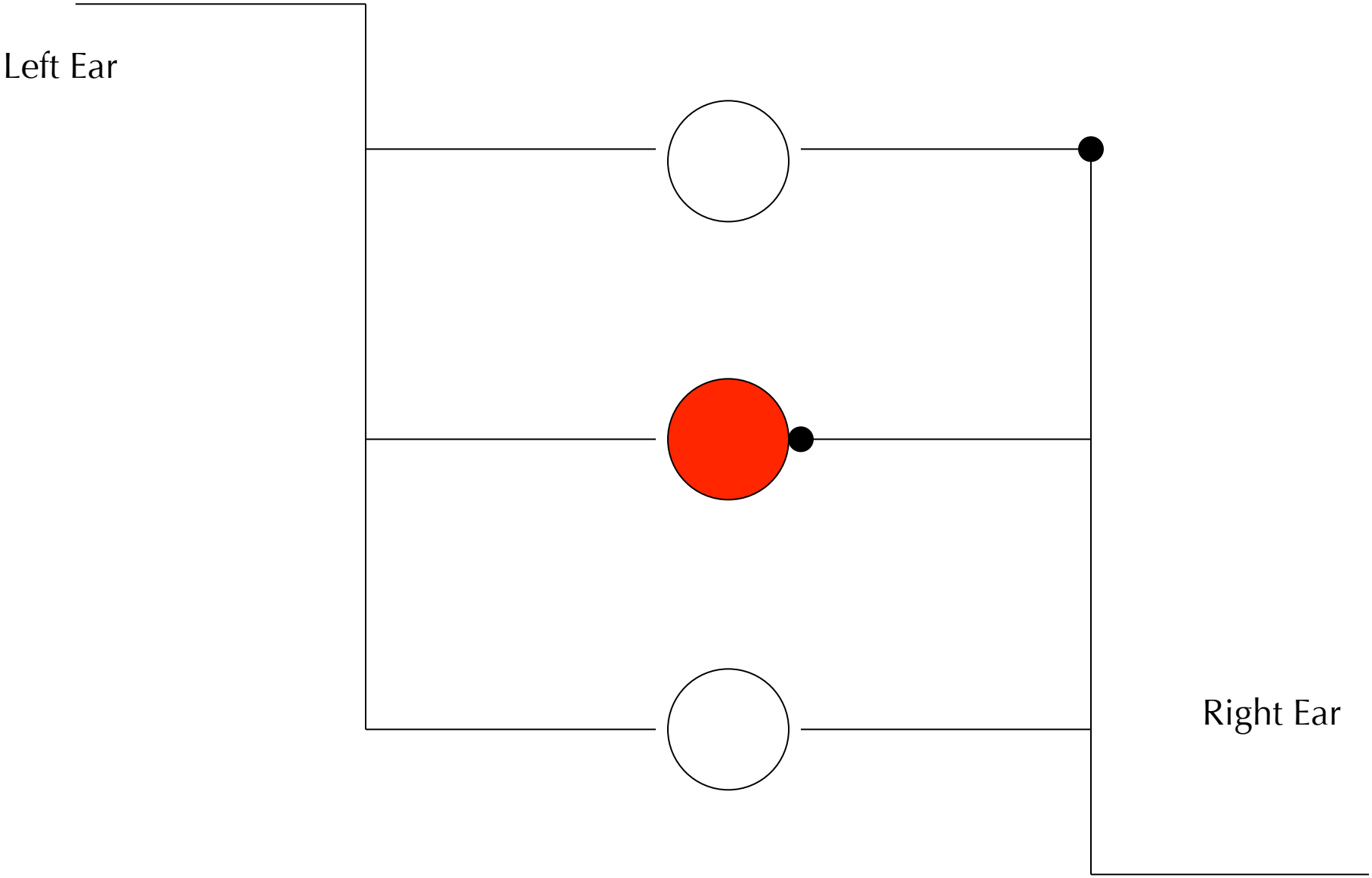
Left Ear
Right Ear

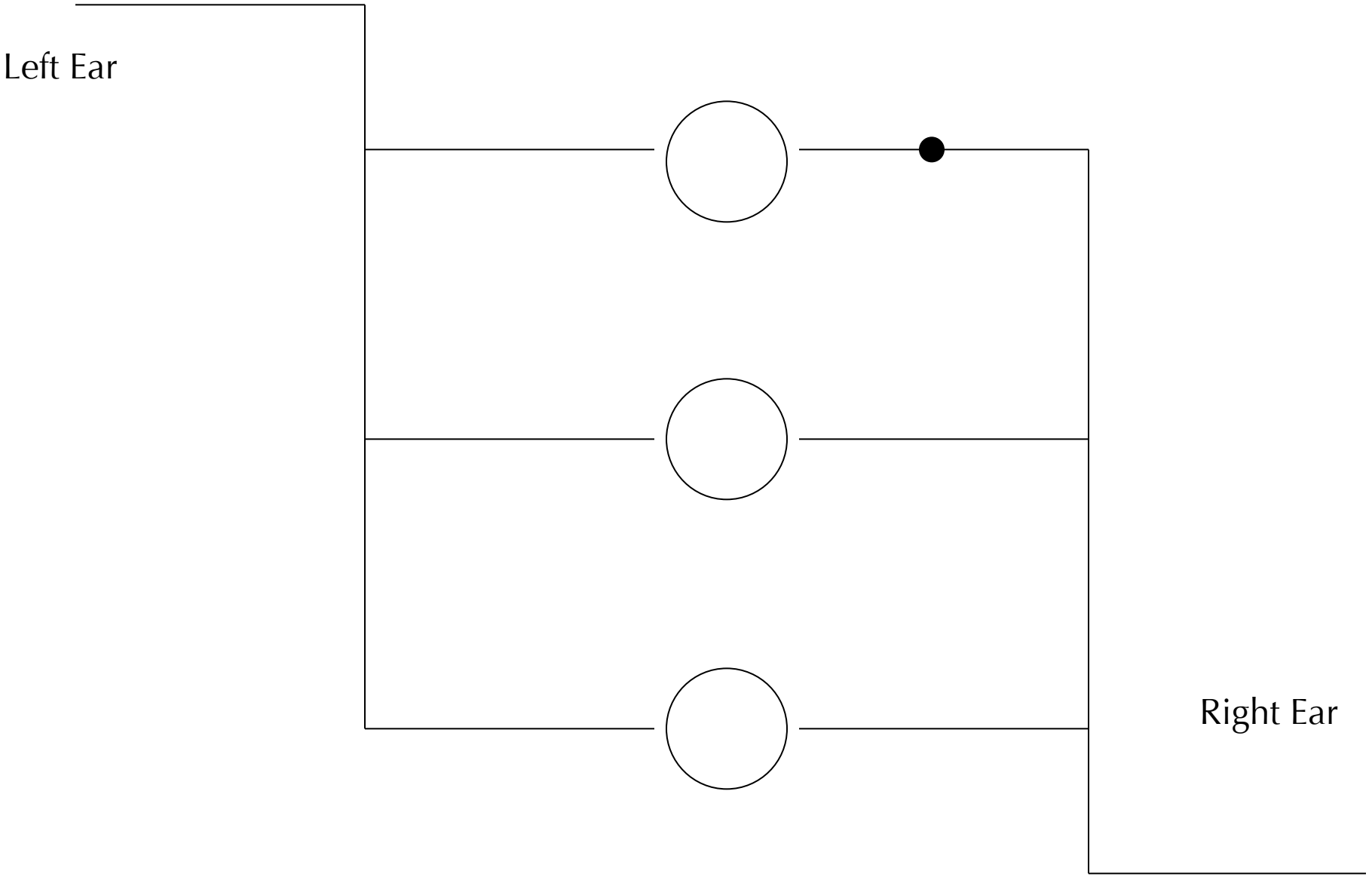
Left Ear
Right Ear

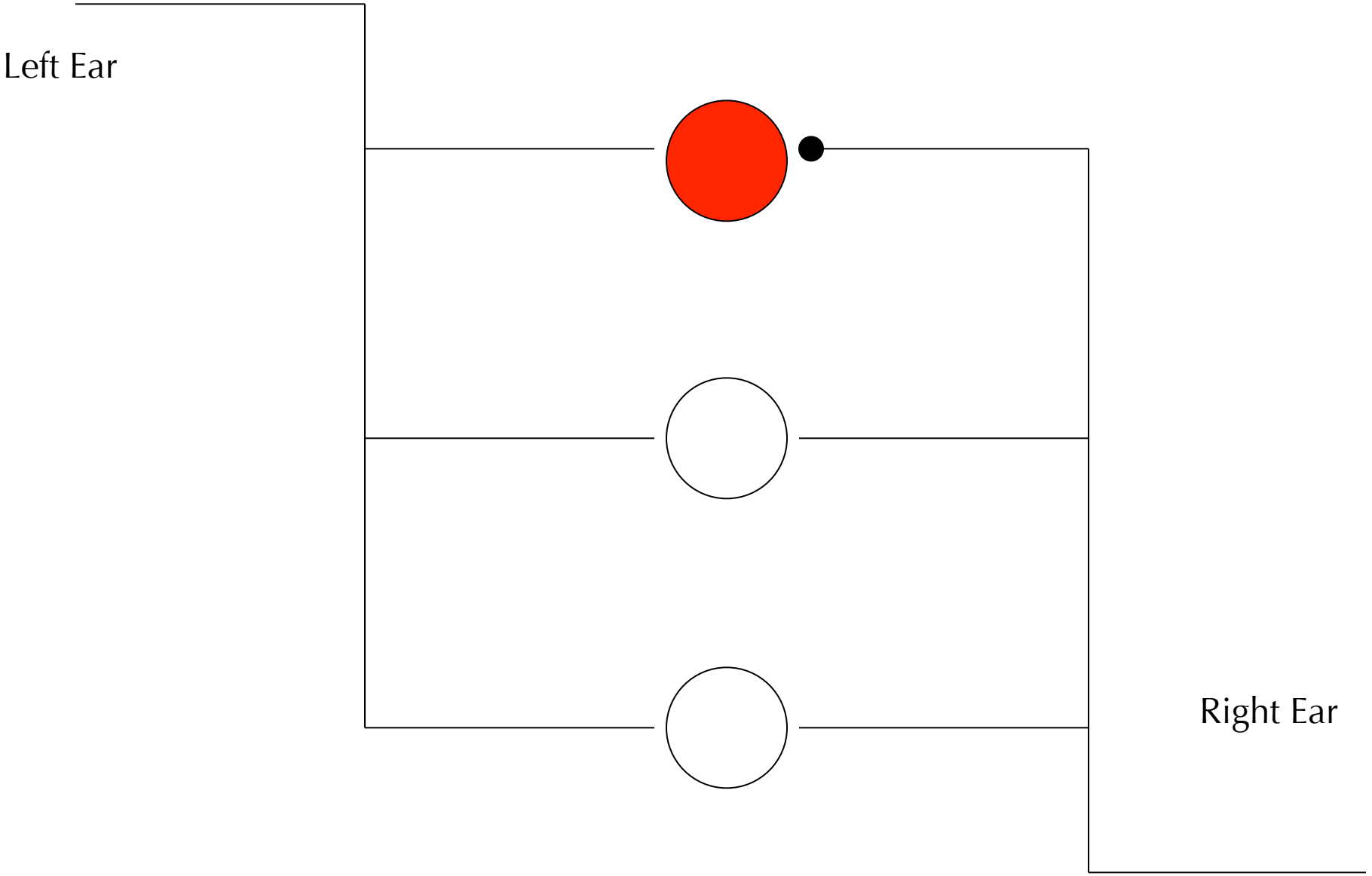
Left Ear
Right Ear

Discriminación de ITD a frecuencias altas

Discriminación de ITD a frecuencias altas

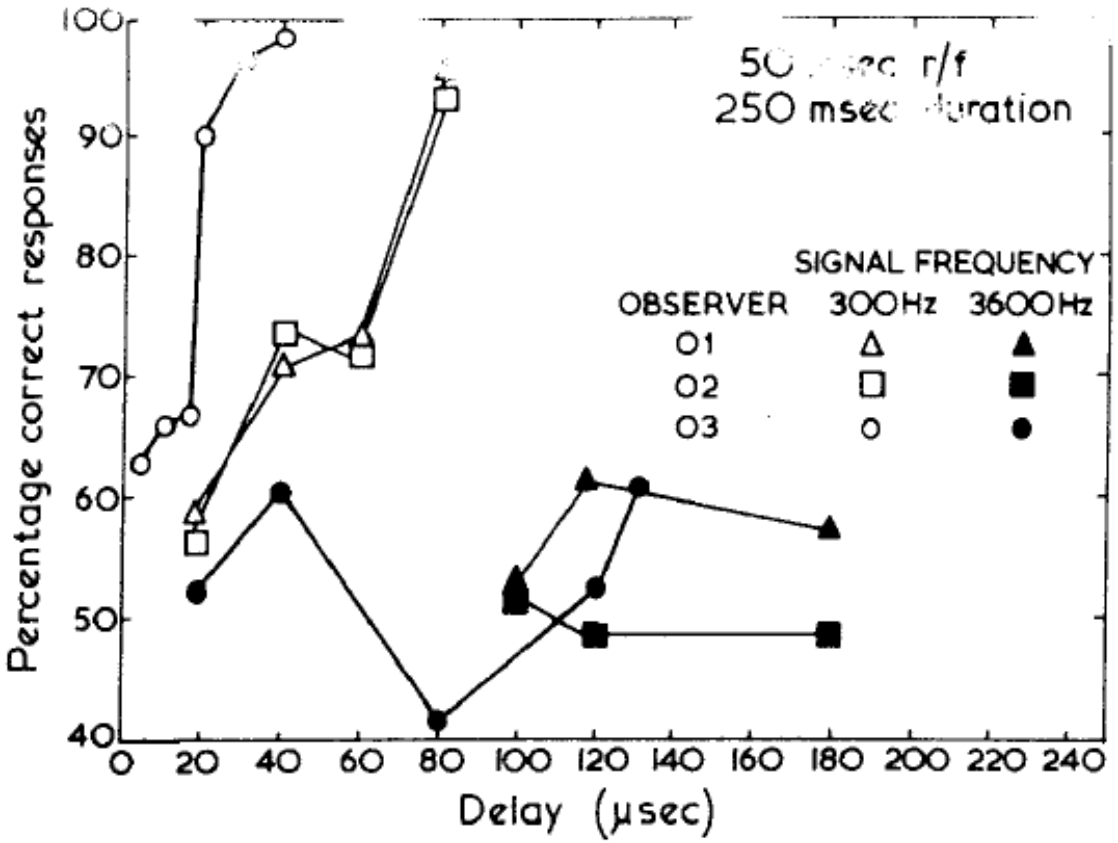

FIG. 1. The percentage of correct lateralization judgments as a function of the interaural delay in microseconds. The signals were 250-msec bursts of either a 300- or 3600-Hz sinusoid with a 50-msec rise-and-fall time. Each data point is based on 200 judgments by each of three observers.

Henning (1974)

Discriminación de ITD a frecuencias altas

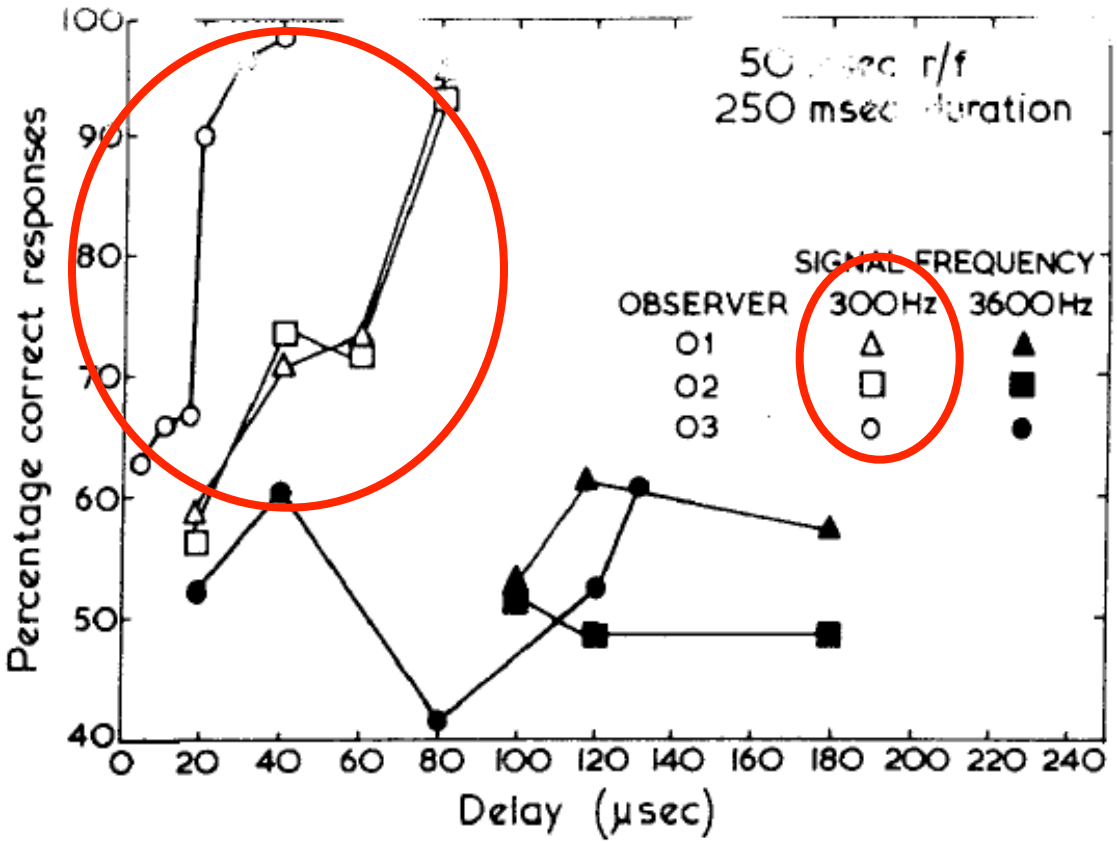

FIG. 1. The percentage of correct lateralization judgments as a function of the interaural delay in microseconds. The signals were 250-msec bursts of either a 300- or 3600-Hz sinusoid with a 50-msec rise-and-fall time. Each data point is based on 200 judgments by each of three observers.

Henning (1974)

Discriminación de ITD a frecuencias altas

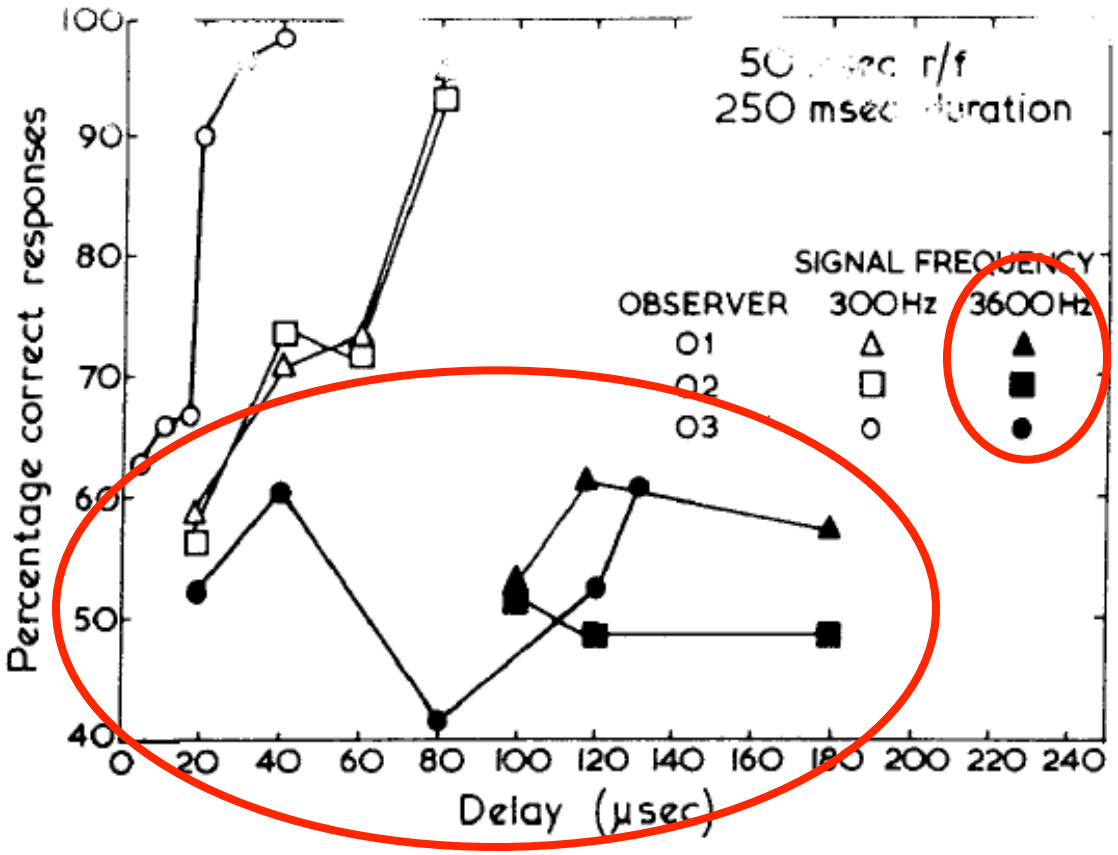

FIG. 1. The percentage of correct lateralization judgments as a function of the interaural delay in microseconds. The signals were 250-msec bursts of either a 300- or 3600-Hz sinusoid with a 50-msec rise-and-fall time. Each data point is based on 200 judgments by each of three observers.

Henning (1974)

Discriminación de ITD a frecuencias altas

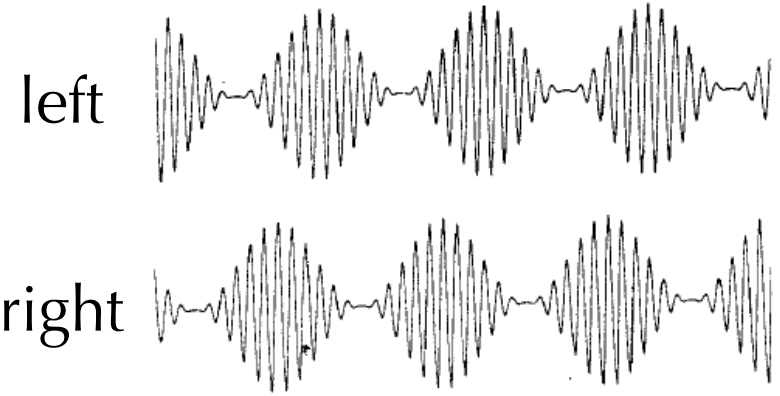

Figure 4. An example of sinusoidal AM presented dichotically. The interaural delay is of the entire waveform. A discussion of the differences between delays of the waveform, of the carrier only, or of the modulator only can be found in Henning (1980).

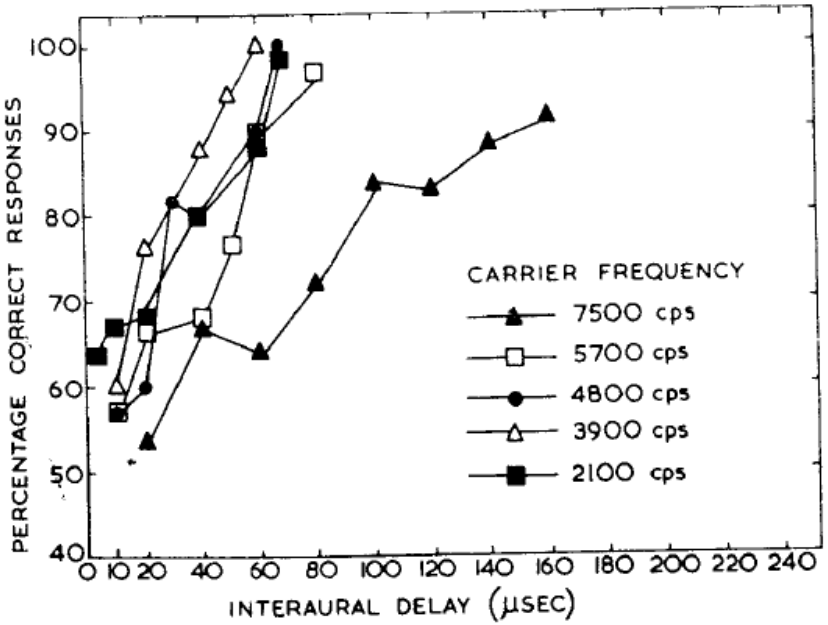

FIG. 4. The percentage of correct lateralization judgments as a function of the interaural delay in microseconds. The signals were 100% amplitude-modulated sinusoidal carriers at the carrier frequency shown. The modulation was also sinusoidal at 300 Hz. The entire signal waveform was delayed. Data points are based on 200 judgments by Observer 3.

Henning (1974)

Discriminación de ITD y pérdidas auditivas

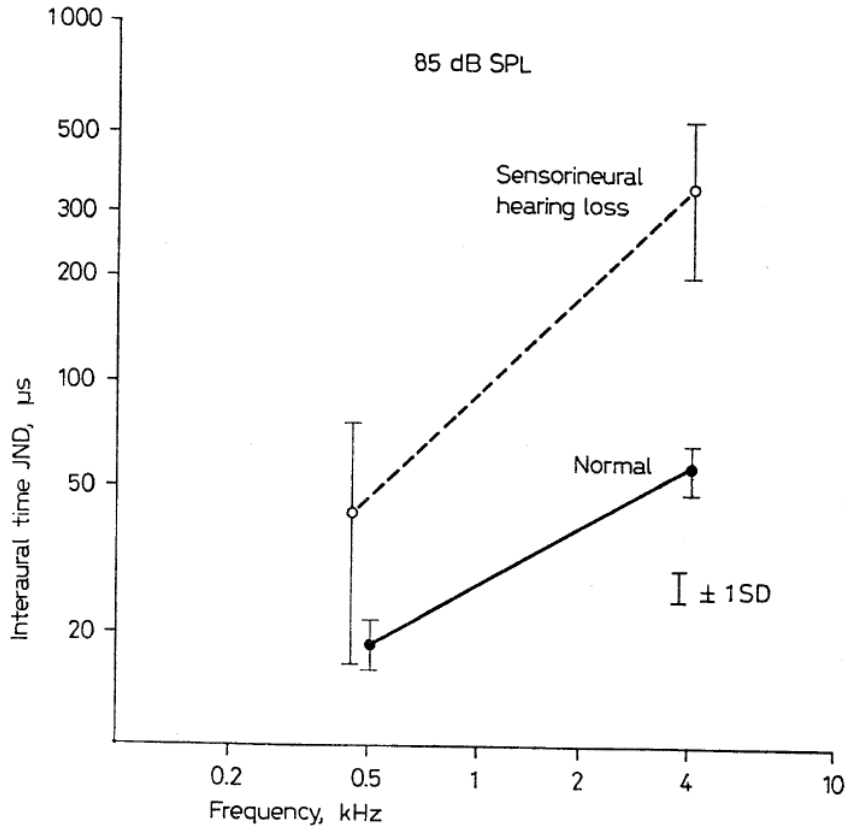

Fig. 3. Mean interaural time JNDs for the normally hearing and sensorineural-impaired listeners with the low- and high-frequency band of noise presented at 85 dB SPL.

Hawkins and Wightman (1980)

Cono de confusión

Cono de confusión

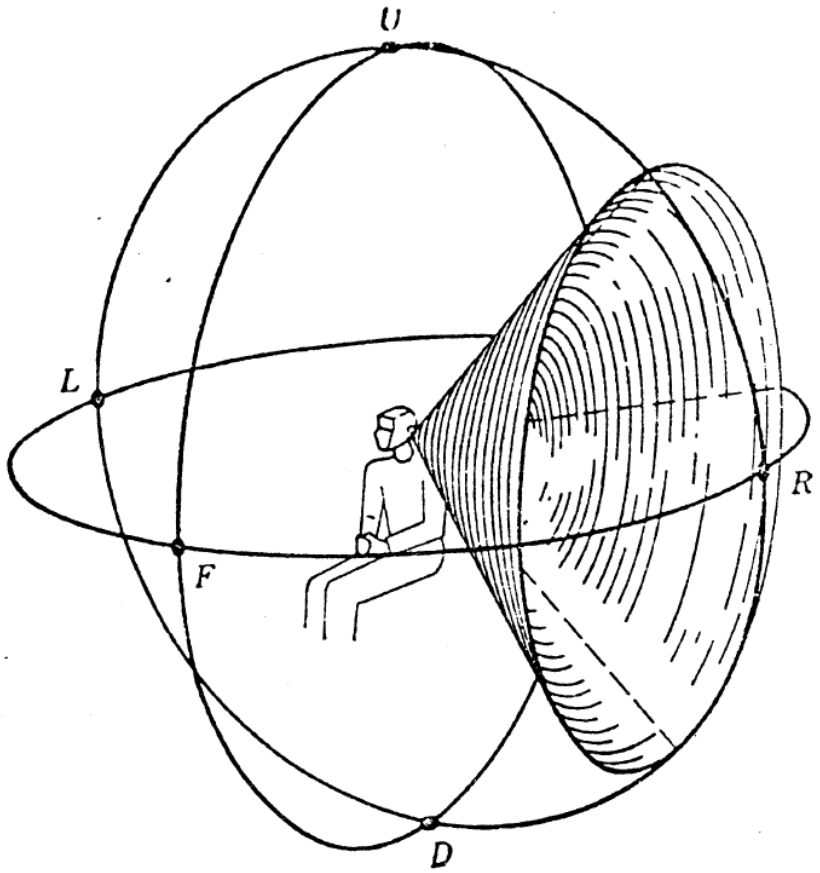

FIGURE 12 A Cone of Confusion for a Stationary Listener on the Assumption that His Head may be Approximated by a Sphere without Pinnae. A sound at any position could not be distinguished from a sound at any other position on the same conical surface. (Reproduced with permission from Boring, E. G., H. S. Langfeld, and H. P. Weld. *Foundations of Psychology*. New York: J. Wiley, 1948, p. 337.)

Cono de confusión

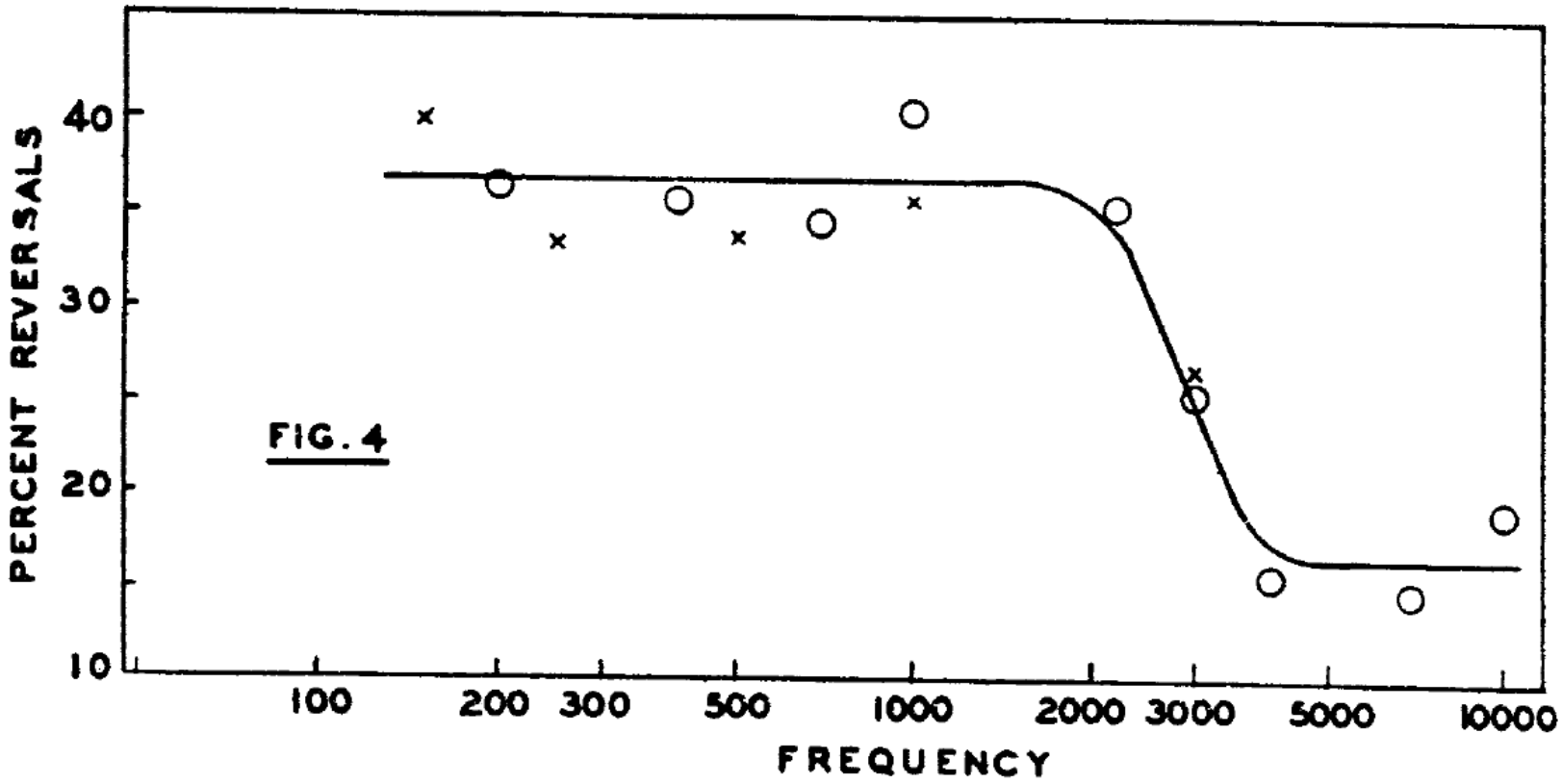

FIG. 4. PERCENTAGE REVERSALS OF THE FRONT-BACK QUADRANTS
The crosses are for the data obtained in 1933, the circles for 1934. The critical region is at about 3000 cycles; cf. Fig. 2.

Stevens and Newman (1936)

Head related transfer function (HRTF)

Head related transfer function (HRTF)

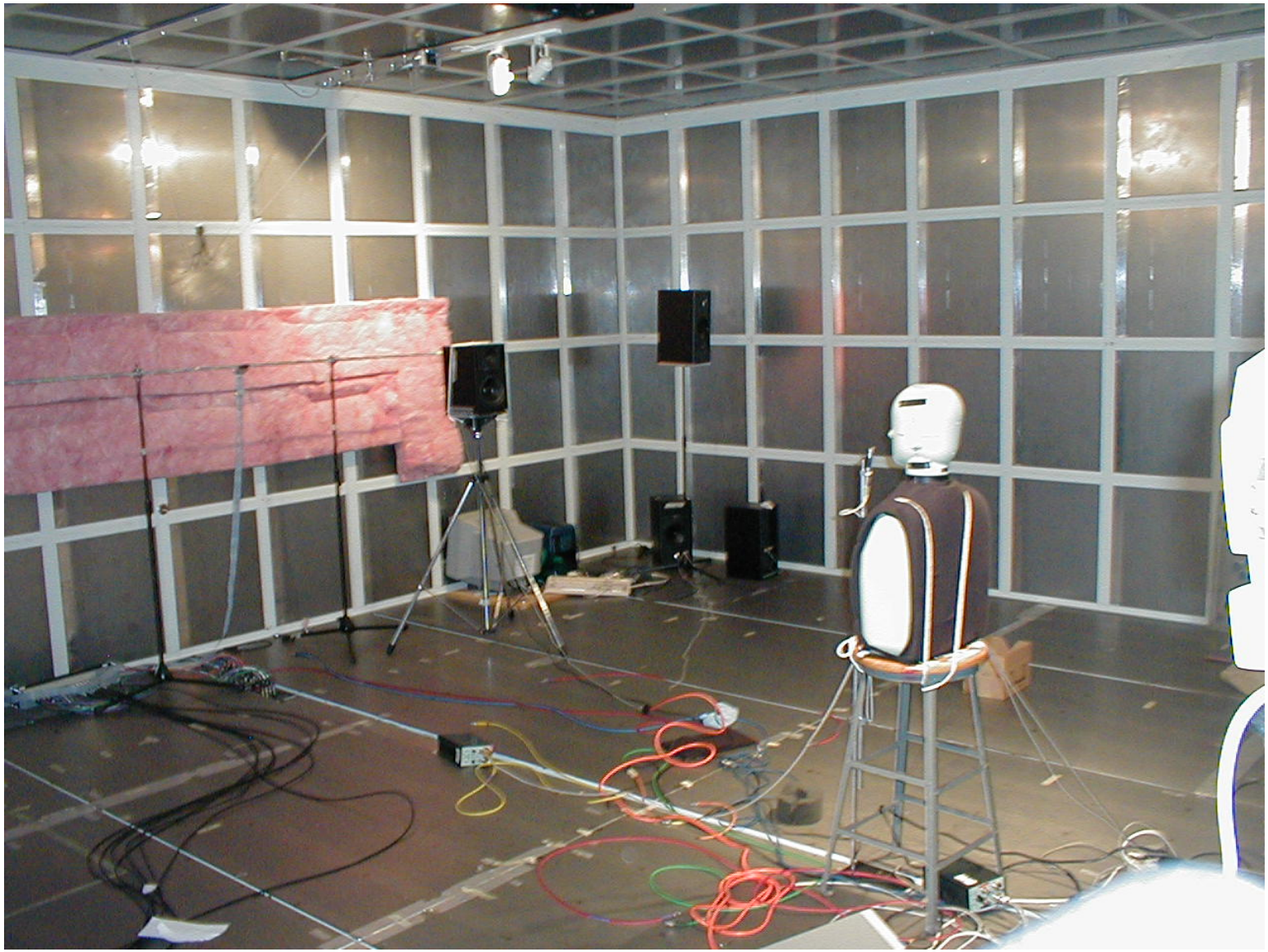

Wightman and Kistler (1989)

Head related transfer function (HRTF)

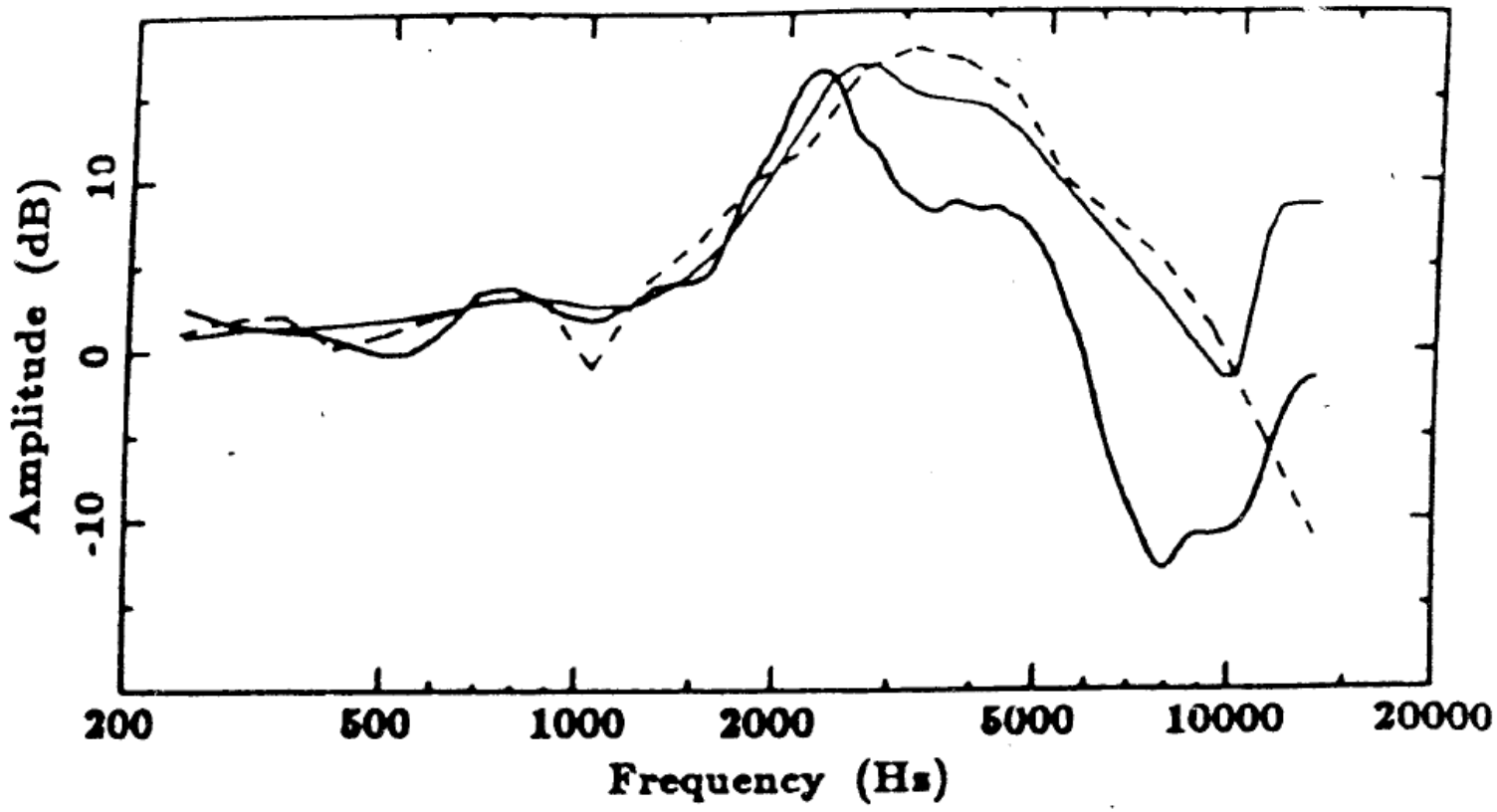

FIG. 6. Average HRTF for a source at 0-deg azimuth, 0-deg elevation, from the ten subjects in the current study (dark solid line) compared to data from the studies of Shaw (1974, light solid line) and Mehrgardt and Mellert (1977, dashed line.)

Wightman and Kistler (1989)

Head related transfer function (HRTF)

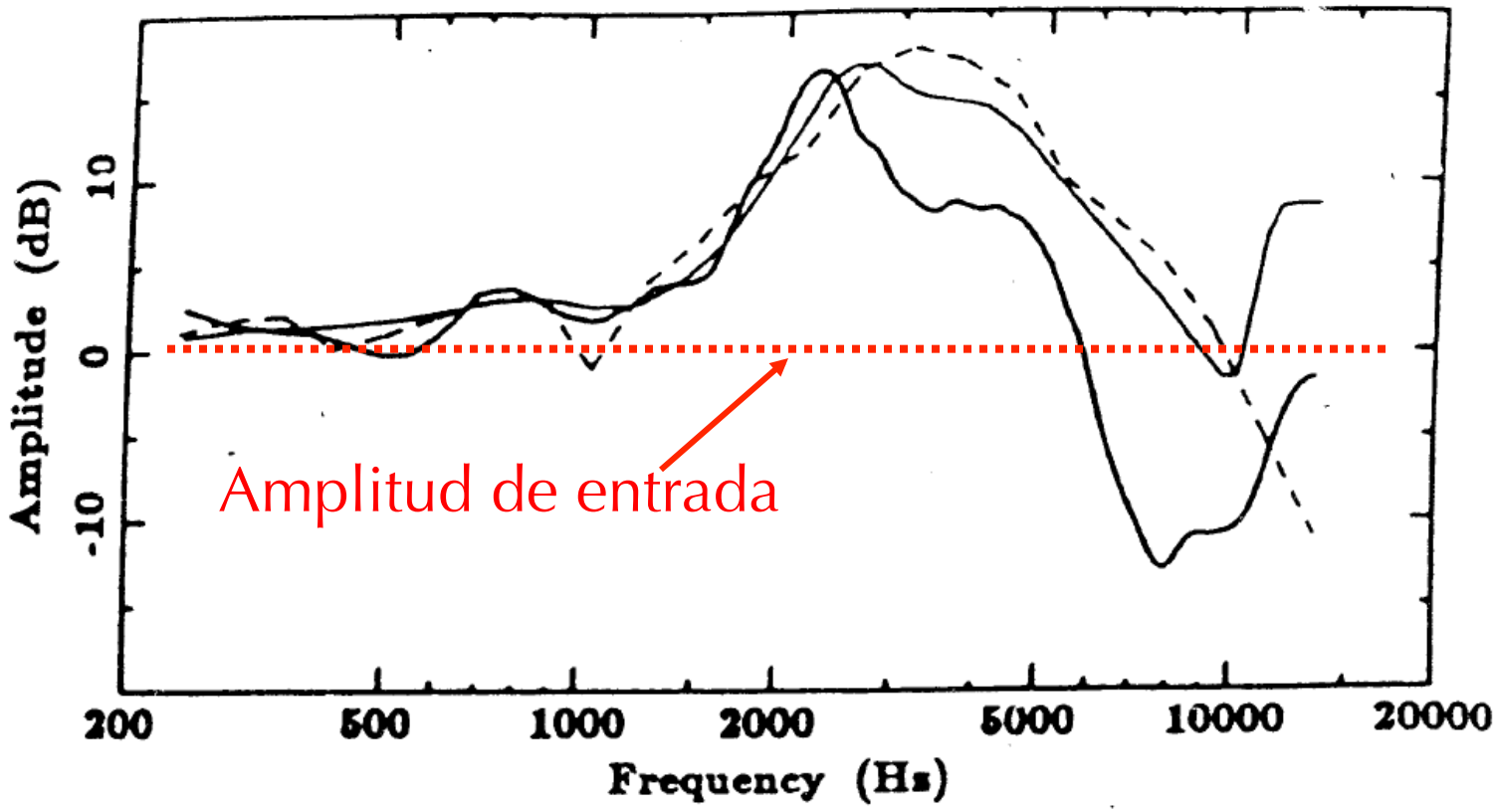

FIG. 6. Average HRTF for a source at 0-deg azimuth, 0-deg elevation, from the ten subjects in the current study (dark solid line) compared to data from the studies of Shaw (1974, light solid line) and Mehrgardt and Mellert (1977, dashed line.)

Wightman and Kistler (1989)

Head related transfer function (HRTF)

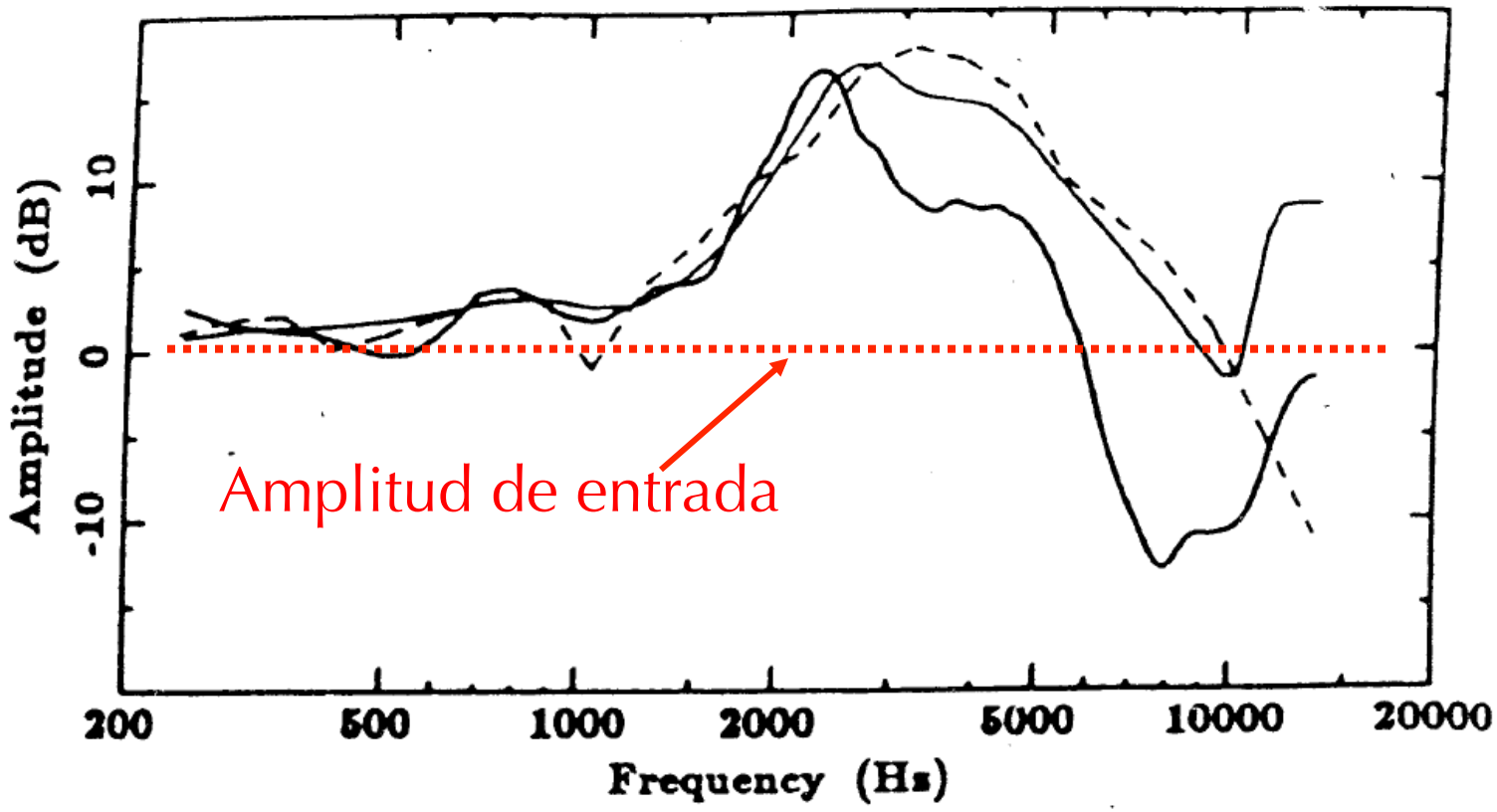

FIG. 6. Average HRTF for a source at 0-deg azimuth, 0-deg elevation from the ten subjects in the current study (dark solid line) compared to data from the studies of Shaw (1974, light solid line) and Mehrgardt and Mellert (1977, dashed line.)

Wightman and Kistler (1989)

Head related transfer function (HRTF)

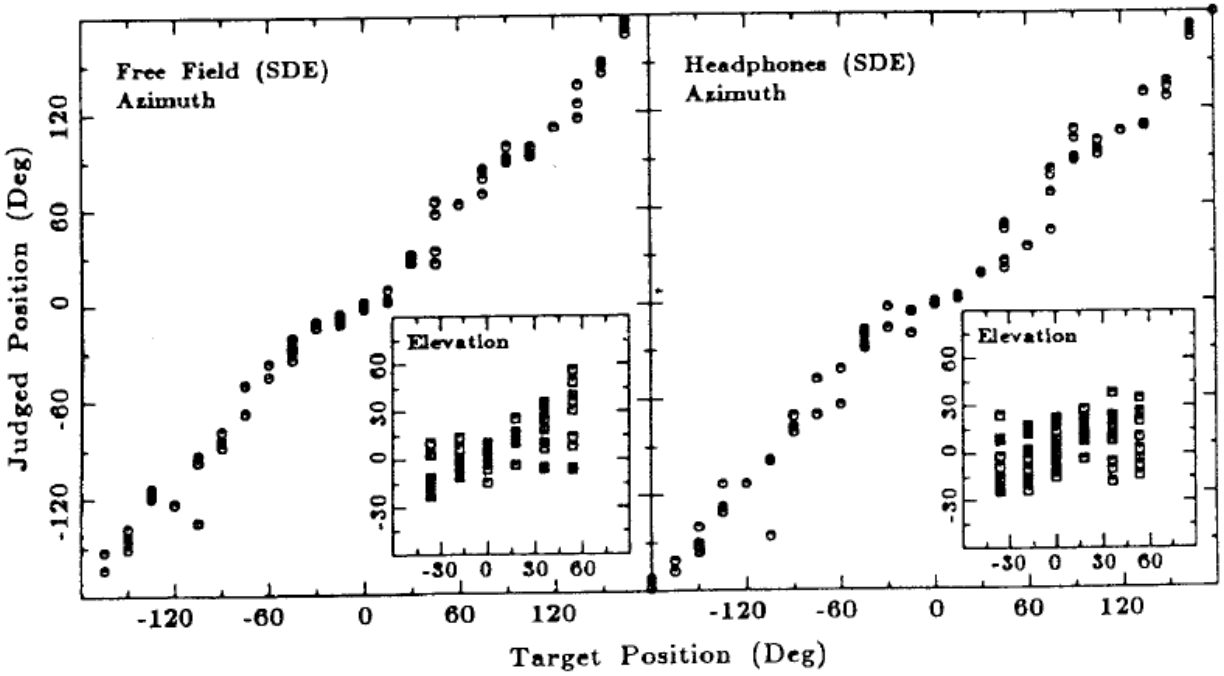

FIG. 2. Scatterplots of actual source azimuth (and, in the insets, elevation) versus judged source azimuth for subject SDE in both the free-field and headphone conditions. Each data point represents the centroid of at least six judgments. All 72 source positions are represented in each panel. Thus data from six different source elevations are combined in the azimuth panels, and data from 24 different azimuths are combined in the elevation panels. Note that the scale is the same for azimuth and elevation plots.

Wightman and Kistler (1989)

Head related transfer function (HRTF)

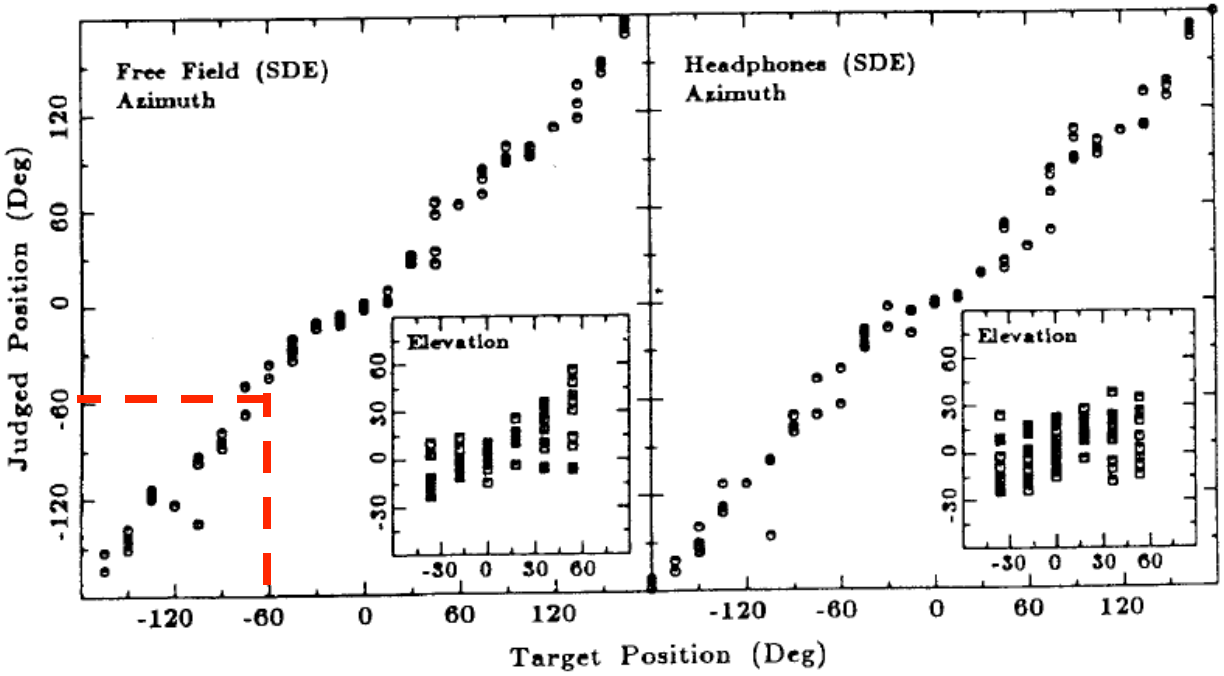

FIG. 2. Scatterplots of actual source azimuth (and, in the insets, elevation) versus judged source azimuth for subject SDE in both the free-field and headphone conditions. Each data point represents the centroid of at least six judgments. All 72 source positions are represented in each panel. Thus data from six different source elevations are combined in the azimuth panels, and data from 24 different azimuths are combined in the elevation panels. Note that the scale is the same for azimuth and elevation plots.

Wightman and Kistler (1989)

Head related transfer function (HRTF)

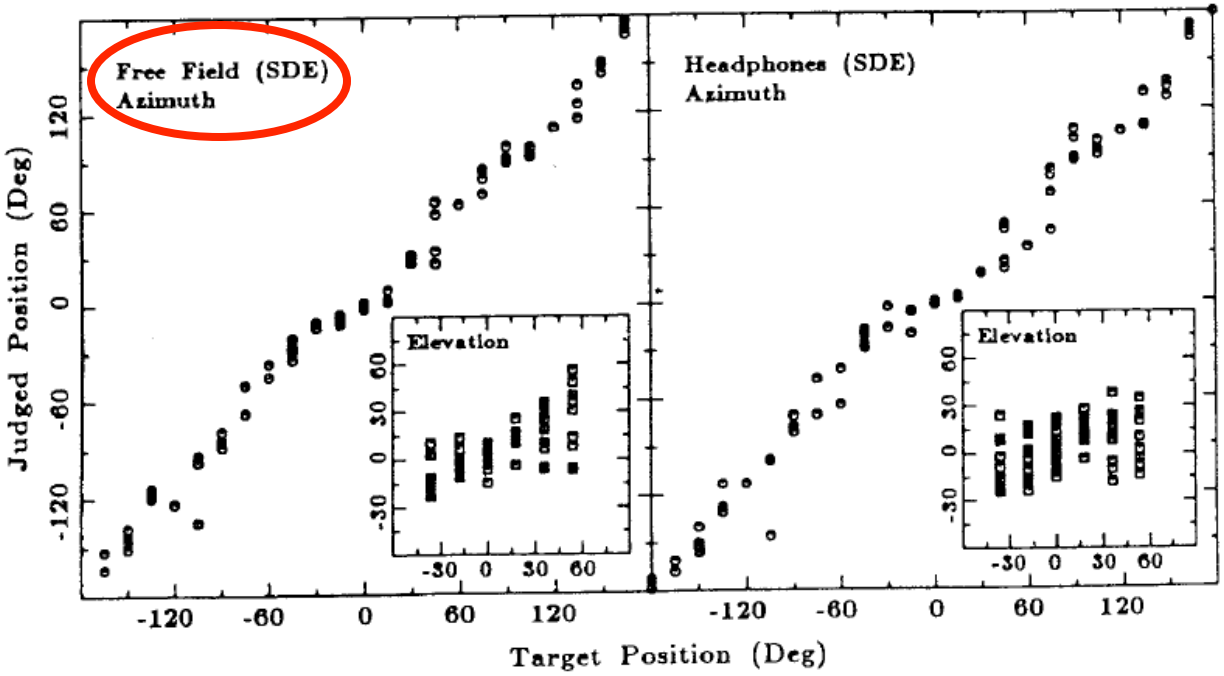

FIG. 2. Scatterplots of actual source azimuth (and, in the insets, elevation) versus judged source azimuth for subject SDE in both the free-field and headphone conditions. Each data point represents the centroid of at least six judgments. All 72 source positions are represented in each panel. Thus data from six different source elevations are combined in the azimuth panels, and data from 24 different azimuths are combined in the elevation panels. Note that the scale is the same for azimuth and elevation plots.

Wightman and Kistler (1989)

Head related transfer function (HRTF)

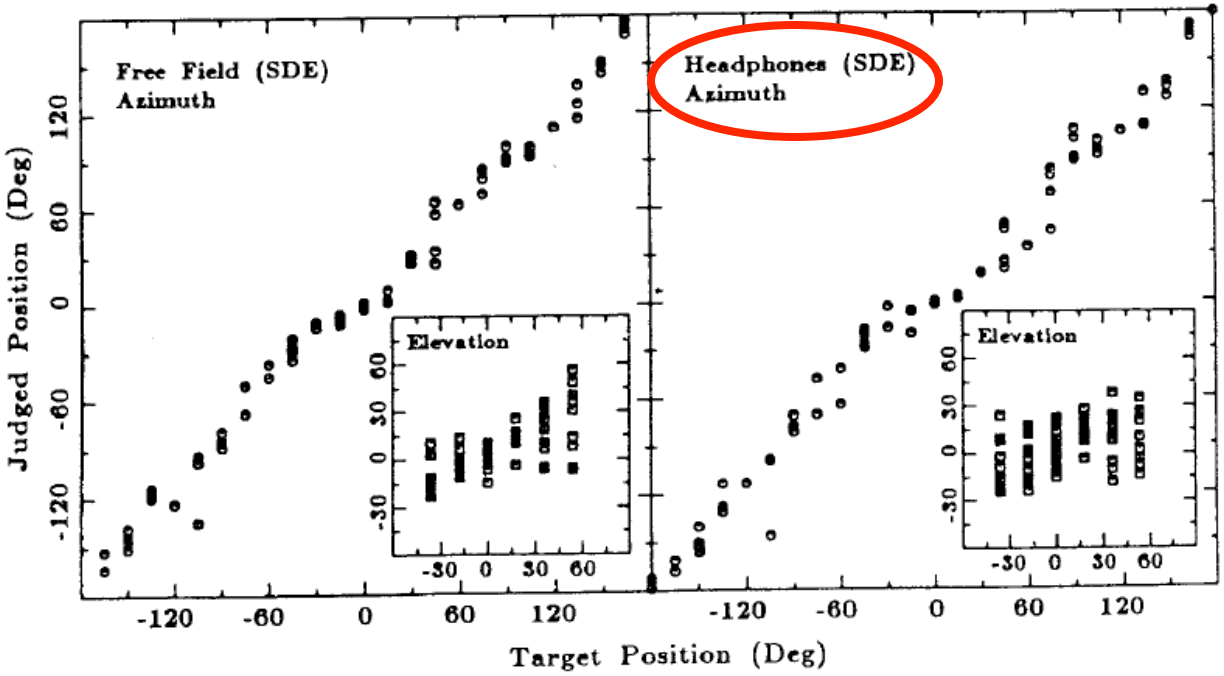

FIG. 2. Scatterplots of actual source azimuth (and, in the insets, elevation) versus judged source azimuth for subject SDE in both the free-field and headphone conditions. Each data point represents the centroid of at least six judgments. All 72 source positions are represented in each panel. Thus data from six different source elevations are combined in the azimuth panels, and data from 24 different azimuths are combined in the elevation panels. Note that the scale is the same for azimuth and elevation plots.

Wightman and Kistler (1989)

Head related transfer function (HRTF)

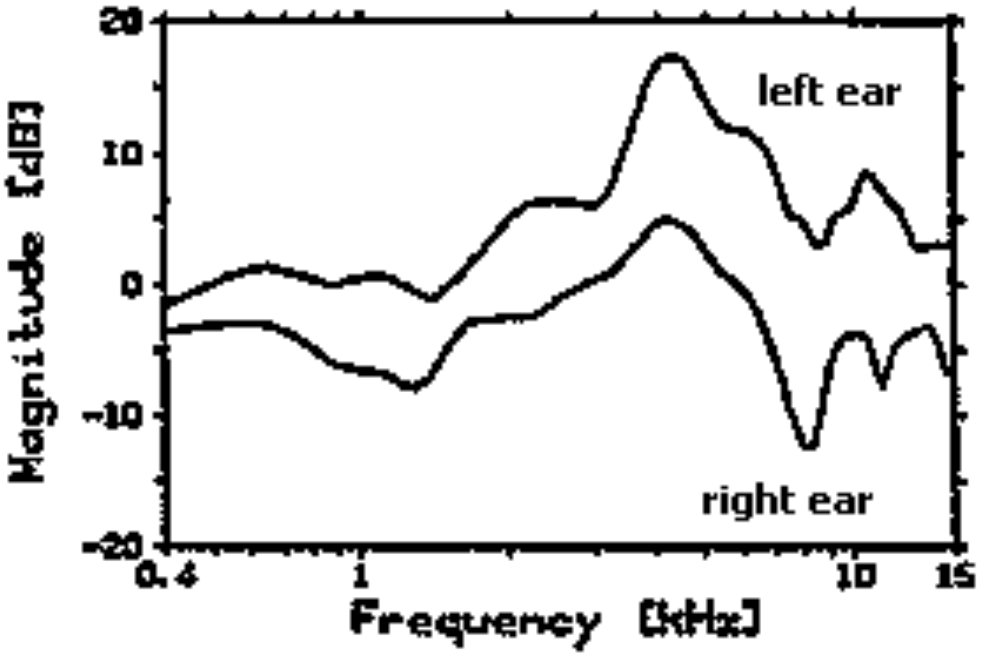

HRTFs of the left and right ears for a sound source at 30-degrees left of center.

source: E. MacPherson, A Computer Model of Binaural Localization for Stereo Imaging Measurement, JAES, September 1991.

Head related transfer function (HRTF)

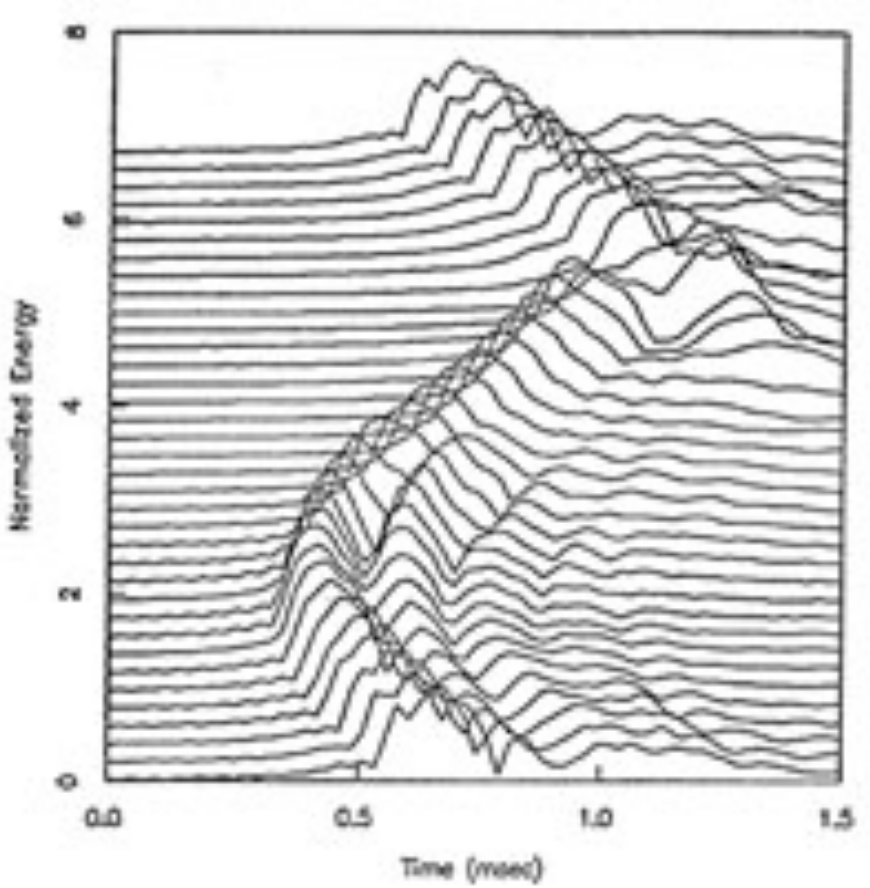

Head related transfer function (HRTF)

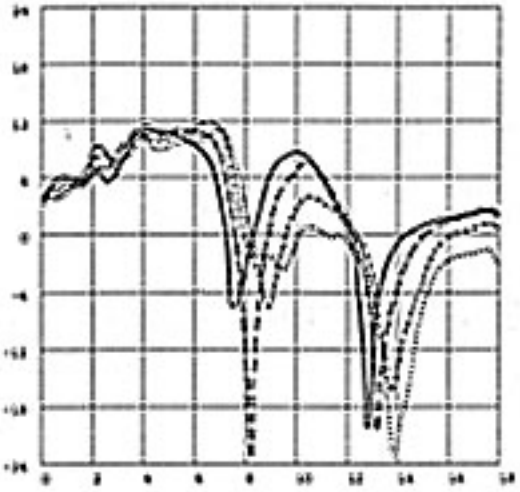

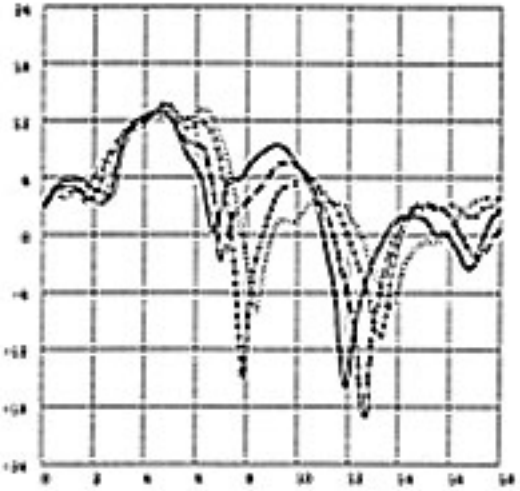

Grabaciones Binaurales

Crosstalk

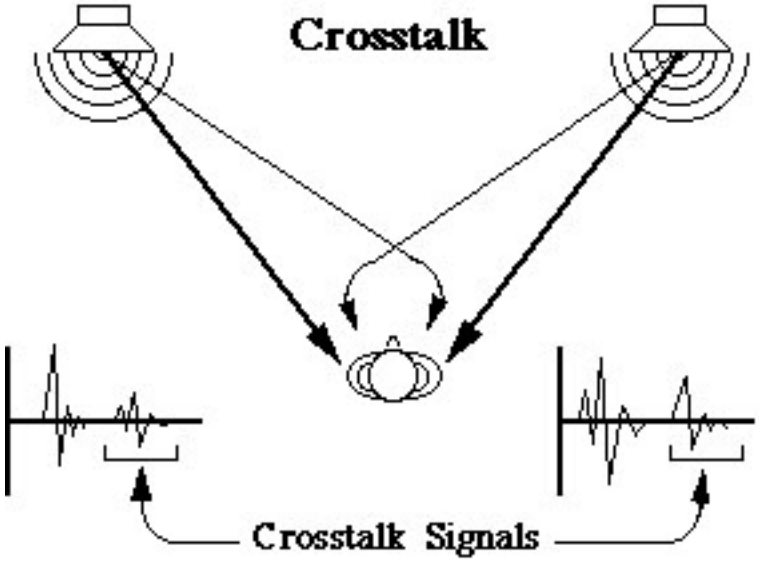

Pistas dinámicas

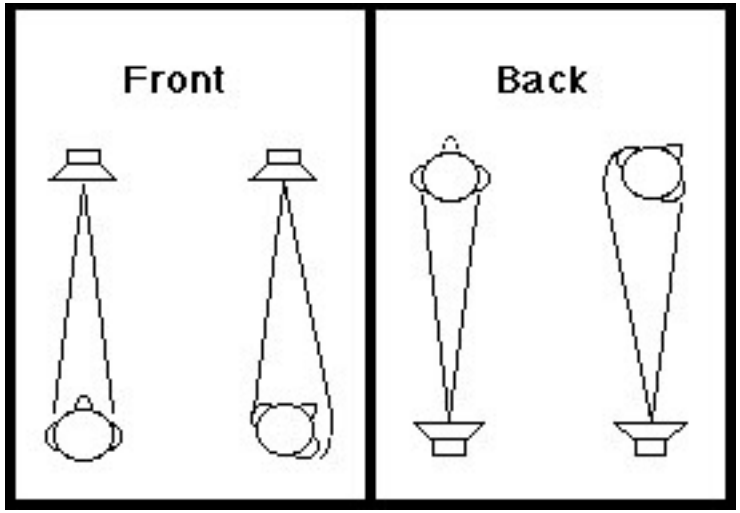

Pistas monaurales para la localización de sonidos

Pistas monaurales

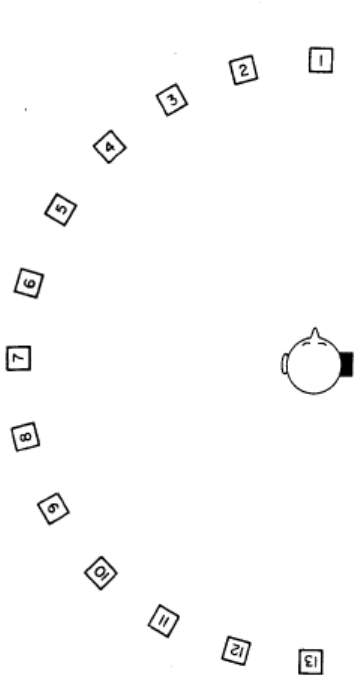

FIG. 1. A diagramatic sketch of the loudspeaker arrangement

Musicant and Butler (1985)

Pistas monaurales

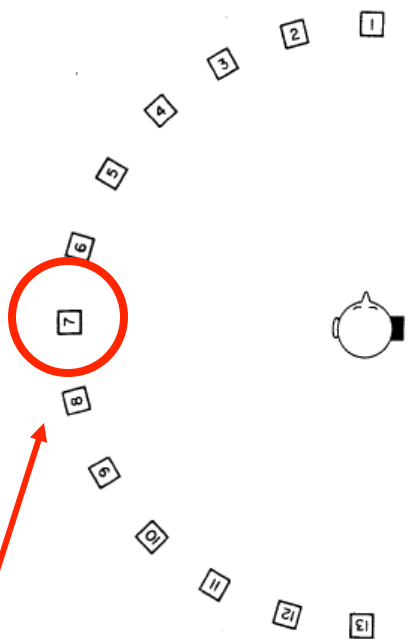

FIG. 1. A diagramatic sketch of the loudspeaker arrangement.

Todos los sonidos fueron producidos mediante este parlante

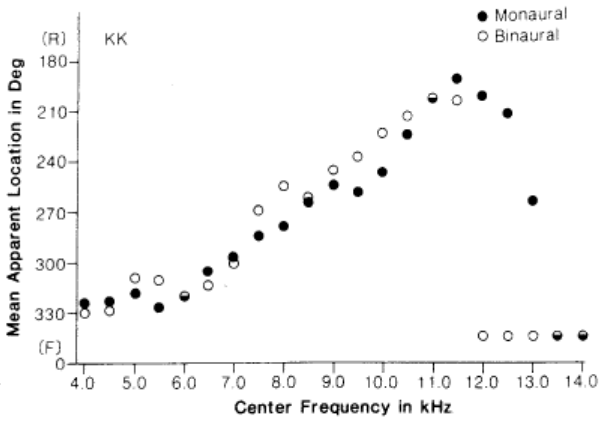

FIG. 2. The mean apparent location of narrow noise bands as a function of center frequency for subject K.K. Actual location was 270 deg azimuth.

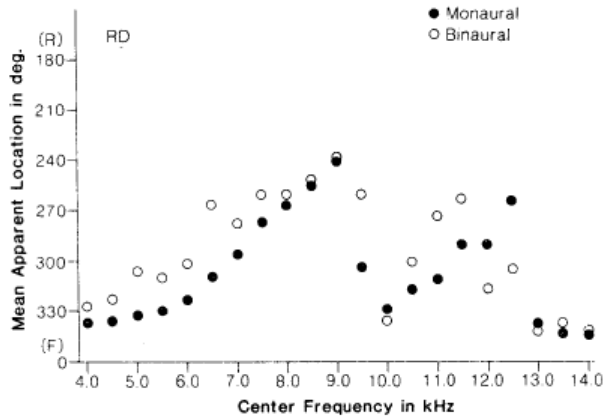

FIG. 3. The mean apparent location of narrow noise bands as a function of center frequency for subject R.D. Actual location was 270 deg azimuth.

Musicant and Butler (1985)

Aprendizaje de localización

Sound localization learning

http://www.mindhacks.com/blogfiles/2006/05/itd_hack.jpg

Re-Aprendiendo a localizar con nuevos oídos

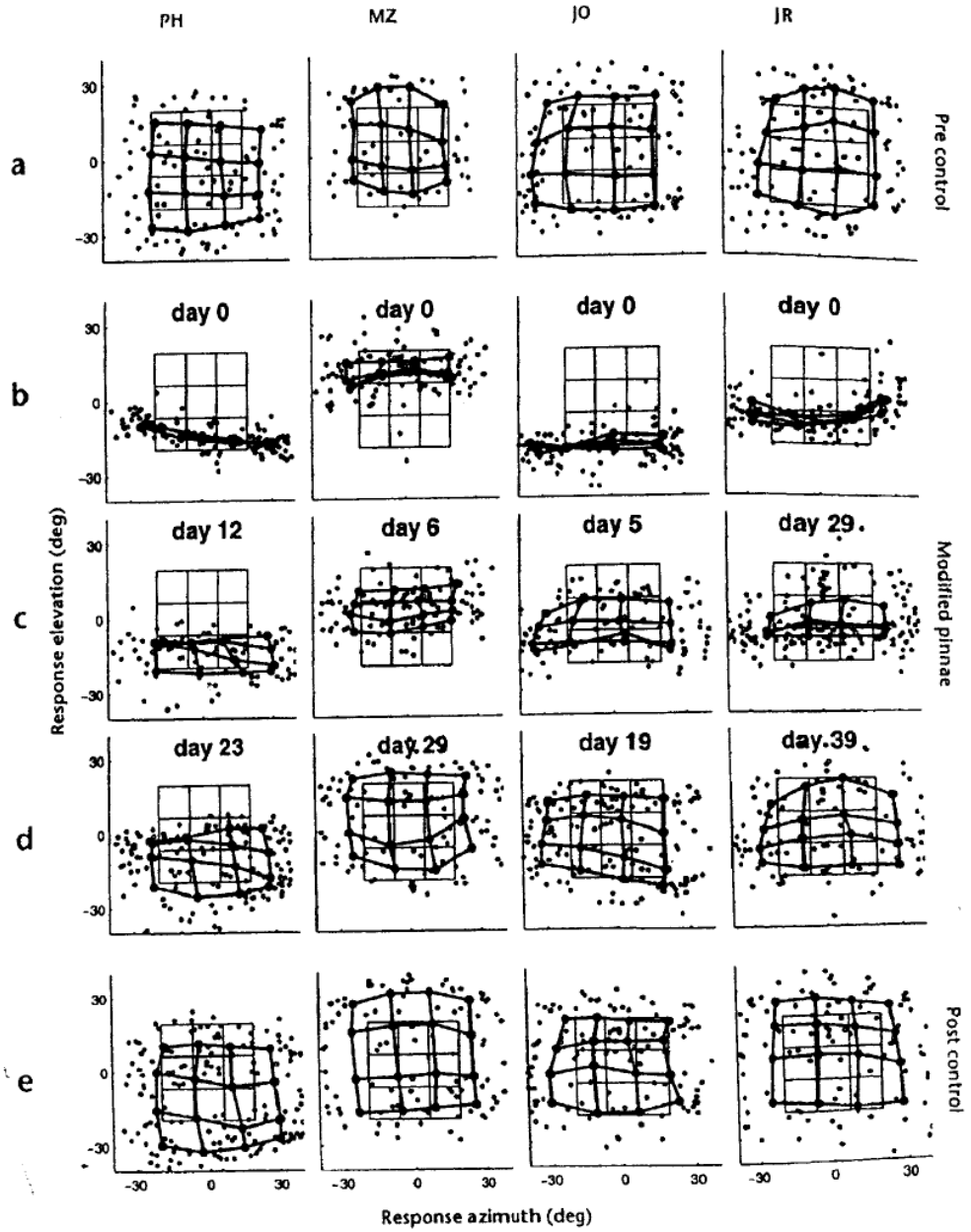

Fig. 2. Adaptation to altered spectral cues. Localization behavior of all four subjects (from left to right) before, during and immediately after the adaptation period. Day zero marks the start of the adaptation experiment. The panels show, for each subject, the individual saccade vector endpoints in the azimuth–elevation plane (symbol ◦). In addition, the saccade vectors were also averaged for targets belonging to similar directions by dividing the target space into sixteen half-overlapping sectors. Averaged data points (symbol •) from neighboring stimulus sectors are connected by thick lines. In this way, a regular response matrix indicates that the subject's saccade endpoints capture the actual spatial distribution of the applied target positions. The target matrix, computed in the same way as the saccade matrix, has been included for comparison (thin lines). **(a)** Results of the pre-adaptation control experiment on day zero, immediately preceding the application of the molds. **(b)** Localization responses immediately after inserting the molds (day 0). Note the dramatic deficit in elevation responses for all subjects. **(c)** Results during the adaptation period after twelve (PH), six (MZ), five (JO) and 29 (JR) days of continuously wearing the ear molds. **(d)** Results near the end of the adaptation period. Stable and reasonably accurate localization behavior has been established in all subjects. **(e)** Results of the control condition, immediately after removal of the molds. All subjects localized sounds with their original ears equally well as before the start of the experiment several weeks earlier.

Hofman et al. (1998)

Re-Aprendiendo a localizar con nuevos oídos

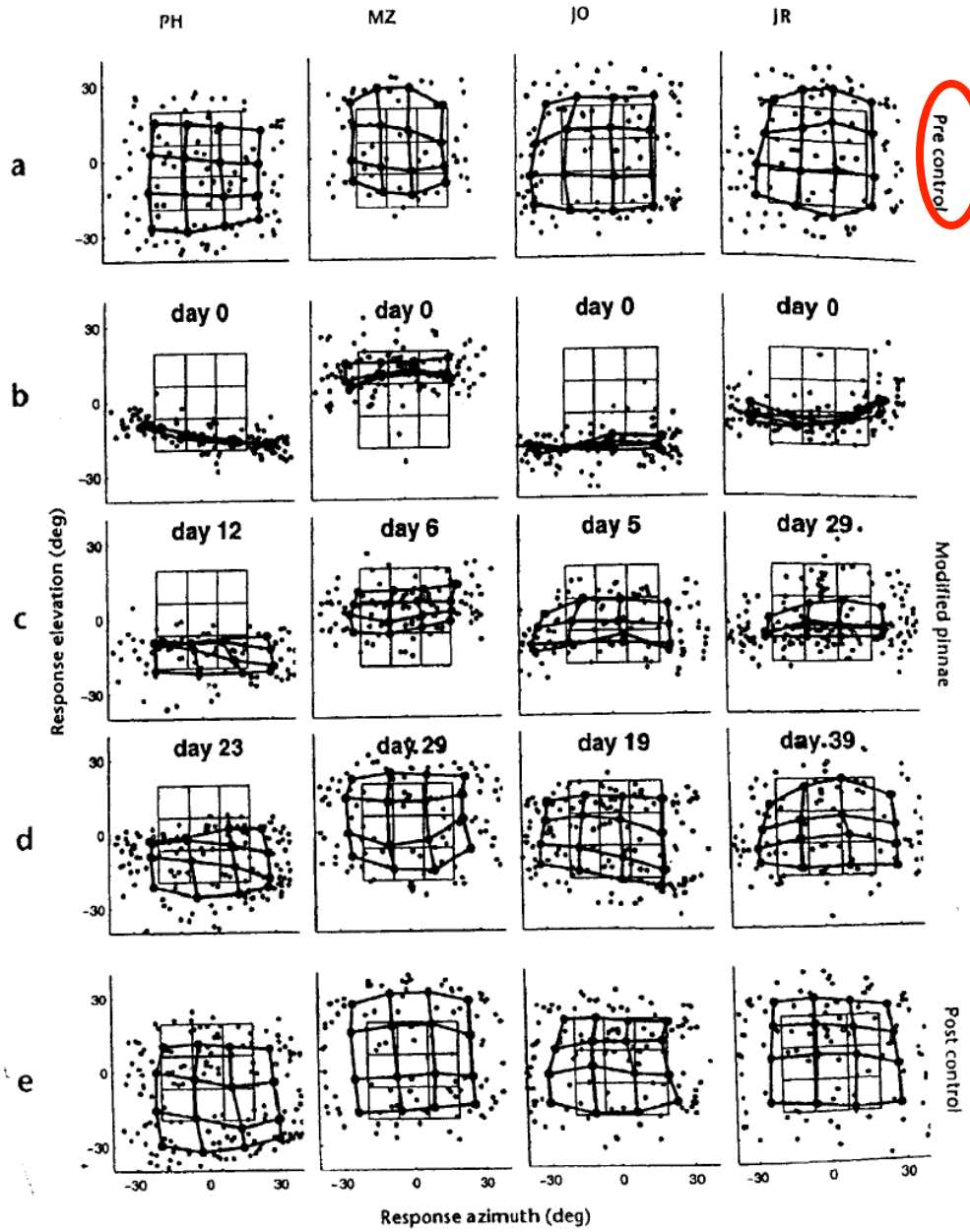

Fig. 2. Adaptation to altered spectral cues. Localization behavior of all four subjects (from left to right) before, during and immediately after the adaptation period. Day zero marks the start of the adaptation experiment. The panels show, for each subject, the individual saccade vector endpoints in the azimuth–elevation plane (symbol •). In addition, the saccade vectors were also averaged for targets belonging to similar directions by dividing the target space into sixteen half-overlapping sectors. Averaged data points (symbol •) from neighboring stimulus sectors are connected by thick lines. In this way, a regular response matrix indicates that the subject's saccade endpoints capture the actual spatial distribution of the applied target positions. The target matrix, computed in the same way as the saccade matrix, has been included for comparison (thin lines). **(a)** Results of the pre-adaptation control experiment on day zero, immediately preceding the application of the molds. **(b)** Localization responses immediately after inserting the molds (day 0). Note the dramatic deficit in elevation responses for all subjects. **(c)** Results during the adaptation period after twelve (PH), six (MZ), five (JO) and 29 (JR) days of continuously wearing the ear molds. **(d)** Results near the end of the adaptation period. Stable and reasonably accurate localization behavior has been established in all subjects. **(e)** Results of the control condition, immediately after removal of the molds. All subjects localized sounds with their original ears equally well as before the start of the experiment several weeks earlier.

Hofman et al. (1998)

Re-Aprendiendo a localizar con nuevos oídos

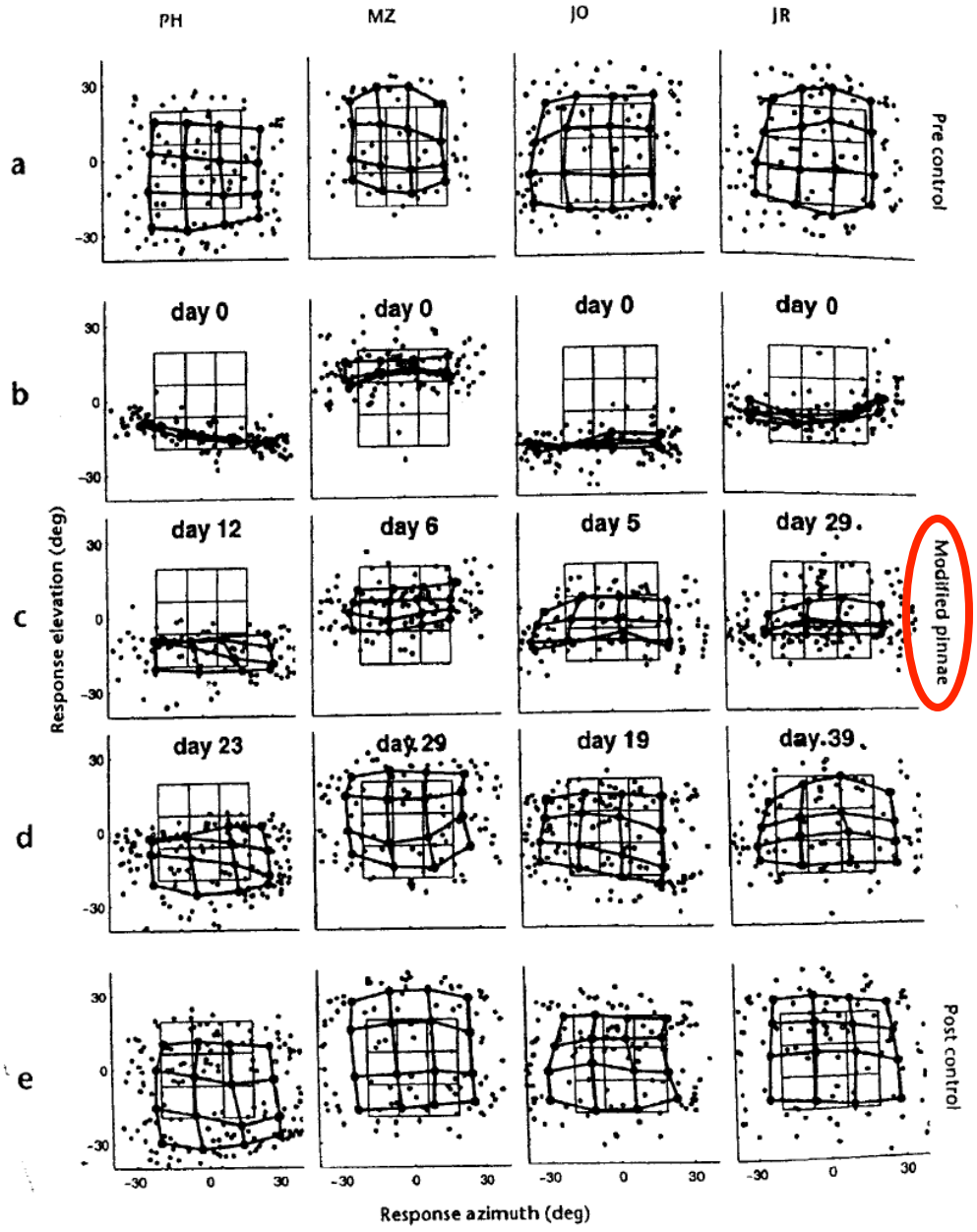

Fig. 2. Adaptation to altered spectral cues. Localization behavior of all four subjects (from left to right) before, during and immediately after the adaptation period. Day zero marks the start of the adaptation experiment. The panels show, for each subject, the individual saccade vector endpoints in the azimuth–elevation plane (symbol ◦). In addition, the saccade vectors were also averaged for targets belonging to similar directions by dividing the target space into sixteen half-overlapping sectors. Averaged data points (symbol •) from neighboring stimulus sectors are connected by thick lines. In this way, a regular response matrix indicates that the subject's saccade endpoints capture the actual spatial distribution of the applied target positions. The target matrix, computed in the same way as the saccade matrix, has been included for comparison (thin lines). **(a)** Results of the pre-adaptation control experiment on day zero, immediately preceding the application of the molds. **(b)** Localization responses immediately after inserting the molds (day 0). Note the dramatic deficit in elevation responses for all subjects. **(c)** Results during the adaptation period after twelve (PH), six (MZ), five (JO) and 29 (JR) days of continuously wearing the ear molds. **(d)** Results near the end of the adaptation period. Stable and reasonably accurate localization behavior has been established in all subjects. **(e)** Results of the control condition, immediately after removal of the molds. All subjects localized sounds with their original ears equally well as before the start of the experiment several weeks earlier.

Hofman et al. (1998)

Re-Aprendiendo a localizar con nuevos oídos

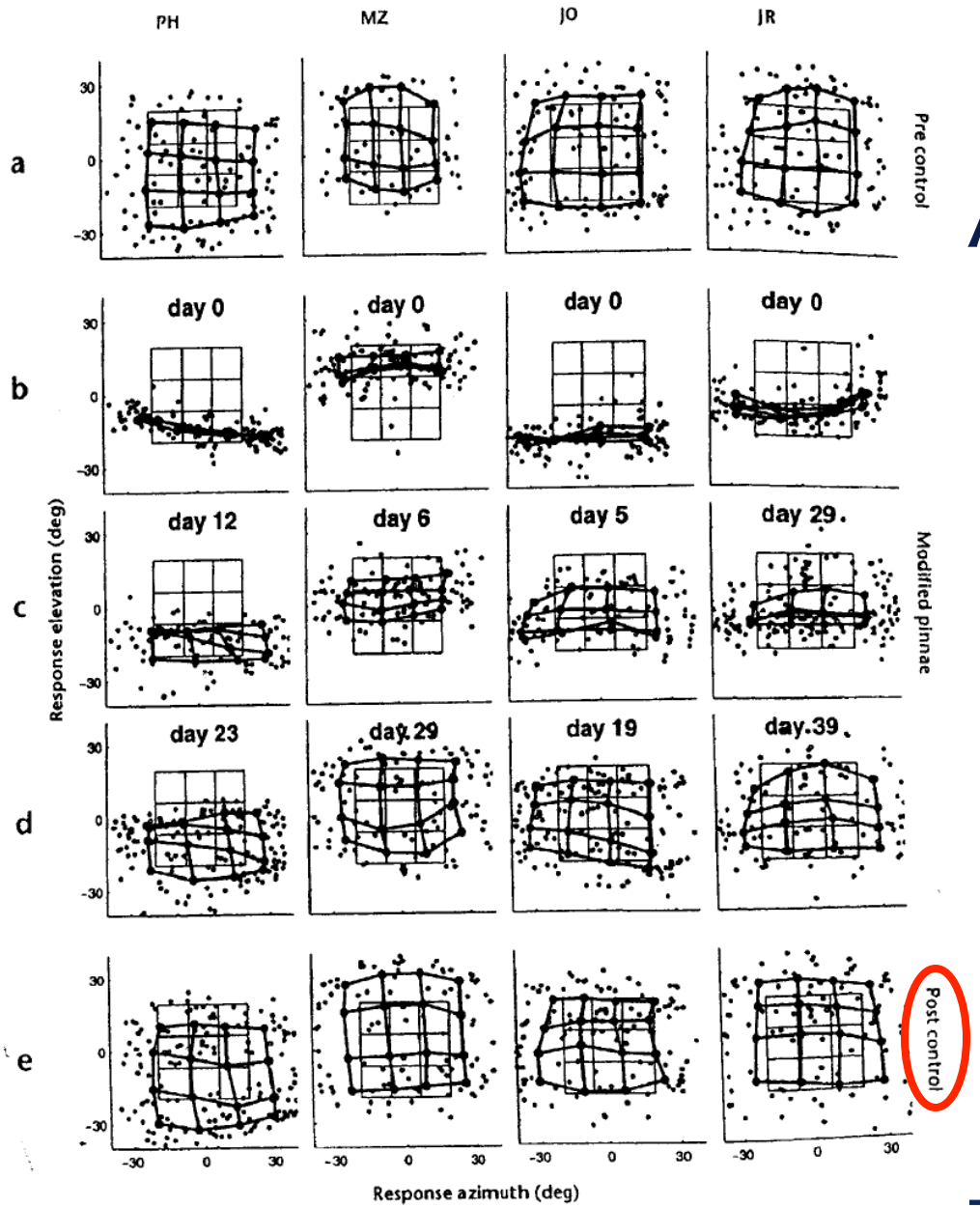

Fig. 2. Adaptation to altered spectral cues. Localization behavior of all four subjects (from left to right) before, during and immediately after the adaptation period. Day zero marks the start of the adaptation experiment. The panels show, for each subject, the individual saccade vector endpoints in the azimuth–elevation plane (symbol ◦). In addition, the saccade vectors were also averaged for targets belonging to similar directions by dividing the target space into sixteen half-overlapping sectors. Averaged data points (symbol •) from neighboring stimulus sectors are connected by thick lines. In this way, a regular response matrix indicates that the subject's saccade endpoints capture the actual spatial distribution of the applied target positions. The target matrix, computed in the same way as the saccade matrix, has been included for comparison (thin lines). **(a)** Results of the pre-adaptation control experiment on day zero, immediately preceding the application of the molds. **(b)** Localization responses immediately after inserting the molds (day 0). Note the dramatic deficit in elevation responses for all subjects. **(c)** Results during the adaptation period after twelve (PH), six (MZ), five (JO) and 29 (JR) days of continuously wearing the ear molds. **(d)** Results near the end of the adaptation period. Stable and reasonably accurate localization behavior has been established in all subjects. **(e)** Results of the control condition, immediately after removal of the molds. All subjects localized sounds with their original ears equally well as before the start of the experiment several weeks earlier.

Hofman et al. (1998)

Efecto de precedencia (Supresión de ecos)

Reflexiones sonoras

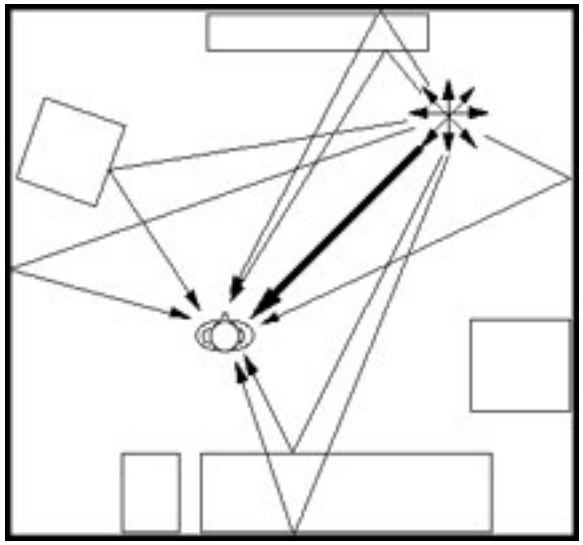

Reflexiones sonoras

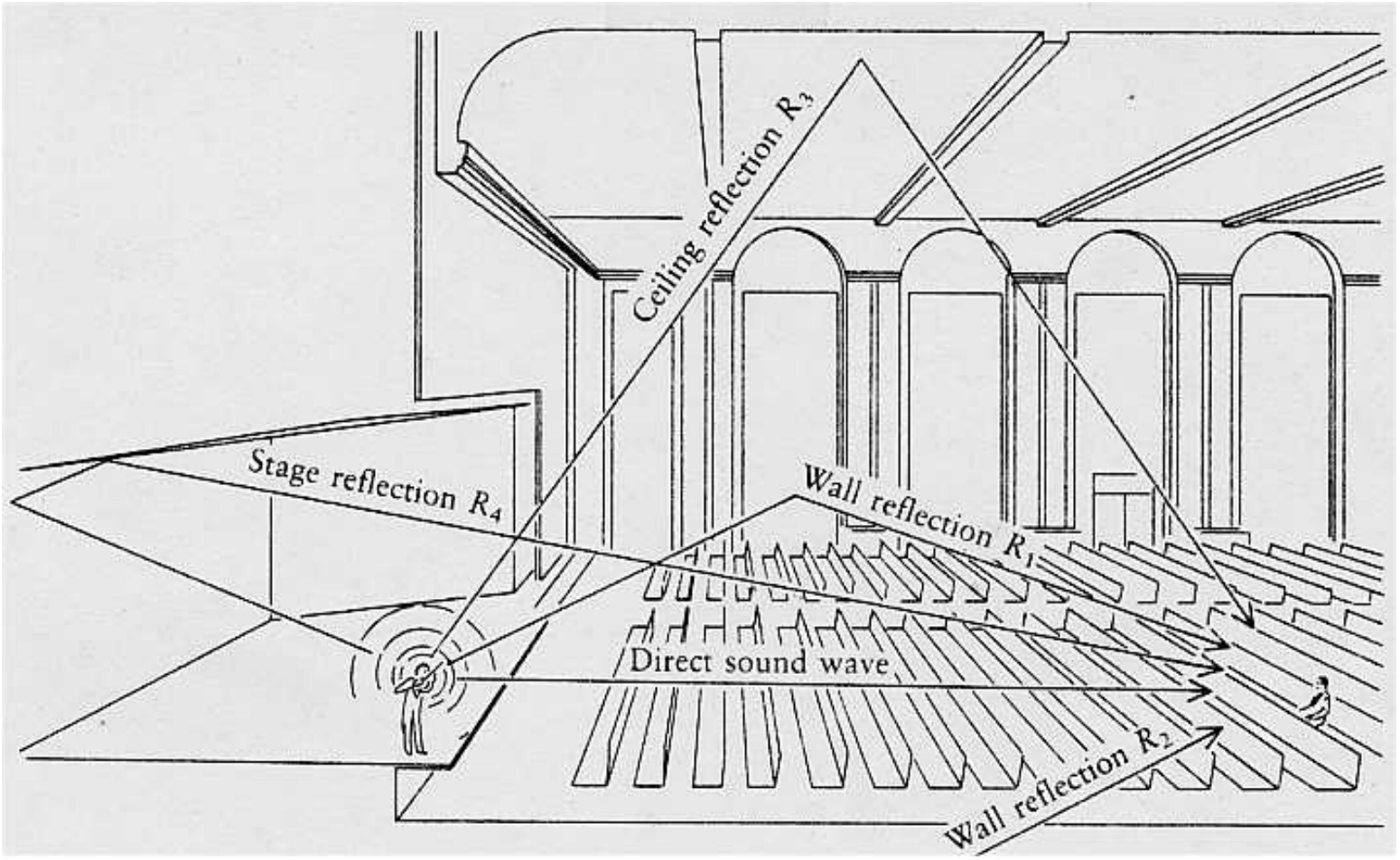

http://www.owlnet.rice.edu/~psyc351/imagelist.htm#Auditory%20Perception

Reflexiones sonoras

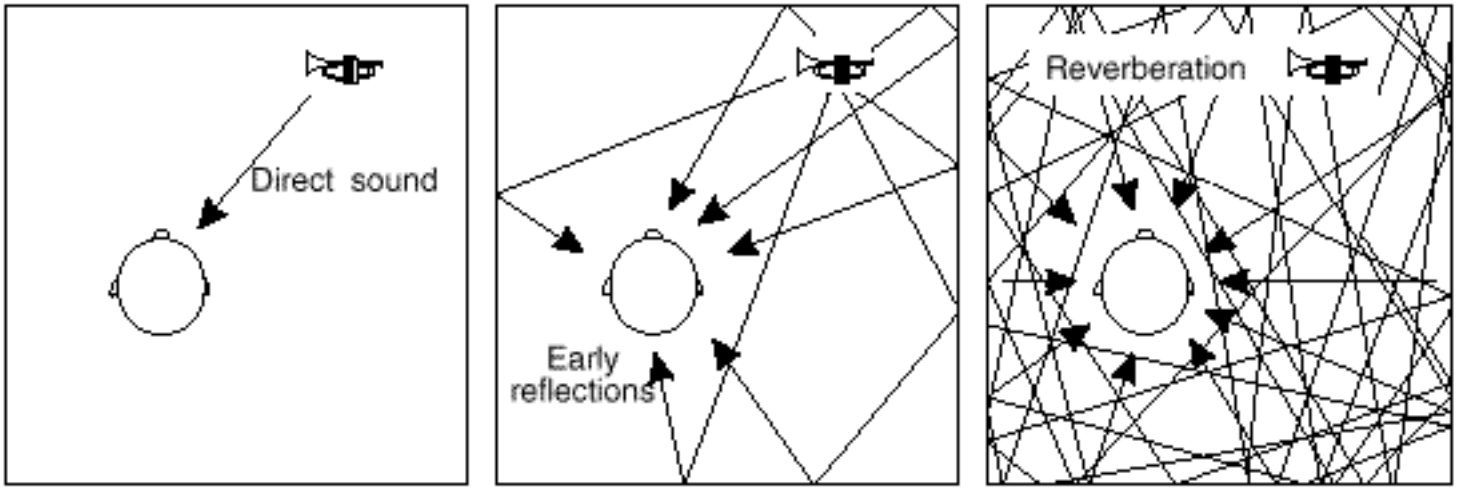

http://www.owlnet.rice.edu/~psyc351/imagelist.htm#Auditory%20Perception

Demonstración de supresión de eco

Demonstration 33: Effect of Echoes (cont.)

This so-called "ghoulies and ghosties" demonstration (No.2 on the "Harvard tapes") has become somewhat of a classic, and so it is reproduced here exactly as it was presented there. The reader is Dr. Sanford Fidell.

An important property of sound in practically all enclosed space is that reflections occur from the walls, ceiling, and floor. For a typical living space, 50 to 90 percent of the energy is reflected at the borders. These reflections are heard as echoes if sufficient time elapses between the initial sound and the reflected sound. Since sound travels about a foot per millisecond, delays between the initial and secondary sound will be of the order of 10 to 20 ms for a modest room. Practically no one reports hearing echoes in typical small classrooms when a transient sound is initiated by a snap of the fingers. The echoes are not heard, although the reflected sound may arrive as much as 30 to 50 ms later. This demonstration is designed to make the point that these echoes do exist and are appreciable in size. Our hearing mechanism somehow manages to suppress the later-arriving reflections, and they are simply not noticed.

The demonstration makes these reflections evident, however, by playing the recorded sound backward in time. The transient sound is the blow of a hammer on a brick, the more sustained sound is the narration of an old Scottish prayer. Three different acoustic environments are used, an anechoic (echoless) room, a typical conference room, similar acoustically to many living rooms, and finally a highly reverberant room with cement floor, hard plaster walls and ceiling. Little reverberation is apparent in any of the rooms when the recording is played forward, but the reversed playback makes the echoes evident in the environment where they do occur.

Note that changes in the quality of the voice are evident as one changes rooms even when the recording is played forward. These changes in quality are caused by differences in amount and duration of the reflections occurring in these different environments. The reflections are not heard as echoes, however, but as subtle, and difficult to describe, changes in voice quality. All recordings were made with the speaker's mouth about 0.3 meters from the microphone.

"First in an anechoic room, then in a conference room, and finally in a very reverberant space, you will hear a hammer striking a brick followed by an old Scottish prayer. Playing these sounds backwards focuses our attention on the echoes that occur."

References

- L.Cremer, H.A.Müller, and T.J.Schultz (1982), *Principles and Applications Room Acoustics*, Vol.1 (Applied Science, London).
- H. Kutruff (1979), *Room Acoustics*, 2nd ed. (Applied Science, London).
- V.M.A.Peutz (1971), "Articulatory loss of constants as a criterion for speech tra mission in a room," J.Audio Eng. Soc. *19*, 915-19.
- M.R.Schroeder (1980), "Acoustics in human communication: room acoustics, n sic, and speech," J. Acoust. Soc. Am. *68*, 22-28.

Efecto de precedencia

Conocido como: supresión de eco, ley del primer frente de onda

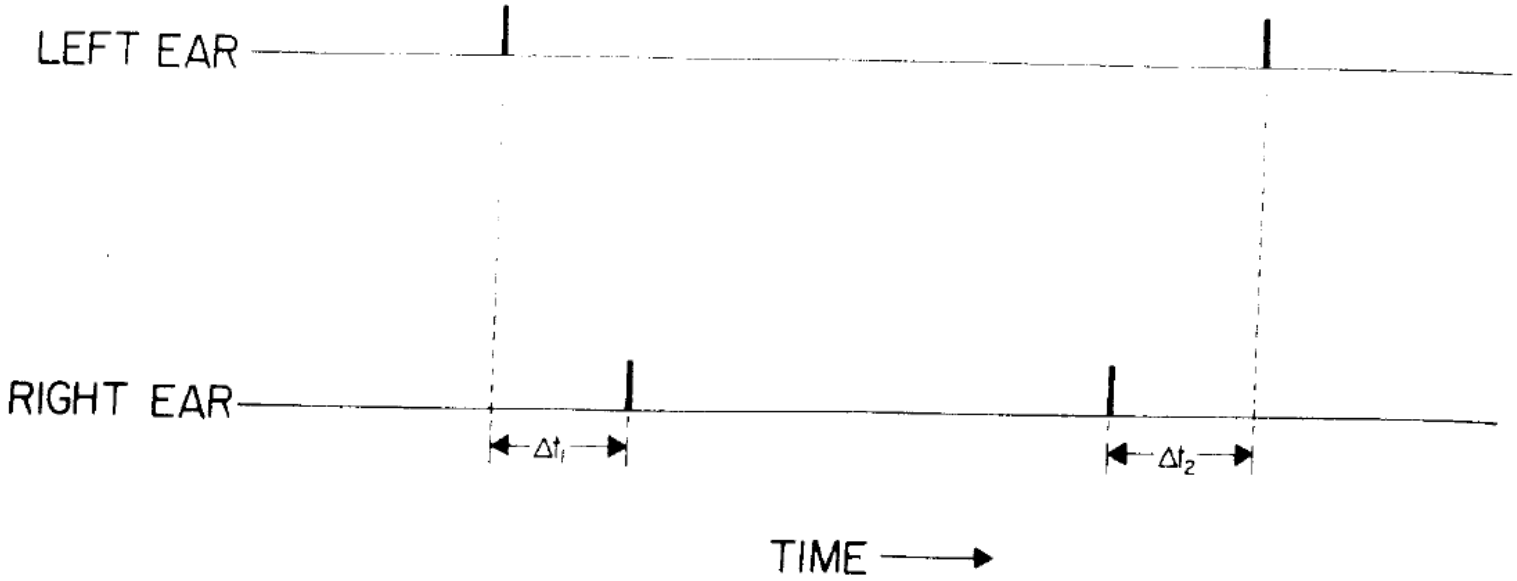

FIG. 8.6 Stimulus conditions in the precedence experiment. Two clicks are presented within a brief interval to both ears. The first click to the left ear arrives Δt_1 before the first click to the right ear. The second click to the right ear arrives Δt_2 before the second click to the left ear. The subject hears a single sound, and by adjusting Δt_2, can "center" the image, thus offsetting Δt_1.

Green, D.M. (1976). *An Introduction to Hearing*. Lawrence Erlbaum Associates, Hillsdale, NJ.

Efecto de precedencia

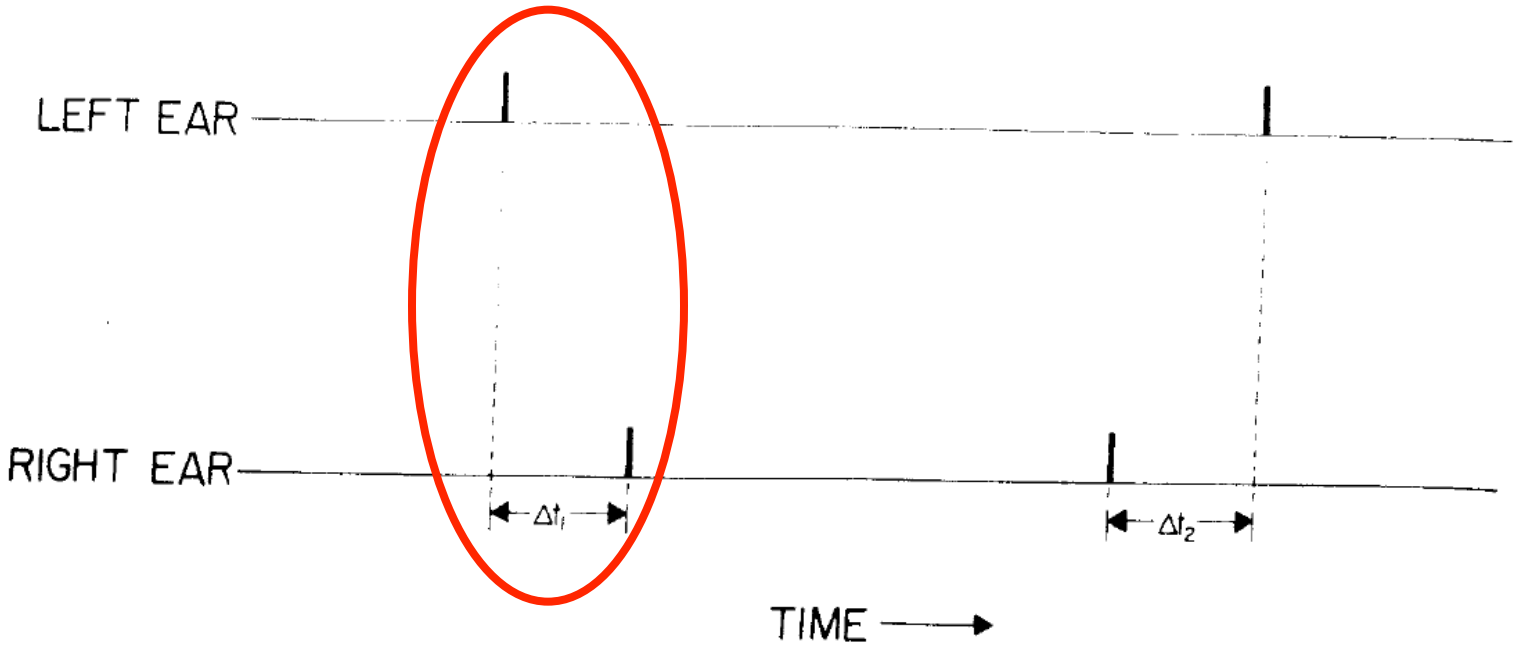

FIG. 8.6 Stimulus conditions in the precedence experiment. Two clicks are presented within a brief interval to both ears. The first click to the left ear arrives Δt_1 before the first click to the right ear. The second click to the right ear arrives Δt_2 before the second click to the left ear. The subject hears a single sound, and by adjusting Δt_2, can "center" the image, thus offsetting Δt_1.

Green, D.M. (1976). *An Introduction to Hearing*. Lawrence Erlbaum Associates, Hillsdale, NJ.

Efecto de precedencia

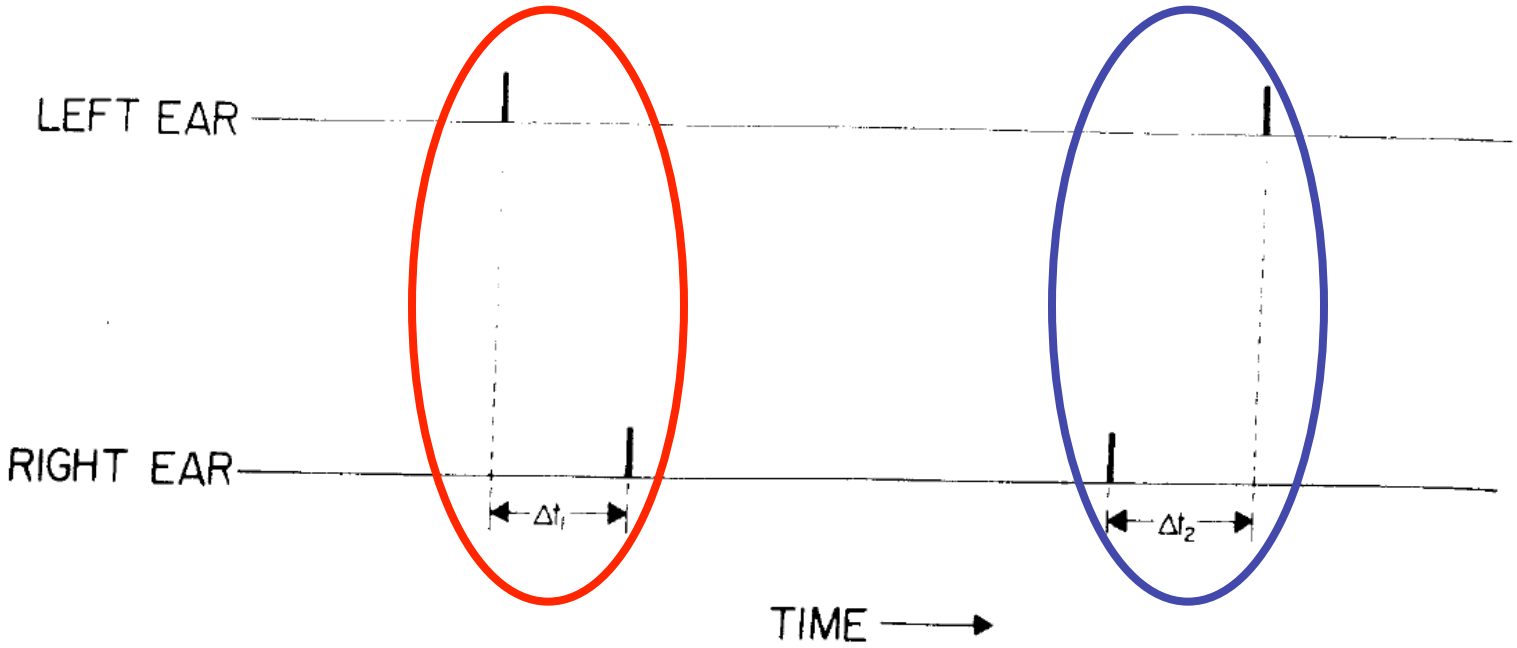

FIG. 8.6 Stimulus conditions in the precedence experiment. Two clicks are presented within a brief interval to both ears. The first click to the left ear arrives Δt_1 before the first click to the right ear. The second click to the right ear arrives Δt_2 before the second click to the left ear. The subject hears a single sound, and by adjusting Δt_2, can "center" the image, thus offsetting Δt_1.

Green, D.M. (1976). *An Introduction to Hearing*. Lawrence Erlbaum Associates, Hillsdale, NJ.

Efecto de precedencia

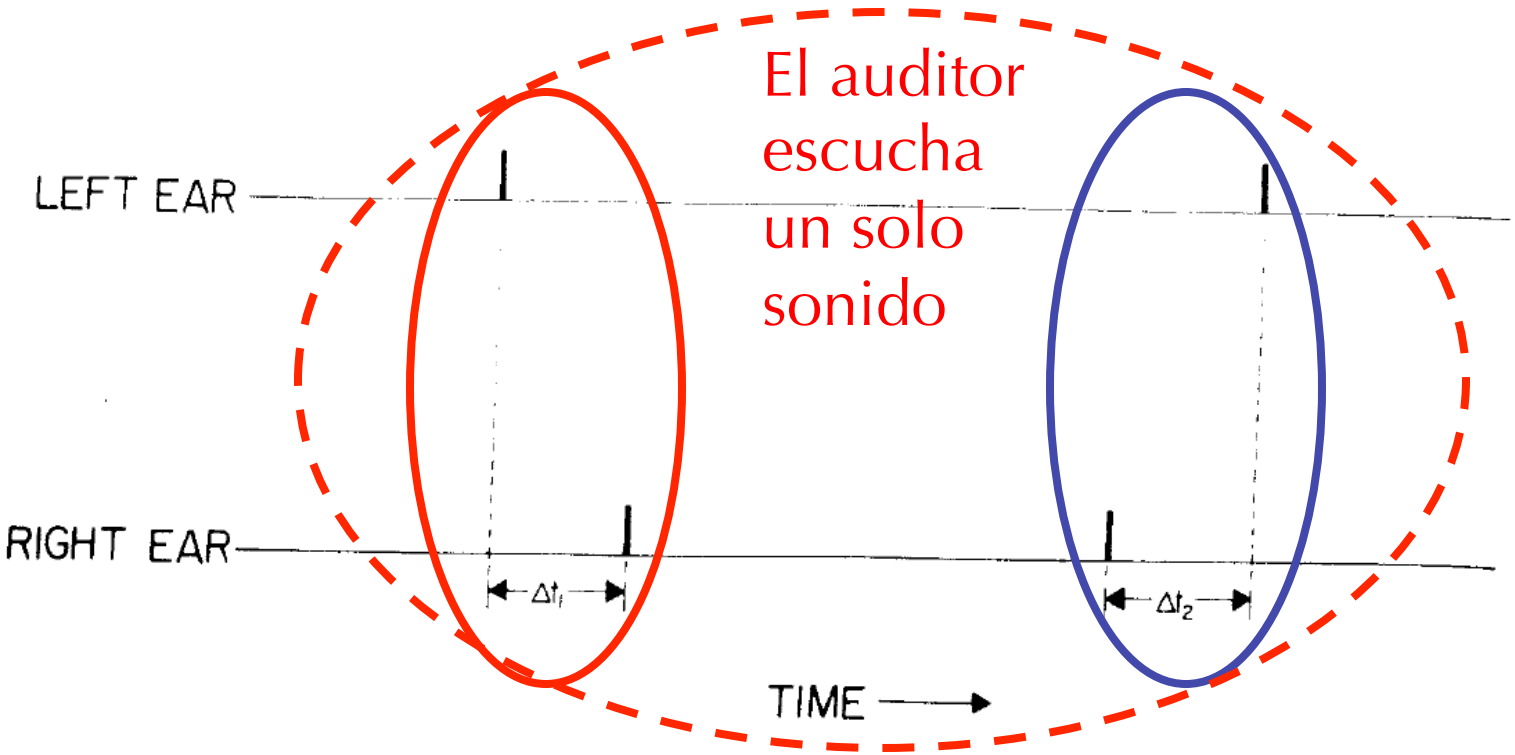

FIG. 8.6 Stimulus conditions in the precedence experiment. Two clicks are presented within a brief interval to both ears. The first click to the left ear arrives Δt_1 before the first click to the right ear. The second click to the right ear arrives Δt_2 before the second click to the left ear. The subject hears a single sound, and by adjusting Δt_2, can "center" the image, thus offsetting Δt_1.

Green, D.M. (1976). *An Introduction to Hearing*. Lawrence Erlbaum Associates, Hillsdale, NJ.

Nivel de diferencia de enmascaramiento
Masking level difference (MLD)

Masking level difference (MLD)

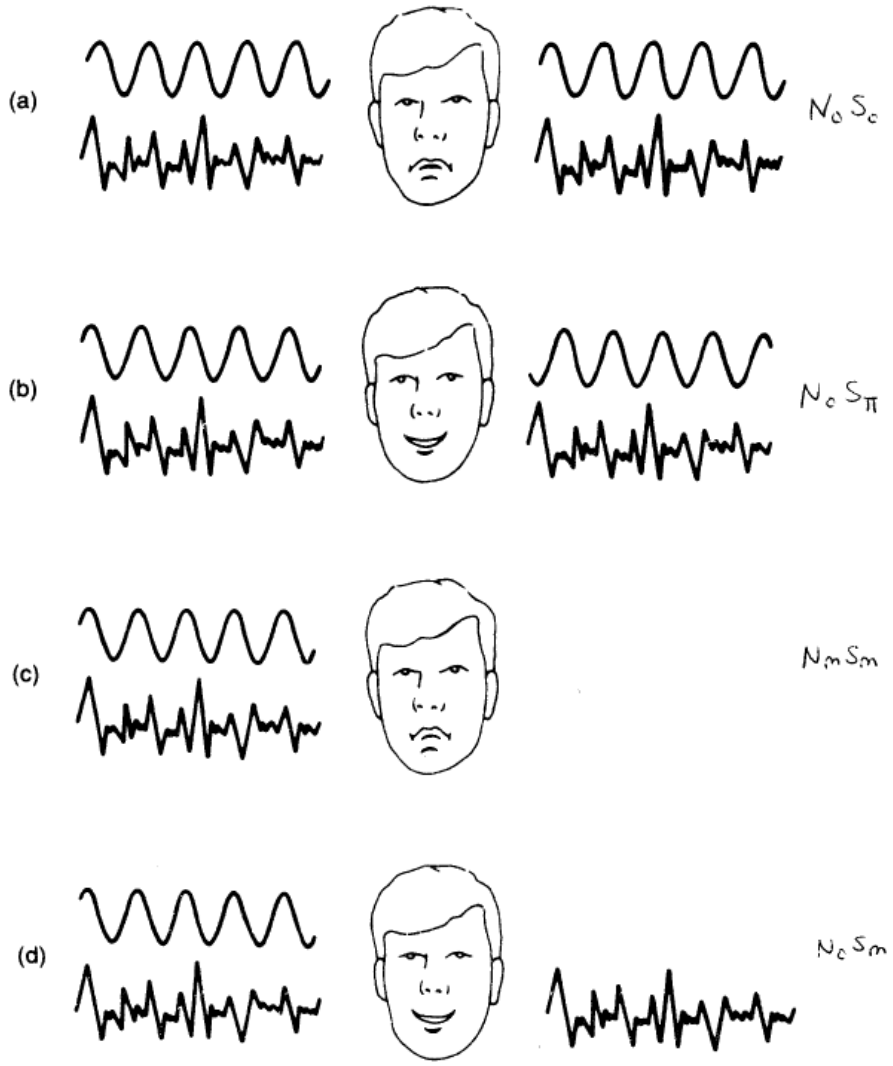

FIG. 6.9 Illustration of two situations in which binaural masking level differences (MLDs) occur. In conditions (a) and (c) detectability is poor, while conditions (b) and (d), where the interaural relations of the signal and masker are different, detectability is good (hence the smiling faces).

Demostración 38

Moore (1997)

S_o: Signal presented to both ears with no interaural differences (lateralized image in center of head).

N_o: Noise presented to both ears with no interaural differences (lateralized image in center of head).

S_m: Signal presented to only one ear, no signal presented at the other ear (sound image at one ear).

N_m: Noise presented to only one ear, no noise presented at the other ear (sound image at one ear).

S_π: Signal presented to both ears but the waveform inverted at one of the ears (sound image at both ears or on a thin line from center toward both ears—distinctly different from S_o).

For a sinusoid this amounts to 180° phase delay between the two ears.

N_π: Noise presented to both ears but inverted at one of the ears, that is, if $n(t)$ presented to the right ear then $-n(t)$ presented at the other (sound image at both ears definitely different from N_o).

N_u: Noise uncorrelated at the two ears (sound image in center of head but very diffuse compared with N_o).

TABLE 8.1

Interaural condition	Relative improvement (in dB, ± .5 dB)
N_oS_o, N_mS_m, N_uS_m, $S_\pi N_\pi$	0
N_uS_π	3
N_uS_o	4
$N_\pi S_m$	6
N_oS_m	9
$N_\pi S_o$	13
N_oS_π	15

Masking level difference (MLD)

Green (1976)

Masking level difference (MLD)

S_o: Signal presented to both ears with no interaural differences (lateralized image in center of head).

N_o: Noise presented to both ears with no interaural differences (lateralized image in center of head).

S_m: Signal presented to only one ear, no signal presented at the other ear (sound image at one ear).

N_m: Noise presented to only one ear, no noise presented at the other ear (sound image at one ear).

S_π: Signal presented to both ears but the waveform inverted at one of the ears (sound image at both ears or on a thin line from center toward both ears—distinctly different from S_o).

For a sinusoid this amounts to 180° phase delay between the two ears.

N_π: Noise presented to both ears but inverted at one of the ears, that is, if $n(t)$ presented to the right ear then $-n(t)$ presented at the other (sound image at both ears definitely different from N_o).

N_u: Noise uncorrelated at the two ears (sound image in center of head but very diffuse compared with N_o).

TABLE 8.1

Interaural condition	Relative improvement (in dB, ± .5 dB)
N_oS_o, N_mS_m, N_uS_m, $S_\pi N_\pi$	0
N_uS_π	3
N_uS_o	4
$N_\pi S_m$	6
N_oS_m	9
$N_\pi S_o$	13
N_oS_π	15

Green (1976)

Demostración 36

Beats binaurales

Si se presenta un sonido de cierta frecuencia en un oído y otro de frecuencia levemente distinta en el otro se producen abatimientos (beatings).

Este fenómeno es distinto al beating físico que se puede percibir con sólo un oído

Green (1976)

Demostración 37

Lateralización binaural

Esta demostración muestra el rol que juegan la ITD y ILD en la localización lateral de los sonidos

Green (1976)